American Mineralogist MS #4425—Revision 3—June 7, 2013

Clay mineral evolution

Robert M. Hazen[1,2*], Dimitri A. Sverjensky[1,3], David Azzolini[3], David L. Bish[4], Stephen C. Elmore[2], Linda Hinnov[3], Ralph E. Milliken[5]

[1]*Geophysical Laboratory, Carnegie Institution of Washington,*
5251 Broad Branch Road NW, Washington, D. C. 20015, USA.
[2]*George Mason University, 4400 University Drive, Fairfax, VA 20444, USA.*
[3]*Department of Earth and Planetary Sciences, Johns Hopkins University, Baltimore, MD 21218, USA*
[4]*Department of Geological Sciences, Indiana University 1001 E. 10th St., Bloomington IN 47405, USA.*
[5]*Department of Geological Sciences, Brown University, Box 1864, Providence, RI 02912 USA*

ABSTRACT

Changes in the mechanisms of formation and global distribution of phyllosilicate clay minerals through 4.567 Ga of planetary evolution in our Solar System reflect evolving tectonic, geochemical, and biological processes. Clay minerals were absent prior to planetesimal formation approximately 4.6 billion years ago but today are abundant in all near-surface Earth environments. New clay mineral species and modes of clay mineral paragenesis occurred as a consequence of major events in Earth's evolution—notably the formation of a mafic crust and oceans, the emergence of granite-rooted continents, the initiation of plate tectonics and subduction, the Great Oxidation Event, and the rise of the terrestrial biosphere. The changing character of clay minerals through time is thus an important part of Earth's mineralogical history and exemplifies the principles of mineral evolution.

Keywords: Clay minerals, biominerals, weathering, diagenesis, Mars mineralogy

---

* E-mail address of corresponding author: rhazen@ciw.edu

INTRODUCTION

The mineralogy of terrestrial planets, moons, and asteroids diversified as physical, chemical, and (in the case of Earth) biological processes modified the initially relatively homogeneous material of the solar nebula into differentiated zones of varied temperature, pressure, and composition. Earth's 4.567 billion year history, as a consequence, can be divided into three eras and ten stages of mineral evolution, each of which has seen significant changes in the planet's near-surface mineralogy (Hazen et al. 2008, 2011; Table 1). These dramatic changes include diversification in the number of different mineral species; shifts in the distribution of those species; systematic changes in major, minor, and trace element compositions of minerals; and the appearance of new grain sizes, textures, and/or morphologies. The concept of mineral evolution thus places mineralogy in a dynamic historical context, in which different mineral species and mineralogical characteristics arose at different stages of planetary history as new modes of mineral paragenesis came into play. However, the initial presentation of this framework by Hazen et al. (2008) did not examine any one group of minerals in detail. Here we consider the important case of the evolution of phyllosilicate clay minerals, which, possibly more than any other mineral groups, exemplify the connections among the geosphere, hydrosphere, and biosphere (Elmore 2009).

It is likely that no phyllosilicate clay minerals were present in the pre-solar molecular cloud, which contained approximately a dozen micro- and nanoscale refractory "ur-minerals" (Hazen et al. 2008). Yet, although clay minerals were absent during the initial high-temperature stages of planet formation, they now represent an important component of the near-surface crustal environment of Earth, Mars, and the parent bodies of carbonaceous chondrite meteorites. They also represent perhaps the most important class of minerals with which mankind interacts on a

daily basis. Therefore, understanding the evolution of clay minerals as products of physical, chemical, and biological alteration processes is critical for understanding the mineralogical history of Earth and other worlds. Indeed, clay minerals provide a revealing case study for Earth's changing mineralogy through time for at least six reasons. (1) Clay minerals first appeared in the early stages of planetary accretion and have been ubiquitous near-surface phases throughout our planet's history. (2) The 10 groups and more than 50 species of phyllosilicate clay minerals officially recognized by the International Mineralogical Association arise through varied paragenetic modes that parallel changing near-surface conditions and processes. (3) All of the principal clay mineral structure types are compositionally adaptable with diverse cations in tetrahedral, octahedral, and interlayer sites. Therefore, major, minor, and trace elements are likely to have varied systematically through time and thus reflect changing near-surface conditions, including compositions of parent rocks, solution chemistry, and redox state. (4) Clay minerals exemplify mineralogical feedback mechanisms: for example, some clay minerals strongly interact with organic molecules, so sedimentary burial of clay minerals can sequester reduced carbon and thus enhance atmospheric oxidation (e.g., Berner 2004), which in turn affects the nature and rate of clay mineral formation. (5) Clay minerals have played a significant role in the mineralogy of Mars, and they hold the potential to reveal details of the evolution of the near-surface martian environment. And (6) clay minerals highlight the co-evolution of Earth's geosphere and biosphere: Clays likely played critical roles in the origin of life, and life has played a dramatic role in the production of near-surface clay minerals. Note, however, that in spite of fascinating "clay origin of life" speculations by Cairns-Smith and coworkers, who posit that the first life forms were self-replicating and evolving clay mineral assemblages (Cairns-Smith and Hartman 1986; Cairns-Smith 2005; Schumann et al. 2012), observational evidence

does not support the contention that clay minerals "evolve" from prior generations by common descent. Mineral evolution instead refers to the tendency of Earth's near-surface environment to display congruent complexification, and thus to parallel other evolving natural and technological systems (Hazen and Eldredge 2010).

Understanding Earth's changing near-surface clay mineralogy through deep time is complicated by the fact that most of Earth's early clay mineral record has been erased as a result of burial, tectonic activity, alteration, and erosion. In this respect, the study of clay mineral evolution presents challenges related to preservational bias that are much more extreme than those of some other mineral systems (Hazen et al. 2009, 2012, 2013; Grew and Hazen 2009, 2010a, 2010b, 2013; Golden et al. 2013). Nevertheless, much about the 4.5 billion year evolutionary history of clays can be inferred from observations of the rock record and studies of modern clay-forming processes.

Our objective is to trace the changing diversity, distribution, and environments of clay minerals from planetary accretion to the modern terrestrial biological era through ten stages of mineral evolution (Table 1). We focus on several overarching questions: What were Earth's first clay minerals? When and how did they form? What new clay minerals were associated with the formation of granitoids, the initiation of plate tectonics, and the Great Oxidation Event? How have the rates of clay mineral production changed over geological time? How does the distribution of clay minerals in the terrestrial environment reflect changes in atmospheric composition? And what effects have biological organisms had on clay mineral production? To address these questions we examine roles of the principal paragenetic modes of clay mineral formation through 10 stages of Earth's mineral evolution.

CLAY MINERAL GROUPS AND SPECIES

Our survey of clay mineral evolution focuses on predominantly fine-grained (< 2 μm) layered phyllosilicate minerals (Guggenheim and Martin 1995), including 56 clay mineral species that have been approved by the International Mineralogical Association based on criteria of composition and structure [see the RRUFF database (http://rruff.info; Downs 2006); Table 2]. The phyllosilicate clay minerals considered here include the kaolin and serpentine groups, the talc and pyrophyllite groups, the expandable smectite and vermiculite groups, the illite group, the chlorite group, and the sepiolite-palygorskite group. Although locally important, we do not systematically treat interstratified clay mineral assemblages, or layered oxide hydroxides, or other phases (including amorphous phases) closely associated with phyllosilicate clay minerals (Table 3).

In spite of the official status of species listed in Table 2, ambiguous terminology complicates the study of clay minerals, which can be defined in terms of particle size, major-element chemistry, and/or structure. Natural "clay" samples are commonly complex mixtures of both layered phyllosilicates and other oxide-hydroxide phases, such as gibbsite [$Al(OH)_3$], brucite [$Mg(OH)_2$], allophane [$Al_2O_3(SiO_2)_{1.3\text{-}2.0}$•$2.5\text{-}3.0H_2O$], imogolite [$Al_2SiO_3(OH)_4$], and nanocrystalline iron oxide-hydroxides. Many clay minerals also lack the three-dimensional order of most mineral species, which complicates accurate description and understanding of their crystal structures. In addition, natural clay accumulations rarely display mono-mineralic properties. Complex solid solutions among multiple end-members and interstratification in fine-grained phyllosilicates make unambiguous identification of valid species difficult, whereas some oft-cited clay-type materials such as attapulgite, bauxite, bentonite, phengite, and steatite are not recognized as valid mineral species (Table 3). Furthermore, the nomenclature approved by the

Association Internationale pour l'Étude des Argiles (AIPEA; Guggenheim et al. 2006, 2007) for clay mineral groups and species is not entirely consistent with that of the IMA.

The Kaolin Group: The kaolin group includes the kaolinite, dickite, nacrite, and halloysite-7Å polymorphs of $Al_2Si_2O_5(OH)_4$, which are dioctahedral 1:1 clay minerals in which a single octahedral sheet is bonded to a single tetrahedral sheet to yield a ~7Å c-axis repeat (Keller 1970; Joussein et al. 2005). Halloysite [$Al_2Si_2O_5(OH)_4 \bullet nH_2O$; $0 < n < 2$] occurs as a solid-solution series between halloysite-7Å with $n = 0$ and halloysite-10Å with $n = 2$ (Bailey 1980; Guggenheim and Eggleton 1988; Joussein et al. 2005). Hisingerite [$(Fe^{3+})_2Si_2O_5(OH)_4 \cdot 2H_2O$] is the ferric iron isomorph of halloysite-10Å (Eggleton and Tilley 1998).

The Serpentine Group: Serpentine group minerals, including several species encompassed by the general formula [$(Mg,Ni^{2+},Fe^{2+},Mn^{2+},Zn,Fe^{3+},Al)_3(Al,Fe^{3+},Si)_2O_5(OH)_4$], are trioctahedral 1:1 layer phyllosilicates with a ~7-Å c-axis repeat. The serpentine group most often occurs in grain sizes larger than those of true clay minerals (i.e., > 2 μm). However, we include it here because of its close structural similarity to the dioctahedral kaolin group and because the serpentine group does include some clay-sized occurrences (including a very early clay-sized fraction in some altered chondrites from stage 2 of mineral evolution; Weaver 1989; Brearley and Jones 1998; Zega et al. 2003). The serpentine group includes at least 15 recognized mineral species, including several Mn, Ni, and Zn species that form in altered ore deposits (Table 2). Note, however, that (as with most clay mineral groups) many of these "species" exhibit complete solid solution among more than a dozen chemical elements and that strict species identification is often difficult.

146

147 ***The Talc and Pyrophyllite Groups:*** The trioctahedral 2:1 talc group, including talc
148 [$Mg_3Si_4O_{10}(OH)_2$] and several isomorphs, are clay minerals with the 10-Å mica-like tetrahedral
149 and octahedral layer arrangement, but without interlayer cations owing to their lack of a layer
150 charge. Pyrophyllite [$Al_2Si_4O_{10}(OH)_2$] is the dioctahedral 2:1 phyllosilicate with no layer charge.

151

152 ***The Smectite and Vermiculite Groups:*** Smectites and vermiculites are expandable 2:1 clay
153 minerals, containing variable amounts of interlayer cations and H_2O molecules (Bailey 1984;
154 Severman et al. 2004; Güven 2009). They include at least 11 IMA-approved species (Table 2),
155 including the important minerals montmorillonite [$(Na,K,½Ca)_{0.3}(Al,Mg)_2Si_4O_{10}(OH)_2•nH_2O$]
156 (the primary constituent of bentonite), beidellite [$(K,Na,½Ca)_{0.3}Al_2(Si,Al)_4O_{10}(OH)_2•nH_2O$], and
157 nontronite [$Na_{0.3}Fe^{3+}{}_2(Si,Al)_4O_{10}(OH)_2•nH_2O$]. These phases expand in the presence of water by
158 hydration of their interlayer cations, and their interlayer cations are readily exchangeable. The
159 weak interlayer bonding leads to poorly ordered crystals, and turbostratic stacking (Bailey 1984)
160 results in broad X-ray diffraction features that complicate identification. Both smectite- and
161 vermiculite-group minerals are generally so disordered that it is not possible to define a three-
162 dimensional crystal structure (Grim 1968; Mering 1975; Brindley 1980).

163

164 ***The Illite Group:*** Illite {$[K_{0.6}(H_3O)_{0.4}]Al_{1.3}Mg_{0.3}Fe^{2+}{}_{0.1}Si_{3.5}O_{10}(OH)_2•(H_2O)$} and glauconite
165 {$[K,Na,(H_3O)^+]_x(Mg,Fe^{2+},Al,Fe^{3+})_2(Al,Si)_4O_{10}(OH)_2·nH_2O$} are 10-Å dioctahedral, non-
166 expandable "hydrated micas" that can incorporate variable amounts of H_2O molecules with
167 interlayer cations, such as sodium and potassium. Illite is commonly found interstratified with
168 other clay minerals, most often with smectite. Note that the official IMA status of illite and

169 glauconite is pending, and phengite [$K(Mg,Al)_2(Si,Al)_4O_{10}(OH)_2$], which was once included in
170 this group, has been discredited as a distinct mineral species. Note, however, that "phengite" is
171 still commonly cited as a morphologically distinct metamorphic modification of illite.
172
173 ***The Chlorite Group:*** All species of the chlorite group, with general formula
174 [$(Li,Mg,Ni,Zn,Cr,Fe^{2+},Mn^{2+},Fe^{3+},Al)_{5\text{-}6}(Si,Al,Fe^{3+},B)_4O_{10}(OH)_8$], have a 14-Å 2:1:1 layer
175 structure; that is they have a 2:1 layer structure with an additional octahedral sheet in the
176 interlayer region. As a result, it is possible to have four structural variants of chlorites, with
177 either a di- or trioctahedral sheet in both the 2:1 layer and the interlayer octahedral sheet.
178 Trioctahedral ferromagnesian chlorite-group minerals, including clinochlore [$Mg_6Si_4O_{10}(OH)_8$]
179 and chamosite [$(Fe^{2+},Mg,Al,Fe^{3+})_6(Si,Al)_4O_{10}(OH,O)_8$], are the most common species and are
180 found in low-grade metamorphic rocks as alteration products of pyroxenes, amphiboles, biotite,
181 and garnet (Alt et al. 1995; Klein and Hurlbut 1999; Alt and Bach 2001).
182
183 ***The Palygorskite and Sepiolite Group:*** Palygorskite and sepiolite [ideally
184 $(Mg,Al)_2Si_4O_{10}(OH)\cdot 4H_2O$ and $Mg_4Si_6O_{15}(OH)_2\cdot 6H_2O$, respectively] are distinctive fibrous
185 chain-structured clay minerals that are relatively uncommon in nature (Bailey 1988a). Minerals
186 of these groups differ by incorporating two (in palygorskite) and three (in sepiolite) pyroxene-
187 like chains. The tetrahedral layers can be considered to be continuous, although they flip every
188 two or three chain widths.
189
190 ***Related "Clay-like" (Non-Phyllosilicate) Materials:*** Although not the main focus of this article,
191 a number of accessory non-phyllosilicate "clay-like" minerals are important in the context of

clay mineral evolution. The amorphous phases allophane, imogolite, and neotocite [$(Mn^{2+},Fe^{2+})SiO_3 \cdot H_2O$], all of which are found in soils associated with the weathering of volcanic ashes and glasses (Bates 1962; Dudas and Harward 1975; Su and Harsh 1998; Dubroeucq et al. 1998; Churchman 2000), possess disordered structures (Wada 1989). Gibbsite, which is commonly found in highly weathered environments such as laterites, and brucite, which occurs in altered or weathered ultramafic rocks and in serpentine-brucite-magnetite assemblages during serpentinization, are common layered hydroxides with ~4-Å layer thickness. These hydroxides are similar to the "octahedral sheet" components of phyllosilicates. Nanophase iron oxide-hydroxides, also commonly associated with clay mineral assemblages, are extremely redox sensitive and thus important in Earth's mineral evolution.

Different sheet arrangements, random stacking of interstratified hydroxide and phyllosilicate layers, variable chemical substitutions, variable hydration states, and numerous other defects complicate the description of natural clay minerals and clay assemblages and often blur a precise formal definition of what constitutes a clay mineral species. In particular, interstratified clays, for example illite/smectite, are ubiquitous in diagenetic sequences in pelitic rocks and are often found in soils and regoliths. In addition, soil smectites also commonly contain partially developed hydroxide interlayers, essentially forming material intermediate between smectite and chlorite.

CLAY MINERAL EVOLUTION

Hazen et al. (2008) described three eras of Earth's mineral evolution, further divided into ten partly overlapping stages (Table 1). The first era of planetary accretion is represented by approximately 60 primary condensate minerals identified in primitive chondrite meteorites (stage 1), and the much more diverse suite of minerals produced by alteration and differentiation in achondrites and other meteorites (stage 2).

The second era of crust and mantle reworking is represented by three stages of mineral evolution. For the purposes of clay mineral evolution, we define stage 3 as the earliest part of the Hadean Eon following Earth's differentiation at ~4.5 Ga—a time characterized by the formation and alteration of an ultramafic and basaltic lithospheric veneer, as well as the first (presumably shallow) hydrosphere. Stage 4, which may also have begun during the Hadean Eon, commenced with the production of granitoids and associated pegmatites by partial melting of stage-3 basalts, as well as by other granitization mechanisms. Stage 5 saw the activation of large-scale plate tectonic processes and fluid-rock interactions associated with subduction, convergent margin orogenesis, and exposure of deep metamorphic terrains. Note that the timings of stages 4 and 5 remain matters of considerable debate. Therefore, for the purposes of this review (and unlike the chronology suggested in Hazen et al. 2008) we do not assign specific time intervals to the earliest occurrences of granite formation and subduction.

The third era of Earth's mineral evolution focuses on the co-evolution of the geo- and biospheres. Prior to ~2.5 Ga microbial activity altered Earth's surface in an anoxic environment (stage 6). The Great Oxidation Event (~2.4 to 2.2 Ga; stage 7) triggered the greatest episode of mineral diversification. The subsequent billion-year interval, an intriguing time known as the "intermediate ocean" (Anbar and Knoll 2002; stage 8), saw no obvious new modes of mineral

234 paragenesis, though additional focus is needed on the apparent mineralogical diversification of
235 this time period associated with the assembly of the Rodinian supercontinent (Grew and Hazen
236 2009, 2010a, 2013; Hazen et al. 2012). Snowball Earth episodes of global glaciation (stage 9)
237 served as preludes for increased atmospheric oxidation and the modern period of
238 biomineralization (stage 10). In this section we explore how each of these three eras and ten
239 stages of mineral evolution are characterized in terms of the diversity, distributions, and
240 environments of clay minerals.

241 The key to understanding the evolution of clay minerals lies in their varied modes of
242 paragenesis. Clay minerals found at or near Earth's surface commonly arise from five partly
243 overlapping processes, each of which was initiated at a different stage of Earth's mineral
244 evolution (Table 1), and each of which introduced new clay species and rates of clay mineral
245 production.

246 *(1) Aqueous alteration:* Aqueous alteration, including hydrothermal alteration and
247 serpentinization, of pre-existing minerals has been an important clay-forming process since
248 before Earth's accretion. Aqueous alteration within planetesimals produced the first minor
249 quantities of clay minerals (stage 2). Subsequently, serpentinization of basalt and other mafic
250 igneous lithologies (stage 3), coupled with seawater-basalt interactions, were the first
251 volumetrically significant engine of clay mineralization. Aqueous alteration of diverse igneous,
252 sedimentary, and metamorphic lithologies has remained an important paragenetic mode for clay
253 minerals throughout Earth history and is active today.

254 *(2) Authigenesis:* Direct precipitation of authigenic clays, especially from solution in marine
255 sediments, alkaline lakes, and restricted marine environments [but also possibly from higher
256 temperature magmatic fluids (Meunier et al. 2012)], represents a second, although volumetrically

less important, mode of clay mineral paragenesis. Such a mechanism may have occurred on a significant scale early in Earth's history, as sediments accumulated on the basaltic floor of the Hadean ocean. This accumulation of thick clay mineral-bearing marine sediments may have preceded the formation and erosion of the first granitic protocontinents (stage 4).

(3) Diagenesis: Clay minerals commonly form during diagenesis in sedimentary basins and during low-grade metamorphism (to greenschist facies) of varied lithologies, often including alteration of pre-existing clay minerals. Such clay-forming processes undoubtedly have operated since early in Earth's history. However, the surface manifestation of initially deep metamorphic terrains and the large-scale production of metamorphic clay minerals were probably not significant prior to the advent of plate tectonics (stage 5) and the exposure of deep crustal rocks through orogenesis. However, the detection of clay minerals associated with large ancient impact craters on Mars suggests that impact events may have played an important role in generating localized hydrothermal systems and excavating deep crustal rocks (Mustard et al. 2008; Carter et al. 2010; Ehlmann et al. 2011), and the same may have been true for early Earth (Pirajno 2009).

(4) Terrestrial weathering: Near-surface terrestrial weathering reactions are an important mode of clay mineral formation. Weathering must have produced minor amounts of clay minerals on early Earth, notably in the acidic environments of active volcanoes (stage 3) and on the earliest anoxic protocontinents (stage 4). However, production of clay minerals through oxidative weathering was not a significant factor until the Great Oxidation Event (stage 7), which not only saw the dramatically increased production of near-surface terrestrial clays, but also likely resulted in several new species of ferric iron clay minerals and extensive formation of lateritic soils.

279 *(5) Biomediated clay mineralization:* The rise of a terrestrial biosphere, most notably the
280 advent of soil-forming microbes, fungi, and plants (stage 10), marked a dramatic transition in the
281 diversity and rate of clay mineral production. Biological weathering in the Phanerozoic Eon may
282 have increased the rate of terrestrial clay production by an order of magnitude (e.g., Ueshima and
283 Tazaki 1998; Kim et al. 2004; Tazaki 2005), and it is likely that the compositional ranges, and
284 possibly some specific clay mineral species formed as products of biological weathering, were
285 distinct from those previously formed abiotically (e.g., Shelobolina et al. 2003; Stucki and
286 Kostka 2006; Dong 2012).
287
288 ***Stage 1—Pre-accretionary Processes (4.56 Ga):*** About a dozen different micro- and nanoscale
289 refractory "ur-minerals" have been identified in presolar grains (Brearley and Jones 1998; Nittler
290 2003; Table 2a in Hazen et al. 2008). Gravitational clumping of nebular material, primarily H,
291 He, small molecular species, and presolar dust, led to star formation and the resultant heating of
292 the protoplanetary disk. This heating produced the primary refractory constituents of chondritic
293 meteorites with their approximately 60 different known mineral phases (stage 1; Table 2b-e in
294 Hazen et al. 2008). All minerals from these earliest stages of mineral diversification are high-
295 temperature condensates and thus clay minerals are unlikely to have formed during (or prior to)
296 these earliest pre-accretionary events in Earth's mineralogical history.
297
298 ***Stage 2—Post-accretionary Processes (4.56-4.55 Ga):*** As chondritic material accumulated
299 through gravitational clumping into planetesimals, core-mantle differentiation and progressive
300 aqueous, thermal, and shock alteration led to the ~250 different minerals that have been
301 identified in meteorite samples (Brearley and Jones 1998; Krot et al. 2006; Brearley 2006;

MacPherson 2004). Low-temperature (<100 °C) aqueous alteration of preexisting condensates produced the earliest known clay minerals, which are now found in a variety of meteorites (Tables 1 and 2). Almost all types of carbonaceous chondrites, including CI, CM, CO, CV, and CR chondrites, experienced secondary aqueous alteration that produced clay minerals (Brearley and Jones 1998).

The matrices of many primitive CI chondrites are dominated (>50 to 60 %) by clay minerals, including Mg-Fe serpentine-group minerals and saponite $[(Ca,Na)_{0.3}(Mg,Fe^{2+})_3(Si,Al)_4O_{10}(OH)_2 \bullet 4H_2O]$, with minor chlorite (Brearley and Prinz 1992). The Mg-Fe serpentine-group minerals cronstedtite $[(Fe^{2+}{}_2Fe^{3+})_3(Si,Fe^{3+})_2O_5(OH)_4]$, chrysotile $[Mg_3Si_2O_5(OH)_4]$, and greenalite $[(Fe^{2+},Fe^{3+})_{2-3}Si_2O_5(OH)_4]$ and berthierine-group minerals also comprise a significant fraction of the matrix in CM chondrites, with reports of the smectite-group mineral saponite, as well (Brearley and Jones 1998; Zega et al. 2003). Saponite is also a common constituent of the altered matrix of CV and CR chondrites, and secondary alteration of Ca-Al inclusions (CAIs) in CV-type chondrites results in montmorillonite and possibly serpentine and saponite (Tomeoka and Buseck 1990). Clay mineral production may have been accelerated in the presence of oxalate and other polar organic molecules found in carbonaceous meteorites (Schumann et al. 2012).

In addition to clay minerals formed during aqueous alteration of chondrite meteorites, interplanetary dust particles also display a range of clay minerals formed by secondary alteration of ferromagnesian silicates (Reitmeijer 1998). Thus, at least 9 Mg- and/or Fe-bearing clay mineral species, most of them serpentines and smectites, were produced in the solar nebula, principally by aqueous alteration contemporaneously with Earth's accretion, and they are recorded from stage 2 (Table 1). Note that Reitmeijer et al. (2006) also propose that some clay-

bearing assemblages might form under metastable eutectic conditions, whereas Meunier et al. (2012) invoke "magmatic precipitation" of clay minerals. However, other modes of clay mineral paragenesis, including authigenic formation in sediments, surface weathering and oxidation, or biologically mediated mineralization, would not have occurred during stage 2.

Stage 3—Earliest Hadean Earth (<4.55 Ga): Stage 3 of Earth's mineral evolution was dominated by the production and subsequent alteration of near-surface ultramafic and mafic rocks. Igneous processes, including volcanism and degassing, fractional crystallization, crystal settling, and assimilation reactions, led to the familiar Bowen's reaction series (Bowen 1928). On volatile-poor (i.e., essentially anhydrous in their near-surface environments) terrestrial bodies such as Mercury and the Moon, which likely only progressed through stage 3 of mineral evolution, clay minerals cannot represent volumetrically significant phases. [A possible exception might occur in hydrothermal zones beneath the shaded margins of ice-filled craters near the poles of these bodies (Lawrence et al. 2013).] However, on volatile-rich bodies such as Earth and Mars, as many as 420 mineral phases, including a potential suite of 25 clay minerals (Tables 1 and 2), may have been present in the near-surface environment from the earliest period, primarily as a result of aqueous alteration and low-temperature metamorphism of ultramafic and mafic lithologies (Hazen 2013). We estimate that 16 of these clay minerals appeared for the first time in Stage 3 (Tables 1 and 2). Several clay minerals with presumed similar parageneses have now been detected in the ancient crust of Mars, which is thought to have formed during this time period.

This mineralogical diversification on Earth was halted when the crust and outer mantle were violently disrupted and melted by the Moon-forming impact event at ~4.55 Ga (Tonks and

Melosh 1993; Ruzicka et al. 1999; Touboul et al. 2007). Immediately following that catastrophic event, Earth's near-surface mineralogy was reset as a consequence of igneous rock crystallization. Intense volcanism and associated mantle outgassing rapidly produced a water-rich near-surface environment, with globe-spanning shallow oceans probably forming prior to 4.4 Ga (Wilde et al. 2001). Aqueous low-temperature reactions, surface weathering, and hydrothermal alteration of the ultramafic and basaltic crust may have resulted in the extensive production of trioctahedral ferromagnesian clay minerals.

Earth's earliest rocks, including komatiities, peridotites, basalts, and other ultramafic and mafic volcanics (Arndt and Nisbet 1982; Rollinson 2007; Papineau 2010), were dominated by the Mg-Fe silicates olivine [$(Mg,Fe)_2SiO_4$], orthopyroxene [$(Mg,Fe)SiO_3$], and clinopyroxene [$(Mg,Fe,Ca)SiO_3$]. Hydrothermal alteration of these ferromagnesian minerals was initiated by the high solubility of Mg. Indeed, primary olivine and pyroxene are often completely altered, making it difficult to determine the initial compositions of some ancient ultramafic rocks. Mg-Fe silicates typically alter via serpentinization reactions (Schrenk et al. 2013) to trioctahedral ferromagnesian clays, including serpentine, talc, and chlorite, which were thus Earth's first volumetrically significant clay minerals. Typical clay-forming alteration reactions of olivine and pyroxenes (Deer et al. 1962; Harder 1976; Fontanaud and Meunier 1983; Newman 1987; Nozaka et al. 2008) include:

$$2(CaMg)Si_2O_6 + 2H^+ \rightarrow Mg_3Si_4O_{10}(OH)_2 + Ca^{2+}_{aq}$$
clinopyroxene talc

$$Mg_2SiO_4 + MgSiO_3 + 2H_2O \rightarrow Mg_3Si_2O_5(OH)_4$$
forsterite enstatite serpentine

$$2Mg_2SiO_4 + 3H_2O \rightarrow Mg_3Si_2O_5(OH)_4 + Mg(OH)_2$$
forsterite serpentine brucite

$$2Mg_2SiO_4 + 2H^+ \rightarrow Mg_3Si_2O_5(OH)_4 + Mg^{2+} + H_2O$$

forsterite serpentine

$$6MgSiO_3 + 3H_2O \rightarrow Mg_3Si_2O_5(OH)_4 + Mg_3Si_4O_{10}(OH)_2$$

enstatite serpentine talc

In addition to serpentinization reactions, interactions between basalt and seawater that lead to seafloor basalt weathering have been a major source of clay minerals throughout Earth history, as well as a significant source of dissolved ionic species in seawater (Scarfe and Smith 1977; Hajash and Archer 1980; Papavassiliou and Cosgrove 1981; Seyfried and Mottl 1982; Thompson 1983; Daughney et al. 2004). Weathering products commonly include dioctahedral and trioctahedral smectites, as well as poorly ordered smectite-chlorite mixed layerings.

Aqueous alteration of ferromagnesian minerals is often characterized by a sequence of clay minerals with decreasing Mg/Si; for example, olivine may be first serpentinized to antigorite, chrysotile, and lizardite [all forms of $Mg_3Si_2O_5(OH)_4$] and later be replaced by other clay minerals, including vermiculite [$Mg_{0.7}(Mg,Fe^{3+},Al)_6(Si,Al)_8O_{20}(OH)_4 \bullet 8H_2O$], mixed-layer saponite-talc, and saponite (Velde 1985; Alt and Bach 2001; Blackman et al. 2006; Caillaud et al. 2006; Nozaka et al. 2008). Note that serpentinization is a significantly exothermic process for compositions more Mg-rich than Fo25 (Oze and Sharma 2006). Consequently, extensive Hadean clay mineralization likely represented a significant component of near-surface heat flow.

Ultramafic and mafic lithologies are also characterized by primary Ca and Al silicates, including amphiboles and plagioclase feldspars, which are subject to deep-sea weathering. The amphiboles tremolite [$\square\, Ca_2Mg_5Si_8O_{22}(OH)_2$], actinolite [$Ca_2(Mg,Fe^{2+})_5Si_8O_{22}(OH)_2$], and magnesiohornblende [$\square Ca_2[Mg_4(Al,Fe^{3+})]Si_7AlO_{22}(OH)_2$] commonly alter to clay minerals (Jayananda et al. 2008). Proust et al. (2006) observed that alteration of calcic amphibole produced a sequence of four clay minerals as a function of crystallization sites in a single amphibole crystal: (1) saponite; (2) montmorillonite; (3) interstratified kaolinite/smectite; and (4)

halloysite. Thus, deposits with multiple coexisting clay mineral species can result from alteration of a single progenitor. Similarly, Garvie and Metcalfe (1997) report a vein occurrence of co-existing talc, saponite, and corrensite [$(Ca,Na,K)_{1-x}(Mg,Fe,Al)_9(Si,Al)_8O_{20}(OH)_{10}\cdot nH_2O$], and Stakes and O'Neil (1982) found coexisting actinolite, smectite, vermiculite, talc, chlorite, saponite, and chlorite-smectite.

In addition to extensive serpentinization, diagenetic clay-forming processes may have been significant at this stage. The ocean floors, covered by fresh basalt with minimal sediment overburden and relatively high heat flow, would have facilitated diagenetic production of saponite and perhaps nontronite. However, given the likely localized and volumetrically minimal deposits of Hadean marine sediments, the production of non-aluminous authigenic clay minerals may have been restricted. Anoxic, CO_2-rich surface weathering of volcanic islands that rose above the global Hadean ocean, with possible associated production of montmorillonite, saponite, and sepiolite, would have been similarly localized and volumetrically minor. Note also that in the absence of extensive felsic granitic lithologies (i.e., stage 4), Fe-Mg trioctahedral clay minerals would have volumetrically exceeded Al-Fe^{3+} dioctahedral clay minerals in anoxic environments.

The presence of an anoxic near-surface environment during stage 3 would have affected the redox state of clay minerals. Ferrous iron would have dominated ferric iron, thereby further exaggerating the dominance of trioctahedral versus dioctahedral clay species. Thus, saponite is likely to have been far more abundant than vermiculite, and ferripyrophyllite [$Fe^{3+}{}_2Si_4O_{10}(OH)_2$], nontronite, and other predominantly ferric iron clay minerals may not have formed at all. Furthemore, unaltered serpentines, smectites, and chlorites from stage 3 are likely to differ systematically in their transition metal chemistry from more recent samples in both major and

minor elements. These distinctive characteristics of Hadean clays are potentially significant for origins-of-life scenarios, as smectites have long been invoked as catalysts for biosynthesis (Schoonen et al. 2004; Meunier et al. 2010), as templates for biomolecular assembly (Ferris and Ertem 1992; Ertem and Ferris 1997; Hanczyc et al. 2003; Chen et al. 2004; Deamer 2011), and even as possible self-replicating proto-life (Cairns-Smith 1968, 2005; Cairns-Smith and Hartman 1986).

Impact processes: An as yet little studied mechanism of clay mineral formation—one that played a significant mineralogical role only in the Hadean Eon—is hydrothermal activity associated with marginal zones of large impacts (Pirajno 2009; Hazen 2013). An estimated 20,000 meteor impacts of objects > 1 km diameter, with many impactors >10 km, altered Earth's near-surface mineralogy during the Hadean Eon (Glickson 1998). Each impact initially melted or vaporized surface phases within a radius significantly greater than that of the impactor, but such events also diversified Earth's mineralogy in three ways—the production of shock minerals, the excavation of high-pressure and temperature lithologies, and the generation of fracture zones with deep circumferential hydrothermal systems possibly lasting for > 10^5 years along crater margins (Abramov and Kring 2005; Versh et al. 2006; Pirajno 2009; Hazen 2013). A significant effect of impact hydrothermal alteration was thus production of clay minerals (Allen et al. 1982; Pirajno 2005).

Stage 4—Granitization (timing uncertain; >3.5 Ga): The fourth stage of Earth's mineral evolution was characterized by extensive partial melting of basalt, the consequent production of extensive intrusive granitoid suites, and ultimately the formation of granitic protocontinents.

While the exact timing of granite formation remains uncertain, we suggest that granite production by partial melting of basalt (stage 4) likely precedes plate tectonics (stage 5) on any terrestrial planet, and that granite formation is likely to occur on some planets that are too small too initiate plate tectonics. All of the aqueous alteration processes of mafic lithologies observed in stage 3 would have continued to operate throughout stage 4. Production of trioctahedral ferromagnesian clay minerals, for example via serpentinization and seawater-basalt interactions, would continue throughout Earth history as major clay-forming mechanisms (albeit at a gradually decreasing rate, depending on exposure of basaltic crust to fluids and heat flow). However, as many as four modes of clay mineral paragenesis must have occurred significantly for the first time as a result of the emergence of granitic protocontinents: Al-silicate alteration, anoxic surface weathering, clay authigenesis, and formation of rare complex pegmatite clay minerals.

Al-silicate alteration: First, and most significantly for stage 4 clay paragenesis, aqueous and hydrothermal processes altered extensive deposits of feldspars, feldspathoids, micas, and other Al-bearing minerals. Note that many of the common Al-bearing clay minerals probably occurred to a limited extent in stage 3 (Tables 1 and 2), but alteration of granite must have led to the first volumetrically significant production of a number of dioctahedral aluminous clay minerals, including kaolinite and its polymorphs (dickite, nacrite, and halloysite), aluminous smectites, vermiculite, and possibly pyrophyllite.

Numerous studies describe the aqueous and hydrothermal alteration of common rock-forming micas, most notably dioctahedral muscovite [$KAl_2(Si_3Al)O_{10}(OH)_2$] and the trioctahedral biotite group [$K(Mg,Fe^{2+})_3(Al,Fe^{3+})Si_3O_{10}(F,OH)_2$]. Stoch and Sikora (1976), for example, described

471 the alteration of biotite, muscovite, and secondary illite directly to kaolinite—a process reflected
472 in the common occurrence of muscovite books containing interlayers of kaolinite. Indeed, many
473 large deposits of kaolinite throughout the world contain remnant muscovite that served as the
474 source for much of the kaolinite (e.g., the Georgia kaolin deposits: Jonas 1964). Where alteration
475 was more gradual, micas may display the following characteristic reaction pathway (Weaver
476 1989):

477 muscovite → muscovite/smectite or muscovite/vermiculite → smectite → kaolinite

478 In related studies, Meunier and Velde (1979) and Velde and Weir (1979) observed that altered
479 granite hosts illite along grain boundaries between muscovite and alkali feldspar, and micas and
480 K-feldspar ($KAlSi_3O_8$) also alter to vermiculite and beidellite. Kaolinite and Fe oxides can occur
481 in fractured granites that experience relatively high water flow and, with time, granite may alter
482 almost entirely to kaolinite and oxides, but it may also transform into other phases such as
483 halloysite and gibbsite, depending on environmental conditions (Weaver 1989).

484 These studies thus indicate that a complex interplay of chemical and physical factors,
485 including temperature, aqueous fluid composition (including activity ratios of cations to H^+),
486 water/rock ratio, and fluid flow rates, is required to explain the varied modes of clay mineral
487 paragenesis from alteration of Al silicate minerals. Temperature, in particular, plays an important
488 role in the hydrothermal alteration of granite. Velde (1985) recognized four types of
489 hydrothermal alteration of granite: potassic, phyllic, argillic, and propylitic, each of which results
490 in different clay-bearing mineral assemblages that reflect different formation temperatures
491 (Lowell and Guilbert 1970; McDowell and Elders 1980). Potassic alteration produces new K-
492 feldspar and Mg-Al-bioite (i.e., with Mg and Al greater than in typical magmatic biotite: Moore
493 and Czamanske 1973; Beane 1974; Jacobs and Parry 1976). Phyllic alteration produces sericite,

494 whereas argillic alteration is notable for producing illite and mixed-layer clay minerals such as
495 rectorite [$(Na,Ca)Al_4(Si,Al)_8O_{20}(OH)_4 \cdot 2H_2O$; a 1:1 ordered interstratification of illite and
496 smectite] that may occur with kaolinite (Velde 1985). Finally, propylitic alteration is
497 characterized by a pairing of chlorite and epidote [$Ca_2Fe^{3+}Al_2(Si_2O_7)(SiO_4)O(OH)$]—an
498 assemblage suggesting formation temperatures of ~200°C (McDowell and Elders 1980).

499 Fluid pH also affects the observed clay mineral assemblage. Neutral to mildly acid conditions
500 commonly result in allophane, kaolinite, or halloysite, and kaolinite has been identified as a
501 surface coating on weathered feldspars, often armoring the remaining feldspar crystal. As cation
502 to H^+ activity ratios increase, which could correspond to pH increase, other minerals such as
503 smectites form in the presence of cations such as K, Na, and Mg (Weaver 1989). Under strongly
504 leached conditions, all species but Al are removed at moderate pH, resulting in precipitation of
505 aluminum hydroxides, such as boehmite and diaspore [both AlO(OH)], and gibbsite, and
506 ultimately the formation of bauxite (Wollast 1967; Weaver 1989). It should be noted that the
507 existence of Paleoarchean or Mesoarchean bauxite deposits is by no means certain. If extensive
508 granitic protocontinents formed by ~3.5 Ga, then development of such Al-rich clay horizons and
509 bauxite is plausible. However, paleobauxites older than the Paleozoic Era are rare (Adusumalli
510 and Schubert 2001).

511 Finally, the flow rate of the aqueous fluid (or water-to-rock ratio) strongly influences feldspar
512 alteration and clay mineral formation: At low or stagnant flow rates, for example,
513 montmorillonite (or illite) forms, whereas kaolinite and gibbsite form at successively higher flow
514 rates, reflecting progressively increased Al/Si in the mineral phase (Berner 1971; Weaver 1989):
515 Stagnant or very low flow rate:
516
517 $$3NaAlSi_3O_8 + Mg^{2+} + 4H_2O \rightarrow 2Na_{0.5}Al_{1.5}Mg_{0.5}Si_4O_{10}(OH)_2 + 2Na^+ + H_4SiO_{4aq}$$
518 albite montmorillonite

519
520 Moderate flow rate:
521
522 $2NaAlSi_3O_8 + 2H^+ + 9H_2O \rightarrow Al_2Si_2O_5(OH)_4 + 2Na^+ + 4H_4SiO_{4aq}$
523 albite kaolinite
524
525 High flow rate:
526
527 $NaAlSi_3O_8 + H^+ + 7H_2O \rightarrow Al(OH)_3 + Na^+ + 3H_4SiO_{4aq}$
528 albite gibbsite
529
530 Thus, high flow-rates and/or water-rock ratios favor more aluminous mineral assemblages.

531

532 *Anoxic surface weathering:* Surface weathering in the absence of molecular oxygen, which
533 represents a second new mode of clay mineral paragenesis associated with growing granitic
534 continents, increased opportunities for soil formation with both di- and trioctahedral Mg-Fe-Al
535 clay minerals, including possibly illite, sepiolite, vermiculite, and kaolinite. Of special
536 importance was subaerial or near-surface alteration of silicic volcanic tuff, which may have led
537 to extensive deposits of montmorillonite-rich bentonites (Caballero et al. 1985; Linares 1985,
538 1987; Christidis and Huff 2009). Montmorillonite, beidellite, and nontronite, the most common
539 dioctahedral smectites, are also found in hydrothermally altered volcanic and igneous rocks
540 (Bischoff 1972; Murnane and Clague 1983; Thompson et al. 1985; Singer and Stoffers 1987; Alt
541 1988; Hekinian et al. 1993). Montmorillonite and related smectites have been invoked in several
542 prominent theories of life's origins (e.g., Cairns-Smith and Hartman 1986; Ferris and Ertem
543 1992; Ertem and Ferris 1997; Meunier et al. 2010), though other clay mineral species may be
544 equally well suited for prebiotic chemistry. Clay mineral diversification is significant, therefore,
545 because a planet may have to progress through at least this stage of mineral evolution as a
546 prerequisite for life.
547

548 *Clay authigenesis:* A third mechanism of clay mineral formation that likely arose in stage 4 is
549 authigenesis of dioctahedral clays. The erosion of granitic continents led to the first significant
550 marine Al-rich sedimentary deposits, where detrital clay minerals from the subaerial crust would
551 have augmented authigenic clay mineral formation. Illite, illite/smectite, bertherine, Al-bearing
552 chlorite, and dickite are all possible authigenic clays from stage 4. In addition, we suggest that
553 the rare aluminous phyllosilicate clay mineral donbassite [$Al_2(Si_3Al)O_{10}(OH)_2{\cdot}Al_{2.33}(OH)_6$],
554 which forms by authigenesis in Al-rich sediments, may have appeared for the first time in stage
555 4.
556
557 *Complex pegmatite clay minerals:* Yet another consequence of granitization, albeit a gradual
558 one that may have taken a billion years of fluid-rock interaction, was the formation of complex
559 pegmatites and their associated suites of the minerals of Li, Be, B, and other incompatible
560 elements (London 2008; Grew and Hazen 2009, 2010a, 2013; Bradley 2011; Tkachev 2011).
561 Complex pegmatites are known to host five unusual clay minerals that arise from hydrothermal
562 alteration of primary pegmatite minerals, all of which probably appeared for the first time in
563 stage 4 (Tables 1 and 2). For example, swinefordite
564 [$Ca_{0.2}(Li,Al,Mg,Fe)_3(Si,Al)_4O_{10}(OH,F)_2{\bullet}nH_2O$] is a dioctahedral Li-rich smectite that forms by
565 alteration of the lithium clinopyroxene spodumene ($LiAlSi_2O_6$). Similarly, the serpentine-group
566 mineral manandonite [$Li_2Al_4(Si_2AlB)O_{10}(OH)_8$], and the chlorite-group minerals cookeite
567 [$(Al,Li)_3Al_2(Si,Al)_4O_{10}(OH)_8$] and borocookeite [$LiAl_4(Si_3B)O_{10}(OH)_8$], are rare clay minerals
568 that form from alteration of tourmaline-group minerals and/or Li-bearing mica ("lepidolite"). In
569 addition, yofortierite [$Mn^{2+}{}_5Si_8O_{20}(OH)_2{\bullet}8\text{-}9H_2O$] is found exclusively in sodalite-nepheline
570 syentite pegmatites enriched in Mn. Other clay minerals formed from weathering of complex

pegmatites, although not new species, may display unusual minor-element compositions. The rare Cs-bearing muscovite "nampingite", for example, weathers to a Cs-bearing illite or smectite. Such Cs-rich clay minerals are very rare in nature but are easily produced by cation-exchange experiments in the laboratory.

Stage 5—Plate Tectonics (timing uncertain; >3.0 Ga): Stage 5 marked the beginning of plate tectonics on Earth—a time that initiated sediment recycling into the mantle at subduction zones (e.g., Koster van Groos 1988) and significantly increased the scale of fluid-rock interactions in the overlying upper mantle and crust. Unfortunately, the minimal rock record prior to 3.5 Ga obscures the chronology of early subduction, orogenic processes, the formation of the cratons, and the assembly of the first continents. The transition from plume–dominated to modern-style plate tectonics for the first time resulted in the orderly accretion of granitic terrains into continents. However, major unresolved questions relate to the timing and rate of continent formation. Estimates range from essentially modern continental coverage by the end of the Hadean Eon at ~4 Ga, to continued continental growth into the late Archean Eon at < 3 Ga (Condie 1989; Rogers and Santosh 2004; Harrison et al. 2005; Smithies et al. 2005a, b; Stern 2005; Witze 2006; Dewey 2007; Groves and Bierlein 2007; Rollinson 2007; Condie and Pease 2008; Van Kranendonk 2011; Cawood et al. 2013; Nance et al. 2013). Similar uncertainties apply to the nature and extent of soils in the Archean Eon. While most land surface prior to the evolution of the terrestrial biosphere was subject to denudation by rainfall and runoff, at what point in Earth history would significant mud deposits have accumulated in terrestrial depressions?

All of the previously mentioned modes of clay mineral paragenesis operated throughout the

initiation of plate tectonics. Aqueous and hydrothermal alteration of a wide range of ultramafic to acidic lithologies produced abundant trioctahedral (Mg-Fe^{2+}) and dioctahedral (Al) clays in the shallow oceanic and continental crust. Growing marine sediment deposits were the loci of authigenic clay formation, whereas anoxic protocontinent weathering may have produced clay-rich terrestrial sedimentary deposits in lakes and valleys.

Plate tectonics also resulted in orogenic processes associated with convergent margins, which exposed significant expanses of deep metamorphic lithologies for the first time. Greenschist facies metamorphic rocks rich in clinochlore, chamosite, and other chlorite-group minerals thus were added to the near-surface environment. In particular, metamorphic Mn- and Ni-chlorites, pennantite [$(Mn^{2+},Al)_6(Si,Al)_4O_{10}(OH)_8$] and nimite [$(Ni,Mg,Al)_6(Si,Al)_4O_{10}(OH)_8$], appeared during stage 5 as a result of the metamorphism and subsequent uplift of Mn and Ni deposits. Thus, whatever the timing, tectonic activity and its associated alteration of near-surface mineralogy, metamorphism, and an increased volume of the crust affected by hydrothermal activity could have increased the number of mineral phases to ~1500, including 37 of the 56 phyllosilicate clay mineral species listed in Tables 1 and 2, prior to the biological innovations of stage 6.

Stage 6—The Anoxic Microbial World (3.9-2.4 Ga): Biological processes began to affect Earth's surface mineralogy by the Eoarchean (~3.9 to 3.6 Ga), when large-scale surface mineral deposits were precipitated under the influences of changing atmospheric and ocean chemistry (e.g., Hazen et al. 2008, 2009). There is no evidence for a significant terrestrial biota at this time, nor were marine microbial populations sufficiently diverse or widespread to have had a major impact on clay mineral formation.

It is likely that all modes of clay mineral paragenesis observed in stages 2 through 5 (i.e., aqueous and hydrothermal alteration, authigenic formation in sediments, anoxic surface weathering, and low- to moderate-grade metamorphic formations exposed by tectonic processes) were active throughout stage 6. One possible mineralogical novelty associated with early life may have been the local production of clay minerals with increased Fe^{3+}/Fe^{2+}, perhaps in zones associated with biologically mediated ferrihydrite [$Fe^{3+}_{4\text{-}5}(OH,O)_{12}$] and banded iron formations (Konhauser et al. 2005; Kendall et al. 2012). Thus, greenalite and minnesotaite [$(Fe^{2+})_3Si_4O_{10}(OH)_2$] may have occurred for the first time. However, it is also likely that anoxic zones hosted populations of iron-reducing microbes, which are known to alter dioctahedral smectite, illite, and chlorite (Dong et al. 2009).

In addition, clay minerals that form through alteration of carbonate-rich zones, including skarn minerals, may also have increased significantly as a consequence of biologically precipitated carbonate platforms. Thus, stage 6 may have seen enhanced production of antigorite and kellyite [$(Mn^{2+},Mg,Al)_3(Si,Al)_2O_5(OH)_4$] (Table 2).

Stage 7—The Great Oxidation Event (2.4-2.2 Ga): The Paleoproterozoic "Great Oxidation Event" (GOE), when atmospheric oxygen may have risen to >1% of modern levels, initiated a remarkable, if prolonged, diversification of Earth's near-surface mineralogy as a consequence of oxidative weathering. Hazen et al. (2008, 2009) estimated that more than 2500 new minerals appeared for the first time after the stabilization of high oxidation states of Fe, Ni, Mn, Cu, Hg, Mo, U, and other redox-sensitive elements. Biochemical processes may thus be responsible, directly or indirectly, for the majority of Earth's > 4,700 known mineral species.

Stage 7 of Earth's mineral evolution likely saw the first appearance, or at least the first

volumetrically significant formation, of at least 13 phyllosilicate clay minerals (Tables 1 and 2). Most of these new phases are ferric iron clay minerals, such as the halloysite isomorph hisingerite, which forms by oxidative weathering of Fe silicates (including Fe-smectites) or sulfides (Kohyama and Sudo 1975); the serpentine group-minerals cronstedtite $[(Fe^{2+}_2Fe^{3+})_3(Si,Fe^{3+})_2O_5(OH)_4]$ and odinite $[(Fe^{3+},Mg,Al,Fe^{2+})_{2.5}(Si,Al)_2O_5(OH)_4]$; the sepiolite/palygorskite-group mineral tuperssuatsiaite $[NaFe^{3+}_3Si_8O_{20}(OH)_2 \bullet 4H_2O]$; the smectite-group mineral nontronite; the Fe^{3+} isomorph of pyrophyllite, ferripyrophyllite, which forms both by hydrothermal alteration in oxic environments and by precipitation from hot and highly saline solutions (Badaut et al. 1992); and glauconite. Glauconite forms in marine sediments, commonly on continental shelfs in proximity to organic matter, which provides a reductive local environment. Glauconite formation is often microbially mediated and is controlled by diffusion of K from seawater and Fe^{2+} from iron minerals (Odin 1988; Meunier and El Albani 2007). Glauconite may also form from biotite by marine diagenesis in shallow water under reducing conditions.

A number of clay minerals are known only from the oxidized weathering zones of ore bodies and thus also likely postdate the Great Oxidation Event. Examples include the serpentine-group minerals brindleyite $[(Ni,Al)_3(Si,Al)_2O_5(OH)_4]$ and fraipontite $[(Zn,Al)_3(Si,Al)_2O_5(OH)_4]$; the smectite-group minerals sauconite $[Na_{0.3}Zn_3(Si,Al)_4O_{10}(OH)_2 \cdot 4H_2O]$, zincsilite $[Zn_3(Si,Al)_4O_{10}(OH)_2 \cdot 4H_2O]$, and yakhontovite $[(Ca,Na,K)_{0.2}(Cu,Fe,Mg)_2Si_4O_{10}(OH)_2.3H_2O]$; and the chlorite-group minerals gonyerite $[Mn^{2+}_5Fe^{3+}(Si_3Fe^{3+})O_{10}(OH)_8]$ and baileychlore $[(Zn,Fe^{2+},Al,Mg)_6(Si,Al)_4O_{10}(OH)_8]$.

The GOE also must have resulted in expanded compositional ranges of numerous other clay minerals as Fe^{3+} increasingly occupied both octahedral and tetrahedral sites, with a

corresponding shift to additional dioctahedral clay mineral phases. For example, ferric iron-rich varieties of vermiculite would have arisen during the oxidative weathering of stage 7 (Velde 1985). Although the GOE would not have immediately triggered dramatic increases in the production of Fe^{3+} minerals in anoxic deep ocean environments, it would have begun a significant modification in the aqueous chemistry of Fe, because iron became less soluble as waters became oxygenated: marine Fe^{2+} would have gradually been depleted by precipitation of Fe-oxyhydroxides (Anbar and Knoll 2002; Klein 2005).

Stage 8—The Intermediate Ocean (2.0-1.0 Ga): The billion years following the Great Oxidation Event encompass one of the most enigmatic stages of Earth's mineral evolution. We suggest that few new species of clays arose, as no significant changes in environmental conditions occurred. All pre-existing modes of clay mineral paragenesis continued, and ongoing sedimentation and recycling via plate tectonics gave rise to increasing volumes of phyllosilicate-bearing rocks. It is worth noting that many clay minerals were being recycled by this point in Earth history, through subduction, regional metamorphism, charnockitization (e.g., Janardhanan et al. 1979; Newton et al. 1980), and other processes. Thus, clay minerals were both added and removed from the near-surface environment (i.e., Koster van Groos 1988).

A caveat to the model of the intermediate ocean as a time of stasis relates to the assembly of the Columbian and Rodinian supercontinents at ~2.0-1.8 and ~1.2-1.0 Ga, respectively. A number of studies have demonstrated pulses of mineralization and associated mineral diversification during those intervals (Meyer 1981; Grew and Hazen 2009, 2010a, 2013; Condie and Aster 2010; Bradley 2011; Condie et al. 2011; Tkachev 2011; Hazen et al. 2012; Golden et al. 2013). If hydrothermal activity associated with collisional orogenies led to mineralization,

686 then clay mineral formation must have been enhanced during those intervals as well.
687 Furthermore, rifting of Columbia at ~1.6-1.2 Ga (e.g., Nance et al. 2013) was accompanied by
688 deposition of thick marginal sediment wedges, which also provided loci for clay formation and
689 accumulation.
690
691 ***Stage 9—The Snowball Earth (1.0-0.542 Ga):*** Dramatic changes in the production of clays and
692 many other minerals occurred during the Neoproterozoic Era, which saw extreme fluctuations in
693 the near-surface environment, coupled with significant biological innovations. These changes
694 include alternating snowball and hothouse climate episodes, increases in atmospheric oxygen,
695 the breakup of the Rodinian supercontinent, and the rise of multicellular animals.
696 At least two major glaciation events between 750 and 650 Ma interupted the terrestrial
697 weathering cycle, as near-surface reaction rates slowed greatly due to decreased temperatures,
698 limited availability of liquid water, and the effects of an extensive ice veneer that may have
699 extended from poles to the Equator. We suggest that only subsurface aqueous/hydrothermal
700 alteration and highly localized oxic weathering of volcanic edifices produced significant clay
701 minerals during snowball Earth episodes, although authigenic clay mineral formation would have
702 continued in the oceans. Minor production of clay minerals may also have occurred via low-
703 temperature alteration of rock flour beneath abundant glaciers.
704 Clay mineral formation must have been correspondingly elevated during intervals between
705 snowball Earth episodes, characterized by relatively brief (~ 10 Ma) "hothouse" periods of rapid
706 warming triggered by elevated CO_2 concentrations and greenhouse gas warming, reinforced by
707 positive albedo feedbacks as ice caps retreated. Increased surface weathering and nutrient-rich
708 runoff, coupled with high atmospheric CO_2, led to extensive algal blooms and significant

709 increases in atmospheric O_2, as well.

710 Perhaps the most significant impact of oxygenation is that it ultimately gave rise to today's
711 range of biochemical mechanisms. Microbial activity enhances clay mineral production, for
712 example by the bio-weathering of feldspar and mica (Schwartzman and Volk 1989; Paris et al.
713 1995; Bennett et al. 1996; Barker et al. 1998; Ueshima and Tazaki 1998, 2001; Ueshima et al.
714 2000; Tazaki 2005), as well as via microbially mediated oxidation and reduction reactions
715 (Shelobolina et al. 2003; Kim et al. 2004; Fisk et al. 2006; Stucki and Kostka 2006; Dong et al.
716 2009; Bishop et al. 2011; Dong 2012). A terrestrial photosynthetic biota may have arisen as early
717 as ~ 850 Ma (Knauth and Kennedy 2009; Hand 2009), and a significant Neoproterozoic increase
718 in clay mineral deposition may have been the result of microbial activity in soils. These
719 processes possibly led to the so-called "clay mineral factory" (Kennedy et al. 2006).
720 Alternatively, Tosca et al. (2010) suggest that the Neoproterozoic Era saw a relative shift in
721 chemical versus physical weathering, with no significant increase in total clay mineral
722 production.

723 An indirect consequence of increased microbial activity was enhanced marine sequestration of
724 organic carbon within clay floccules and onto clay mineral surfaces (Hedges and Keil 1995;
725 Mayer et al. 2004). Clay mineral surfaces actively adsorb a number of organic compounds,
726 particularly polar organic molecules, and clay minerals can participate in reactions that modify
727 the organic molecules (Ransom et al. 1997, 1998, 1999; Blair and Aller 2012). In addition, it has
728 often been inferred that clay minerals can play a role in protecting organic molecules from
729 subsequent oxidation and other reactions, thereby effectively preserving the organic molecules
730 (Gordon and Millero 1985; Baldock and Skjemstad 2000; Lalonde et al. 2012). Subsequent
731 burial of this organic carbon with clay minerals, which was possibly the first major global-scale

carbon sequestration process, contributed to a rise in atmospheric oxygen by decreasing the opportunity for organic carbon to oxidize.

Stage 10—Phanerozoic Biomineralization (0.542 Ga to present): The Neoproterozoic rise in atmospheric oxygen, with the consequent formation of the UV-blocking ozone layer, ultimately facilitated the evolution of multicellular life and led to skeletal biomineralization—events that irreversibly transformed Earth's near-surface mineralogy. Skeletal biomineralization of carbonates had the indirect effect of sequestering large amounts of carbon in Earth's crust, further modifying the composition of the atmosphere, and changing the pH of the oceans. The rise in oxygen also altered Earth's surficial aqueous geochemistry, changing near-surface redox chemistry (most importantly for Fe in the context of clay minerals) as well as minor and trace element speciation.

Soil formation: Grim (1968), Velde (1985), Newman (1987), and Weaver (1989) provide overviews of rock weathering, soil formation, and phyllosilicate clay mineralogy resulting from near-surface rock alteration. Weathered rocks are not altered homogeneously; rather they develop rock alteration horizons, grading from the deepest unaltered rock, through saprock, saprolite, laterite, and the topmost soil layer. Resulting clay mineral assemblages can therefore be classified into chemical systems based on their alteration processes and conditions. For example, alkali, alkaline earth, and Fe^{2+} minerals tend to decrease upwards, whereas Al, Fe^{3+}, and hydrated species increase toward the soil horizon (Velde 1985; Newman 1987; Weaver 1989). These details, particularly with respect to redox-sensitive elements such as Fe, would

754 differ significantly on Earth before the Great Oxidation Event or before biological activity was
755 important on the surface.

756 Details of weathering profiles also differ significantly depending on the primary lithology.
757 The two most important factors controlling the weathering of komatiites and other ultramafic
758 rocks are the loss of Mg from the rocks and oxidation of Fe. Prior to about 2.4 Ga (the start of
759 the Great Oxidation Event), ultramafic rocks probably did not experience significant oxidation
760 (Sverjensky and Lee 2010). However, after 2.4 Ga, oxidation became much more important to
761 the evolution of Earth's clay minerals, primarily by oxidation of Fe^{2+} to Fe^{3+} (a process that was
762 accelerated by microbially mediated redox reactions; e.g., Cheah et al. 2003; Shelobolina et al.
763 2003; Bishop et al. 2011).

764 Loss of Mg in ultrabasic rocks does not contribute substantially to soil clay minerals because
765 Mg-saponite, chlorite, sepiolite, or palygorskite are unstable during weathering (Velde 1985). In
766 this regard the role of Mg in solution is of special interest. Harder (1972) investigated smectite
767 paragenesis at surface conditions and concluded that the presence of Mg in solution favors the
768 formation of smectite minerals. He found that montmorillonite and talc can be synthesized from
769 Mg-hydroxide silica gel, but Mg-Al-hydroxide silica gel precipitated both di- and trioctahedral
770 smectites. Low silica was observed to be favorable for formation of montmorillonite, a
771 significant result given the predominantly ultramafic to mafic crustal composition of early Earth,
772 and a result at odds with recent research supporting the formation of smectites under high silica
773 activity conditions (Bish and Aronson 1993; Abercrombie et al. 1994).

774 Olivine weathering would have provided the needed chemical reactants for such reactions, so
775 saponite is likely to have been a significant clay mineral from the earliest stages of Earth history.
776 Indeed, Mg-rich clay minerals such as saponite appear to be a common alteration product of the

777 ancient basaltic crust of Mars (e.g., Poulet et al. 2005; Bibring et al. 2006; Mustard et al. 2008;
778 Ehlmann et al. 2009, 2010; Milliken et al. 2009; Carter et al. 2010; Milliken and Bish 2010).

779 Oxidative weathering of mafic lithologies yields a distinctive sequence of clay minerals. For
780 example, Ildefonse (1980) described weathering of a metagabbro with a saprock zone of Fe
781 beidellite, nontronite, and talc, as well as Fe oxides overlying a saprolite zone containing coarse-
782 grained vermiculite. This sequence reflects a loss of Ca and Mg coupled with Fe oxidation. Note
783 that iron oxidation facilitates the transition from tri- to dioctahedral clay minerals [$(Fe^{2+})_3$ →
784 $(Fe^{3+})_2$] ; i.e., serpentine, chlorite, and/or saponite transform to nontronite as follows (Ducloux et
785 al. 1976): chlorite + trioctahedral smectite → dioctahedral smectite + interstratified minerals.

786 Alteration of ultramafic rocks under humid conditions commonly results in formation of
787 laterites that contain a variety of phyllosilicates, including vermiculite, chlorite, kerolite, and
788 smectites (including Ni-bearing varieties). Vermiculite (di- or trioctahedral) is commonly
789 produced during basic rock weathering (Jackson et al. 1952; Bassett 1959; Rich and Cook 1963;
790 Johnson 1964; Tardy and Gac 1968; Proust 1982; Velde 1985). Vermiculite paragenesis often
791 reflects a coupled loss of K, Ca, and Mg, together with oxidation of Fe. Crystallization occurs in
792 response to the incorporation of more Al and Fe^{3+} in the octahedral sites from the leaching of Mg
793 and oxidation of Fe^{2+} (Velde 1985).

794 Weathering of granite and other felsic rocks contrasts with the alteration of more mafic
795 lithologies. Kaolinite is present with oxides in the fracture systems of granites but has a minor
796 effect on the mass balance of the system (Meunier 1980; Newman 1987). Gibbsite is common in
797 the lowest parts of granitic alteration profiles and the rock may also be kaolinized (Helgeson
798 1970; Calvert et al. 1980; Macias-Vazquez 1981; Newman 1987). Feldspar weathering in acidic
799 lithologies is influenced by a number of factors. Composition strongly affects feldspar

dissolution rates, and Na and Ca removal rates are greater than for K. Thus, plagioclase weathers more rapidly than K-feldspar and mica (Johnson et al. 1968; Nesbitt et al. 1980; Nesbitt and Young 1984; Weaver 1989).

The role of root systems: Fungi and plants, which established a terrestrial foothold ~ 430 Ma, dramatically changed the rate of terrestrial mineral alteration to clays. Plant root systems change soil chemistry by producing organic acids that accelerate clay mineral formation (Weed et al. 1969; Silverman and Munoz 1970; Huang and Keller 1970, 1972; Kodama et al. 1983). For example, fulvic acid has been used to facilitate synthesis of kaolinite at low temperatures (Siffert 1978). It is likely, therefore, that organic acids began to play an important role in many low-temperature, near-surface mineral dissolution reactions soon after the development of surface vegetation.

Plant roots also facilitate removal of potassium from biotite (Spyridakis et al. 1967; Cecconi et al. 1975; Weaver 1989); thus micas serve as a biological source of potassium as they alter to vermiculite (Bassett 1959) and eventually to kaolinite. A major effect of plants on clay mineral chemistry was the differential removal of cations other than Si, thereby gradually transforming soil horizons to more silicious minerals, including smectites, illites, and kaolinite, compared with oxide-hydroxides such as gibbsite (B. Velde, personal communication). Plants also dramatically increased the volume of terrestrial clay minerals: Throughout the Paleozoic Era, plants established progressively deeper soil profiles, which provided the foundation for progressively taller plants. Thus, terrestrial clay mineral formation exemplifies the co-evolution of the geo- and biospheres.

Few of the 56 IMA recognized phyllosilicate clay mineral species appeared in the Phanerozoic Eon for the first time. The serpentine-group mineral odinite [$(Fe^{3+},Mg,Al,Fe^{2+})_{2.5}(Si,Al)_2O_5(OH)_4$] is known today only as an authigenic species in tropical reefs. The sepiolite-group mineral loughlinite [$Na_2Mg_3Si_6O_{16}\cdot 8H_2O$], a product of dolomite alteration, and the soil mineral palygorskite are found exclusively in Phanerozoic formations and may thus also be restricted to stage 10. Similarly, if laterite formation is a unique characteristic of the terrestrial biosphere then the rare species orthochamosite [$Fe^{2+}{}_5Al(Si,Al)O_{10}(O,OH)_8$] and falcondoite [$Ni_4Si_6O_{15}(OH)_2\cdot 6H_2O$] are also found only in stage 10. Given the varied clay-forming environments of the Phanerozoic Eon, we speculate that all 56 clay species cited in Table 2 have formed during the past 500 million years (and likely still are forming).

PHANEROZOIC CLAY MINERALS AND ATMOSPHERIC CHEMISTRY

Studies of clay mineral evolution are hindered by early Earth's meager clay mineral record—the consequence of burial, alteration, subduction, and erosion. Accordingly, much of the preceding analysis has relied on speculation based on studies of clay mineral stabilities and mechanisms of contemporary clay mineral paragenesis. However, detailed compilations of the temporal distribution of clay minerals over the past 1.3 Ga, and especially the last 600 Ma, by Ronov and coworkers provide an unparalleled record of relative clay abundances during the late Proterozoic and Phanerozoic Eons and thus offer the possibility of a more quantitative statistical approach to clay mineral evolution. Especially useful in this regard is the geographically extensive and sample intensive compilation of Ronov et al. (1990) for select clay-group mineral abundances from ~10,000 dated shale samples to 1,300 Ma from the Russian platform. Ronov and colleagues analyzed the modal abundances of four predominant groups of clay minerals, as distinguished by their characteristic (001) X-ray diffraction peaks—kaolin group (7 Å), illite group (10 Å), "montmorillonite" (i.e., smectite group; expandable ≥10 Å), and chlorite group (14 Å)—for each shale sample.

Starting with the assumption that terrestrial clay mineral abundances may reflect both diagenetic processes and variations in atmospheric composition, we examined correlations between pairs of clay mineral abundances versus time, as well as for clay abundances versus recent quantitative models of global O_2 and CO_2 levels in Earth's atmosphere extending back 543 Ma through the Phanerozoic Eon (Berner 2004, 2006a, 2009; Arvidson et al. 2007).

We find two significant pair correlations between the relative abundances of clay mineral groups. As expected, the most significant correlation is found for sediment concentrations of the two most abundant clay mineral groups, illite and smectite ("montmorillonite" of Ronov et al.).

856 Illite-group clay minerals dominate in sediments of the early Phanerozoic Era but tend to be less
857 abundant in more recent formations. Smectite-group minerals, on the other hand, are more
858 abundant in younger sediments (Fig. 1). We employed the Pearson product-moment correlation
859 coefficient (PMCC; see Supplementary Text) to quantify the negative correlation of illite with
860 smectite (PMCC = –0.74)—a significant overall trend that is consistent with the well-known
861 alteration sequence from smectite to illite during burial diagenesis (Hower et al. 1976; Weaver
862 1989).

863 We also observe a significant negative correlation (PMCC = –0.55) between kaolinite and
864 chlorite, which are the least abundant of the four clay mineral groups reported in these samples
865 (Fig. 2). This result suggests that a significant amount of kaolinite might be derived from
866 weathering of chlorite, probably during the weathering of mafic volcanic rocks—a major process
867 in the GEOCARBSULF model (Berner 2006b; see below).

868 In addition to the diagenetic smectite-illite and chlorite-kaolinite transitions, we find four
869 significant correlations between clay mineral abundances and atmospheric chemistry—
870 correlations that may reflect net effects of geological processes such as weathering,
871 sedimentation, metamorphism, and hydrothermal alteration, as well as biological processes such
872 as photosynthesis, bacterial sulfate reduction, and Fe^{2+} oxidation. Variations in the relative
873 abundances of the clay mineral groups kaolinite, illite, smectite, and chlorite in shales on a
874 regional spatial scale have been correlated with changes in climate, particularly humidity, during
875 parts of the Paleozoic Era (Ronov et al. 1990; Hallam et al. 1991; Hesselbo et al. 2009), and it
876 has been hypothesized that Neoproterozoic clay mineral production increased globally in
877 association with a rise in O_2 level (Kennedy et al. 2006; but see also Tosca et al. 2010).

878 However, correlations between atmospheric composition and relative clay mineral group
879 abundances have not been reported.

880 The procedure used in Ronov et al. (1990) provides a platform-wide average over different
881 clay mineral depositional environments and assumes a uniform and similar diagenetic history for
882 all samples—an assumption that is at best an approximation. We suggest that by correlating
883 relative abundances of different clay mineral groups with atmospheric CO_2 and O_2, we test the
884 extent to which variations in relative proportions of clay mineral groups reflect their genesis in a
885 weathering environment, as opposed to diagenetic and other factors. For example, illite
886 commonly forms by diagenetic alteration of K-feldspars, as well as by the progressive
887 transformation of smectite evident in Figure 1. We assumed that each sample is representative of
888 a global environmental condition for a specific geologic age (Gradstein et al. 2004). We plotted
889 relative abundances of the four clay mineral groups (Supplementary Tables S1 and S2) as time
890 series with the model-calculated O_2 or CO_2 levels from GEOCARBSULF (Berner 2006a, 2009;
891 Figs. 3-6; Supplementary Table S3), which employs a chronology consistent with Gradstein et al.
892 (2004). Similar correlations were obtained using the CO_2 model values from the Magic model
893 (Arvidson et al. 2007), but O_2 values for the entire Phanerozoic Eon were not reported by these
894 authors and may differ from those in GEOCARBSULF.

895 A matrix of eight possible correlations between the four different clay mineral groups and O_2
896 and CO_2 levels is given in Supplementary Table S4. We find four significant correlations (i.e.,
897 PMMC < -0.5 or PMMC > 0.5) between the Ronov et al. (1990) clay abundance data and the
898 Berner (2009) atmospheric composition model for CO_2 and O_2, as described below.

899

Kaolinite and chlorite versus O_2: Figure 3 illustrates a negative correlation between the relative abundance of kaolinite and O_2 levels over the entire Phanerozoic Eon (PMCC = –0.50), in contrast to the lack of significant correlation with CO_2 levels (PMCC = –0.14). The O_2 and CO_2 levels in the GEOCARBSULF model (Berner 2006a) are controlled by the following overall reactions:

$$(Ca,Mg)SiO_3 + CO_2 \longleftrightarrow (Ca,Mg)CO_3 + SiO_2 \quad (1)$$

$$CO_2 + H_2O \longleftrightarrow CH_2O + O_2 \quad (2)$$

$$15O_2 + 4FeS_2 + 8H_2O \longleftrightarrow 2Fe_2O_3 + 8SO_4^{2-} + 16H^+ \quad (3)$$

Equation 1 exerts primary control on CO_2 levels, whereas O_2 levels are controlled primarily by Equation 2 and are also influenced by Equation 3. Low levels of O_2 in Figure 3 correspond to net model shifts of Equation 2 to the left and Equation 3 to the right; both shifts are associated with higher levels of acidity. If we assume that kaolinite is detrital and originally derived by weathering of silicates, then higher acidity during weathering corresponds to lower values of the ratios of aqueous cations to H^+, e.g., $\frac{a_{Mg^{2+}}}{(a_{H^+})^2}$ or $\frac{a_{Ca^{2+}}}{(a_{H^+})^2}$, which favor the kaolinite stability field relative to Ca- and/or Mg-bearing silicates on aqueous activity diagrams (Drever 1988). Low O_2 levels thus correspond to greater amounts of kaolinite relative to primary silicates or other clay minerals. It should also be emphasized that it is the weathering of Ca- and/or Mg-bearing silicates that is of the greatest global importance for the coupled O_2 and CO_2 cycles, because it is Ca and Mg that form carbonates in the oceans (Berner 2006a).

Relative abundances of chlorite through time (Fig. 4) correlate positively with O_2 levels over the Phanerozoic Eon as a whole (PMCC = +0.51), whereas no correlation occurs with CO_2 levels (PMCC = –0.04). These results suggest that chlorite could have formed by direct oxidative

922 weathering of other mafic silicates at values of $\frac{a_{Mg^{2+}}}{(a_{H^+})^2}$ unfavorable for kaolinite. However, some
923 of the observed chlorite-group minerals could represent detrital phases, whose relative
924 abundance is a monitor of what could be termed chemically assisted physical weathering,
925 particularly of mafic and ultramafic rocks that contain chlorite from prior hydrothermal alteration
926 processes. It is likely that physical weathering of such rocks rich in Mg^{2+} and Fe^{2+} (and also
927 containing Fe^{3+}) was assisted by high levels of O_2, which would oxidize any rapidly weathering
928 Fe^{2+}-bearing minerals (e.g., olivine) to iron oxides and facilitate mechanical breakup of the
929 rocks, resulting in a greater relative abundance of residual, ultimately detrital, chlorite.
930 Figure 4 suggests that the above modes of weathering were important from 550 Ma until
931 about 200 Ma ago, after which the correlation between chlorite and O_2 appears weak.
932 Interestingly, ~200 Ma ago corresponds to the rise of ectomycorrhizal fungi (EMF; Taylor et al.
933 2009). EMF are distinguished from the earlier arbuscular mycorrhizal fungi (AMF) by their
934 ability to secrete oxalate and siderophores, which in combination have been shown in laboratory
935 experiments to be particularly effective in solubilizing Fe-oxide (Cheah et al. 2003). EMF can
936 facilitate solubilization of Fe-bearing minerals (Courty et al. 2010) and mechanical-chemical
937 weathering of sheet silicates (Bonneville et al. 2009), which, in turn, could facilitate the
938 incorporation of Fe^{2+}/Fe^{3+} into weathering products such as smectites. Thus the rise of EMF at
939 about 200 Ma would have resulted in a complex style of combined physical, chemical, and
940 biological weathering similar to that at the present day. We suggest that this new weathering
941 behavior is reflected in the relative abundance of both chlorite- and smectite-group (see below)
942 minerals from about 200 Ma to the present.
943

944 *Smectite and illite versus CO_2*: Relative abundances of smectite-group minerals versus time
945 correlate with decreasing CO_2 levels (Fig. 5; PMCC = –0.62). Unlike kaolinite- and chlorite-
946 group minerals, smectite abundance is not correlated with O_2 levels over the Phanerozoic Eon as
947 a whole (PMCC = +0.12). For smectite formed during weathering processes, this behavior
948 suggests control through Equation 1. Decreasing atmospheric CO_2 levels are potentially
949 associated with less acidic weathering conditions corresponding to increased values of activity
950 ratios such as $\frac{a_{Mg^{2+}}}{(a_{H^+})^2}$, which favor smectites relative to illite-group minerals if the Mg-contents
951 of the smectites are higher than those of illite. Despite progress in the thermodynamic
952 characterization of these minerals (Vidal and Dubacq 2009; Dubacq et al. 2010), the
953 compositions of the Russian platform clays are not known, which hampers more quantitative
954 evaluations of the stability of smectite relative to illite.

955 This scenario, in which clay mineral formation links to atmospheric CO_2, requires that
956 atmospheric CO_2 levels control CO_2 concentrations in the weathering zone, which is not the case
957 in the present day (CO_2 partial pressures in modern soil zones are typically much higher than in
958 the atmosphere). However, in the early Phanerozoic Eon, atmospheric CO_2 levels could have
959 directly controlled CO_2 concentrations in the shallow subsurface. Before the rise and spread of
960 deeply rooted vascular land plants about 350 to 300 Ma ago, the partial pressure of CO_2 in the
961 soil zone was significantly lower than at present (owing to fewer respiratory processes) and thus
962 more directly responsive to the level of CO_2 in the atmosphere (Berner 2004). Consequently, a
963 decrease of atmospheric CO_2 resulted in a CO_2 decrease in the soil zone, lower acidity, and more
964 smectite relative to illite. After ~350 Ma, deep root activity and associated biological activity
965 (e.g., AMF) resulted in greater levels of CO_2 respiration in the soil zone. In turn, this biological

966 processing resulted in CO_2 concentrations in the soil zone that were not directly controlled by
967 atmospheric CO_2 levels.

968 Figure 5 offers tentative support for the above arguments; namely, the negative correlation of
969 smectite-group minerals and CO_2 levels is particularly strong from 550 to about 350 Ma;
970 however, after ~300 Ma the correlation appears weaker. A new pattern of smectite abundances
971 may have emerged between ~200 Ma and the present in terms of O_2 instead of CO_2. The relative
972 abundance of smectite-group minerals during the last 200 Ma increases directly with O_2 levels,
973 as would be expected based on the rise of EMF discussed above. Increasing O_2 in the presence of
974 EMF facilitated oxidation reactions, thereby favoring the formation of Fe^{3+}-bearing smectites at
975 the expense of chlorite-group minerals (and presumably other mafic minerals, e.g., Sugimori et
976 al. 2008).

977 Relative illite abundances correlate with CO_2 levels (Fig. 6; PMCC = +0.72) but not with O_2
978 levels (PMCC = +0.13). Although significant illite must have formed by the well-documented
979 process of smectite diagenesis (Fig. 1), the correlation with CO_2 levels over hundreds of millions
980 of years suggests a strong influence of the weathering environment on illite formation as well.
981 The correlation is consistent with the notion discussed above that lower CO_2 levels favor lower
982 acidity and less illite relative to smectite. It is also plausible that the rise of terrestrial plant life
983 from the Silurian Period through the end of the Permian Period might have caused an increased
984 demand for K^+ in soil and weathering zones, which contributed to destabilizing illite relative to
985 kaolinite-group minerals (Knoll and James 1987). Recent studies have suggested that illite may
986 be stabilized in the uppermost parts of modern soil zones, but this stabilization depends on the
987 development of abundant decayed surface organic matter such as leaf litter (Barre et al. 2009). In

the early to mid-Paleozoic Era, the near-surface soil zone could have been quite different (Knoll and James 1987; Berner 2004).

Overall, the relative abundances of kaolinite- and chlorite-group minerals show negative and positive correlations, respectively, with O_2 levels, whereas smectite- and illite-group minerals show negative and positive correlations, respectively, with CO_2 levels. Within these overall correlations, changes in the patterns of the correlations suggest that relative clay mineral abundances are sensitive indicators of major biological events relevent to the weathering zone, including the rise of deep-rooted vascular plants and their associated mycorrhizal fungi. These correlations point to the viability of mineralogical proxies for paleo-atmospheric compositions, and they emphasize the tightly linked nature of the evolution of Earth's biosphere, atmosphere, and minerals deep into geologic time (Hazen et al. 2008; Sverjensky and Lee 2010).

CLAY MINERAL EVOLUTION ON MARS

In contrast to Earth, recent observations have shown that the ancient surface of Mars contains a diversity of clay minerals, most of which are thought to be more than 3 billion years old (Poulet et al. 2005; Bibring et al. 2006; Mustard et al. 2008; Ehlmann et al. 2009, 2010; Milliken et al. 2009; Carter et al. 2010; Milliken and Bish 2010), though it is as yet unresolved whether these clay minerals represent primarily surface/near-surface processes (e.g., weathering, diagenesis, precipitation from fluids) or subsurface hydrothermal processes (Poulet et al. 2005; Tosca and Knoll 2009; Ehlmann et al. 2011; Meunier et al. 2012). Paradoxically, we may have much to learn about the lost evolutionary record of clay minerals on early Earth by studying their surviving counterparts in the ancient (and largely preserved) rock record of Mars.

The successful landing of NASA's *Curiosity* rover in Gale Crater, coupled with observations from earlier lander, rover, and orbiter missions, provides an opportunity for comparing clay mineral evolution on Earth and Mars. Of the several modes of clay mineral paragenesis on Earth described in this study, the earliest—subsurface aqueous/hydrothermal alteration—has unambiguously occurred on Mars (Griffith and Shock 1997; Poulet et al. 2005; Bibring et al. 2006; Mustard et al. 2008; Ehlmann et al. 2011; Meunier et al. 2012). The alteration of basalt and other crustal mafic lithologies to trioctahedral ferromagnesian clay minerals must have commenced early in the Pre-Noachian (>4.1 Ga) history of Mars and may continue to this day in deep hydrothermal zones. Strong evidence from regional mineralogical surveys also points to possible authigenic clay mineral formation in martian sediments (Chevier et al. 2007; Murchie et al. 2009; Milliken et al. 2009), including possible authigenesis by high-temperature fluids associated with intrusive bodies (Meunier et al. 2012).

Significant evidence has accumulated that suggests Mars had abundant surface and near-surface water during its first half- to one-billion years, making it likely that a suite of authigenic clay minerals and products of water-rock interactions formed in the sediments associated with these ancient bodies of water. The timing, extent, and duration of a warm, wet martian surface environment are less certain (Squyres and Kasting 1994; Ehlmann et al. 2011). The clay minerals detected at the martian surface are found predominantly in terrains that are dated to the Noachian Eon (>3.5 Ga) based on crater counts, consistent with this time period being favorable for clay mineral formation if the clays in these deposits are detrital (Poulet et al. 2005; Mustard et al. 2008; Murchie et al. 2009). However, the ages of these clay minerals would be relatively unconstrained if they are instead authigenic, as they could have formed later than the rocks in which they are contained. In contrast, younger (Hesperian-aged) terrains are characterized by the presence of sulfate salts and a paucity of clay minerals.

This apparent mineralogical dichotomy has led to the hypothesis that Mars experienced a dramatic climatic change that is directly recorded in the mineralogy of martian strata (Bibring et al. 2006). Unlike Earth, which has experienced an increase in the diversity and production of clay minerals through time, the martian crust may record the opposite. Alternatively, martian clay minerals may not reflect conditions in the near-surface environment if they instead formed deep in the crust or are the products of magmatic processes (Ehlmann et al. 2011; Menuier et al. 2012).

Unraveling the physical and chemical weathering processes on Mars is, by necessity, quite difficult. Data returned by the *Spirit*, *Opportunity*, and *Curiosity* rovers currently provide the best *in situ* geochemical and mineralogic information. Specifically, recent X-ray diffraction data acquired by the CheMin instrument on the *Curiosity* rover have confirmed the presence of clay

minerals on Mars in rock powder collected by a drill from what has been classified as a mudstone (http://www.nasa.gov/mission_pages/msl/news/msl20130312.html; accessed 04/12/2013). These clay minerals and other associated minerals and elements indicate formation in circum-neutral pH fluids. This formation environment is in contrast to those previously explored by the *Opportunity* and *Spirit* rovers which, coupled with laboratory experiments, suggest acidic conditions, iron oxidation, and low water-to-rock ratios dominating surface chemical weathering over the past several billion years of Mars' history (Hurowitz and McLennan 2007; Tosca et al. 2009; Altheide et al. 2010; Hurowitz et al. 2010). Such conditions are not favorable to extensive clay formation, in direct opposition to orbital observations of clay mineral deposits in the oldest (Noachian) terrains on Mars. The presence of a putative ancient northern ocean on Mars or a more vigorous hydrologic cycle in the first billion years would alleviate some of these discrepencies, and *Curiosity*'s *in situ* observations of the clay minerals reported in Gale crater from orbital data (Milliken et al. 2010) will continue to provide new insight into water-rock interactions on ancient Mars.

A fourth association of near-surface clay minerals on Earth is related to the exposure of low-grade, chlorite-bearing metamorphic rocks (greenschist facies) through plate tectonics processes. Plate tectonics is not active on Mars, though Yin (2012) suggested the existence of large-scale strike-slip faulting in Valles Marineris on Mars. However, asteroid impacts may have played a role in excavating clay-bearing formations of deep crustal origin (Fairén et al. 2010; Ehlmann et al. 2011). In addition, asteroid impacts may have played an indirect role in the formation of clays through the generation of deep hydrothermal zones in the vicinity of impact craters (Newsom 1980; Rathbun and Squyres 2002; Abramov and Kring 2005; Schwenzer and Kring 2009; Marzo et al. 2010). Intriguingly, the vast majority of clay minerals detected from orbit thus far on Mars

do not require high-temperature conditions to form. Instead, smectites, mixed-layer chlorite/smectite, and chlorite-group minerals appear to be the dominant phases and may indicate temperatures <100°C, although occurrences of prehnite and serpentine have been reported in some locations (Ehlmann et al. 2009, 2011). In the early history of Mars, impacts into a water-bearing crust would surely have produced clay minerals, and the same was likely true for Earth at that time. However, the extent to which such martian clays were altered, recycled, or exposed by erosion and later impacts remains to be determined.

Based on this analysis, the diversity and relative abundances of clay minerals on Mars likely differ from Earth in several significant ways. On Mars, with a global basaltic crust and minimal granitization, trioctahedral ferromagnesian clay minerals will occur more abundantly than dioctahedral Al-Fe^{3+} species. Furthermore, dioctahedral ferric species will dominate over those of Al, at least if the clays formed at the surface. Conditions of the shallow subsurface on Mars are likely to be more reducing, suggesting that Fe^{2+} will predominate over Fe^{3+} varieties.

The diversity of clay mineral species is likely to be significantly less than on Earth—perhaps limited to the 25 species suggested to occur in stage 2 and 3 environments (Tables 1 and 2). Minerals associated with Li, Zn, Ni, Cu, and Cr enrichment (through volumetrically extensive fluid-rock interaction) and subsequent weathering and secondary alteration processes on Earth are less likely to occur on Mars. By the same token, minor and trace element distributions of clay minerals on Mars are likely to differ significantly from those on Earth.

Finally, there is as yet no evidence for microbially-induced clay mineral formation, much less the modes of biological weathering associated with the rise of a terrestrial biosphere—processes associated with stage 10 of Earth's clay mineral evolution. An important open question is whether any combination of clay minerals might represent a convincing biomarker. Summons et

al. (2011) identified a number of biosignatures that could potentially be identified using the instruments on the *Curiosity* rover. These potential biomarkers include organism morphologies, biofabrics, diagnostic organic molecules, isotopic signatures, evidence of biomineralization and bioalteration, spatial patterns in chemistry, and biogenic gases. They considered biogenic organic molecules and biogenic atmospheric gases to be most definitive and most readily detectable by the SAM instrument on MSL.

Beyond these differences in clay mineral diversity, relative abundances, and extent, a fascinating and as yet unresolved question relates to the differences in clay mineral preservation on Earth versus Mars. On Earth there is a paucity of clays > 1 Ga, but on Mars the majority of clay minerals appear to date from the planet's first billion years. These differences can be ascribed in part to the recycling of Earth's clay minerals through subduction, as well as the destruction of clay minerals through thermal metamorphism and possibly dehydration by CO_2-rich fluids (Janardhanan et al. 1979; Newton et al. 1980; Peterson and Newton 1989; Santosh et al. 1990). Nevertheless, it remains an open question why we find so few Archean clay minerals on Earth even in relatively unaltered sedimentary basins (e.g., Tosca and Knoll 2009).

CONCLUSIONS

Of the more than 4,700 known minerals on Earth, only a few dozen are classified as clay minerals, yet these species have played a major role in the evolution of Earth's near-surface environment throughout our planet's history. The four-billion-year rock record on Earth provides scant direct evidence of clay mineral diversification and increased distribution through geologic time, particularly for its first three billion years. Nevertheless, observations of more recent clay-bearing formations, coupled with our growing knowledge of the modes of clay paragenesis, provide a sound basis for understanding clay mineral evolution. Thus, it appears that the variety and volume of clay minerals present at Earth's surface has increased dramatically since planetary accretion.

This overview of clay mineral evolution has focused on the appearance of new clay mineral species and groups, with hints regarding the changing distributions and volumes of those crustal phases. However, the most revealing changes in clay mineralogy through Earth history may be related to as yet unrecognized compositional variations, including trace and minor element compositions, as well as their isotopic subtleties. The effects of Earth's evolving near-surface environment, including variations in redox conditions; atmospheric, ocean, and groundwater geochemistry; tectonic processes, notably associated with orogenic activity; and the origin of life and subsequent evolution of marine and terrestrial ecosystems; must be reflected in chemical variations that have been little studied. Future work will undoubtedly shed additional light on the remarkable effects of biological activity on Earth's near-surface mineralogy, and the continuing co-evolution of the geosphere and biosphere.

ACKNOWLEDGMENTS

A. Meunier and B. Velde contributed detailed, thoughtful, and constructive reviews that significantly improved this work. The authors greatly appreciate discussions with G. D. Cody, R. E. Cohen, R. T. Downs, C. Estrada, J. M. Ferry, E. S. Grew, K. Klochko, A. H. Knoll, F. A. Macdonald, and C. M. Schiffries, and comments by R. A. Berner, R. J. Hemley, D. Rumble, and an anonymous reviewer. Financial support was provided to R.H. and D.S. by the National Science Foundation, the NASA Astrobiology Institute, the Deep Carbon Observatory, and the Carnegie Institution of Washington.

REFERENCES

Abercrombie, H.J., Hutcheon, I.E., Bloch, J.D., and de Caritat, P. (1994) Silica activity and the smectite-illite reaction. Geology, 22, 539-542.

Abramov, O. and Kring, D.A. (2005) Impact-induced hydrothermal activity on early Mars. Journal of Geophysical Research, 110, E12S09.

Adusumalli, C.I. and Schubert, W. (2001) Geochemistry of metabauxites in the Bergsträsser Odenwald (Mid German Crystalline Rise) and paleoenvironmental implications. Mineralogy and Petrology, 72, 45-62.

Allen, C.C., Gooding, J.L., and Keil, K. (1982) Hydrothermally altered impact melt rock and breccia: contributions to the soil of Mars. Journal of Geophysical Research, 87, 10083-10101.

Alt, J.C. (1988) Hydrothermal oxide and nontronite deposits on seamounts in the eastern Pacific. Marine Geology, 81, 227-239.

Alt, J.C. and Bach, W. (2001) Data report: Low-grade hydrothermal alteration of uplifted lower oceanic crust, Hole 735B: mineralogy and isotope geochemistry. In J.H. Natland, Jr., H.J.B. Dick, D.J. Miller and R.P. Von Herzen, (Eds.), Proceedings of the Ocean Drilling Program. Scientific Results, 176, 1-24.

Alt, J.C., Zuleger, E., and Erzinger, J. (1995) Mineralogy and stable isotopic compositions of the hydrothermally altered lower sheeted dike complex, Hole 504B, Leg 140. In J. Erzinger, K. Becker, H.J.B. Dick and L.B. Stooking, (Eds.), Proceedings of the Ocean Drilling Program. Scientific Results, 137/140, 155-166.

Altheide, T.S., Chevrier, V.F., and Dobrea, E.N. (2010) Mineralogical characterization of acid weathered phyllosilicates with implications for secondary martian deposits. Geochimica et Cosmochemica Acta, 74, 6232-6248.

Ames, L.L. and Sands, L.B. (1958) Factors affecting maximum hydrothermal stability in montmorillonites. American Mineralogist, 43, 641-648.

Anbar, A.D. and Knoll, A.H. (2002) Proterozoic ocean chemistry and evolution: A bioinorganic bridge? Science, 297, 1137-1142.

Arndt, N.T. and Nisbet, E.G. (Eds.) (1982) Komatiites. George Allen and Unwin, London.

Arvidson, R.S., Mackenzie, F.T., and Guidry, M. (2007) Magic: A Phanerozoic model for the geochemical cycling of major rock-forming components—reply. American Journal of Science, 307, 858-859.

Badaut, D., Decarreau, A., and Besson, G. (1992) Ferripyrophyllite and related Fe^{3+} 2:1 clays in recent deposits of Atlantis II Deep, Red Sea. Clay Minerals, 27, 227-244.

Bailey, S.W. (1980) Structures of layer silicates. In G.W. Brindley and G. Brown, (Eds.), Crystal structures of clay minerals and their X-ray identification, Monograph 5, p.1-24. Mineralogical Society, London.

Bailey, S.W. (1984) Classification and structures of the micas. In S.W. Bailey, (Ed.), Micas. Reviews in Mineralogy, 13, 1-12. Mineralogical Society of America, Washington, DC.

Bailey, S.W. (1988a) Hydrous phyllosilicates (exclusive of Micas). In S.W. Bailey, (Ed.), Reviews in mineralogy, 19, 1-12. Mineralogical Society of America, Washington, DC.

Bailey, S.W. (1988b) Odinite, a new dioctahedral-trioctahedral Fe^{3+}-rich 1:1 clay mineral. Clay Minerals, 23, 237-247.

1183 Baldock, J.A. and Skjemstad, J.O. (2000) Role of the soil matrix and minerals in protecting
1184 natural organic materials against biological attack. Organic Geochemistry, 31, 697-710.
1185 Barker, W.W., Welch, S.A., and Banfield, J.F. (1998) Experimental observations of the effects of
1186 bacteria on aluminosilicate weathering. American Mineralogist, 83, 1551–1563.
1187 Barre, P., Berger, G., and Velde, B. (2009) How element translocation by plants may stabilize
1188 illitic clays in the surface of temperate soils. Geoderma, 151, 22-30.
1189 Bassett, W.A. (1959) Origin of the vermiculite deposit at Libby, Montana. American
1190 Mineralogist, 44, 282-299.
1191 Bates, T.F. (1962) Halloysite and gibbsite formation in Hawaii. Clays & Clay Minerals, 9, 315-
1192 218.
1193 Beane, R.E. (1974) Biotite stability in the porphyry copper environment. Economic Geology, 69,
1194 241-256.
1195 Bennett, P.C., Hiebert, F.K., and Choi, W.J. (1996) Microbial colonization and weathering of
1196 silicates in petroleum-contaminated groundwater. Chemical Geology, 132, 45–53.
1197 Berner, R.A. (Ed.) (1971) Principles of chemical sedimentology. McGraw-Hill Book Co., New
1198 York.
1199 Berner, R.A. (2004) The Phanerozoic Carbon Cycle: CO_2 and O_2. Oxford University Press, UK.
1200 Berner, R.A. (2006a) Geocarbsulf: A combined model for Phanerozoic atmospheric O_2 and CO_2.
1201 Geochimica et Cosmochimica Acta, 70, 5653-5664.
1202 Berner, R.A. (2006b) Inclusion of the weathering of volcanic rocks in the Geocarbsulf model.
1203 American Journal of Science, 306, 295-302.
1204 Berner, R.A. (2009) Phanerozoic atmospheric oxygen: New results using the Geocarbsulf model.
1205 American Journal of Science, 309, 603-606.

Bibring, J.P., Langevin, Y., Mustard, J.F., Poulet, F., Arvidson, R., Gendrin, A., Gondet, B., Mangold, N., Pinet, P., Forget, F., and the OMEGA team (2006) Global mineralogical and aqueous Mars history derived from OMEGA/Mars Express data. Science, 312, 400-404.

Bischoff, J.L. (1972) A ferroan nontronite from the Red Sea geothermal system. Clays and Clay Minerals, 20, 217-223.

Bish, D.L. and Aronson, J.L. (1993) Paleogeothermal and paleohydrologic conditions in silicic tuff from Yucca Mountain, Nevada. Clays and Clay Minerals, 41, 148-161.

Bishop, M.E., Dong, H., Kukkadapu, R.K., Lin, C., and Edelmann, R.E. (2011) Bioreduction of Fe-bearing clay minerals and their reactivity toward pertechnetate (Tc-99). Geochimica et Cosmochimica Acta, 75, 5229-5246.

Blackman, D.K., Ildefonse, B., John, B.E., Ohara, Y., Miller, D.J., MacLeod, C.J., and the Expedition 304/305 Scientists (2006) Oceanic core complex formation, Atlantis Massif. Proceedings of the Integrated Ocean Drilling Program, 304/305, College Station, Texas. (Available at http://iodp.tamu.edu/publications/exp304_305/30405title.htm).

Blair, N.E. and Aller, R.C. (2012) The fate of terrestrial organic carbon in the marine environment. Annual Review of Marine Science, 4, 401-423.

Bonneville, S., Smits, M.M., Brown, A., Harrington, J., Leake, J.R., Brydson, R., and Benning, L.G. (2009) Plant-driven fungal weathering: Early stages of mineral alteration at the nanometer scale. Geology, 37, 615-618.

Bowen, N.L. (Ed.) (1928) The evolution of the igneous rocks. Princeton University Press, New Jersey.

Bradley, D.C. (2011) Secular trends in the geologic record and the supercontinent cycle. Earth-Science Reviews, 108, 16-33.

1229 Brearley, A.J. (2006) The action of water. In D.S. Lauretta and H.Y. McSween, Jr., (Eds.),
1230 Meteorites and the Early Solar System, II, p.587-624. University of Arizona Press, Tuscon.
1231 Brearley, A.J. and Jones, R.H. (1998) Chondritic meteorites. In J.J. Papike, (Ed.), Planetary
1232 Materials. Reviews in Mineralogy and Geochemistry, 36, 3.1-3.398. Mineralogical Society of
1233 America, Chantilly, Virginia.
1234 Brearley, A.J. and Prinz, M. (1992) CI-like clasts in the Nilpena polymict urelite: Implications
1235 for aqueous alteration processes in CI chondrites. Geochimica et Cosmochimica Acta, 56,
1236 1373-1386.
1237 Brindley, G.W. (1980) Order-disorder in clay mineral structures. In G.W. Brindley, and G.
1238 Brown, (Eds.), Crystal structures of minerals and their X-ray identification, Monograph 5,
1239 125-195. Mineralogical Society, London.
1240 Brindley, G.W. (1982) Chemical composition of berthierines—a review. Clays and Clay
1241 Minerals, 30, 153-155.
1242 Brindley, G.W. and Goodyear, J. (1948) X-ray studies of halloysite and metahalloysite. Part II.
1243 The transition of halloysite to metahalloysite in relation to relative humidity. Mineralogical
1244 Magazine, 28, 407-422.
1245 Brindley, G.W. and Wan, H.-M. (1975) Compositions, structures, and thermal behavior of
1246 nickel-containing minerals in the lizardite-népouite series. American Mineralogist, 60, 863-
1247 871.
1248 Caballero, E., Reyes, E. Linares, J., and Huertas, F. (1985) Hydrothermal solutions related to
1249 bentonite genesis. Cabo de Gata region, Almeria, SE Spain. Mineralogy and Petrography
1250 Acta, 29A, 187-196.

1251 Caillaud, J., Proust, D, and Righi, D. (2006) Weathering sequences of rock-forming minerals in a
1252 serpentinite: influence of microsystems on clay mineralogy. Clays and Clay Minerals, 54, 87-
1253 100.
1254 Cairns-Smith, A.G. (1968) The origin of life and the nature of the primitive gene. Journal of
1255 Theoretical Biology, 10, 53-88.
1256 Cairns-Smith, A.G. (2005) Sketches for a mineral genetic material. Elements, 1, 157-161.
1257 Cairns-Smith, A.G. and Hartman, H. (1986) Clay Minerals and the Origin of Life. Cambridge
1258 University Press, UK.
1259 Calvert, C.S., Buol, S.W., and Weed, J.B. (1980) Mineralogical characteristics and
1260 transformation of a vertical rock-saprolite-soil sequence. Soil Science Society of American
1261 Journal, 44, 1056-1103.
1262 Carter, J., Poulet, F., Bibring, J.P., and Murchie, S. (2010) Detection of hydrated silicates in
1263 crustal outcrops in the northern plains of Mars. Science, 328, 1682-1686.
1264 Cawood, P.A., Hawkesworth, P.J., and Dhuime, B. (2013) The continental record and generation
1265 of continental crust. Geological Society of America Bulletin, 125, 14-32.
1266 Cecconi, S., Ristori, G.G., and Vidrich, V. (1975) The role of octahedral Fe in biological
1267 weathering of biotite. Proceedings of the International Clay Conferences, Mexico City, p.623-
1268 628.
1269 Cheah, S., Kraemer, S.M., Cervini-Silva, J., and Sposito, G. (2003) Steady-state dissolution
1270 kinetics of goethite in the presence of desferrioxamine B and oxalate ligands: Implications for
1271 the microbial acquisition of iron. Chemical Geology, 198, 63-75.
1272 Chen, I.A., Roberts, R.W., and Szostak, J.W. (2004) The emergence of competition between
1273 model protocells. Science, 305, 1474-1476.

Chevrier, V., Poulet, F., and Bibring, J.P. (2007) Early geochemical environment of Mars as determined from thermodynamics of phyllosilicates. Nature, 448, 60-63.

Christidis, G.E. and Huff, W.D. (2009) Geological aspects and genesis of bentonites. Elements, 5, 93-98.

Chukanov, N.V., Pekov, I.V., Zadov, A.E., Chukanova, V.N., and Mokkel, S. (2003) Ferrosaponite $Co_{0.3}(Fe^{2+},Mg,Fe^{3+})_3(Si,Al)_4O_{10}(OH)_2 \cdot 4H_2O$, the new trioctahedral smectite. Zapiski Vserossijskogo Mineralogicheskogo Obshchestva, 132, 68-74.

Churchman G.J. (2000) The alteration and formation of soil minerals by weathering. In M.E. Sumner, (Ed.), Handbook of soil science, p.3-76. CRC Press, Boca Raton, Florida.

Condie, K.C. (1989) Plate tectonics and Crustal Evolution. 3rd edition. Pergamon Press, New York.

Condie, K.C. and Aster, R.C. (2010) Episodic zircon age spectra of orogenic granitoids: The supercontinent connection and continental growth. Precambrian Research, 180, 227-236.

Condie, K.C. and Pease, V. [Editors] (2008) When Did Plate Tectonics Begin on Earth? Geological Society of America Special Paper, 440, 294 p.

Condie, K.C., Bickford, M.E., Aster, R.C., Belousova, E., Scholl, D.W. (2011) Episodic zircon ages, Hf isotopic composition, and the preservation rate of continental crust. GSA Bulletin, 123, 951-957.

Courty, P.E., Buee, M., Diedhiou, A.G., Frey-Klett, P., Le Tacon, F., Rineau, F., Turpault, M.P., Uroz, S., and Garbaye, J. (2010) The role of ectomycorrhizal communities in forest ecosystem processes: New perspectives and emerging concepts. Soil Biology and Biochemistry, 42, 679-698.

Daughney, C.J., Rioux, J.-P., Fortin, D. and Pichler, T. (2004) Laboratory investigation of the role of bacteria in the weathering of basalt near deep sea hydrothermal vents. Geomicrobiology Journal, 21, 21-31.

Deamer, D. (2011) First Life. University of California Press, Berkeley.

Deer, W.A., Howie, R.A., and Zussman, J. (Eds.) (1962) Volume 3, Rock-Forming Minerals: Sheet Silicates. Longmans, Green & Co., London.

De Waal, S.A. (1970a) Nickel minerals from Barberton, III. Willemseite, a nickelian talc. American Mineralogist, 55, 31-42.

De Waal, S.A. (1970b) Nickel minerals from Barberton, II. Nimite, a nickel-rich chlorite. American Mineralogist, 55, 18-30.

Dewey, J.F. (2007) The secular evolution of plate tectonics and the continental crust: an outline. Geological Society of America Memoir, 200, 1-7.

Dong, H. (2012) Clay-microbe interactions and implications for environmental mitigation. Elements, 8, 113-118.

Dong, H., Jaisi, D.P., Kim, J., and Zhang, G. (2009) Microbe-clay mineral interactions. American Mineralogist, 94, 1505-1519.

Downs, R.T. (2006) The RRUFF Project: an integrated study of the chemistry, crystallography, Raman and infrared spectroscopy of minerals. Program and Abstracts of the 19th General Meeting of the International Mineralogical Association in Kobe, Japan, O03-13.

Drever, J.I. (1988) The Geochemistry of Natural Waters. Prentice Hall, Princeton, New Jersey.

Dubacq, B., Vidal, O., and De Andrade, V. (2010) Dehydration of dioctahedral aluminous phyllosilicates: Thermodynamic modelling and implications for thermobarometric estimates. Contributions to Mineralogy and Petrology, 159, 159-174.

Dubroeucq, D., Geissert, D., and Quantin, P. (1998) Weathering and soil forming processes under semi-arid conditions in two Mexican volcanic ash soils. Geoderma, 86, 99-122.

Ducloux, J., Meunier, A., and Velde, B. (1976) Smectite, chlorite, and a regular interlayered chlorite-vermiculite in soils developed on a small serpentinite body, Massif Central, France. Clay Minerals, 11, 121-135.

Dudas, M.J. and Harward, M.E. (1975) Weathering and authigenic halloysite in soil developed in Mazama ash. Soil Science Society American Journal, 39, 561-566.

Eggleton, R.A. and Bailey, S.W. (1967) Structural aspects of dioctahedral chlorite. American Mineralogist, 52, 673-689.

Eggleton, R.A. and Tilley, D.B. (1998) Hisingerite: A ferric kaolin mineral with curved morphology. Clays and Clay Minerals, 46, 400-413.

Ehlmann, B.L., Mustard, J.F., Swayze, G.A., Clark, R.N., Bishop, J.L., Poulet, F., Des Marais, D.J., Roach, L.H., Milliken, R.E., Wray, J.J., Barnouin-Jha, O., and Murchie, S.L. (2009) Identification of hydrated silicate minerals on Mars using MRO-CRISM: Geologic context near Nili Fossae and implications for aqueous alteration. Journal of Geophysical Research, 114, E00D08.

Ehlmann, B.L., Mustard, J.F., and Murchie, S.L. (2010) Geologic setting of serpentine on Mars. Geophysical research Letters, 37, L06201.

Ehlmann, B.L., Mustard, J.F., Murchie, S.L., Bibribg, J.P., Meunier, A., Fraeman, A.A., and Langevin, Y. (2011) Subsurface water and clay mineral formation during the early history of Mars. Nature, 479, 53-60.

Elmore, S. C. (2009) Clay Mineral Evolution. MS Thesis, Department of Atmospheric, Oceanic and Earth Sciences, George Mason University, Fairfax, Virginia.

Ertem, G. and Ferris, J.P. (1997) Template-directed synthesis using the heterogeneous templates produced by montmorillonite catalysis: A possible bridge between the prebiotic and RNA worlds. Journal of the American Chemical Society, 119, 7197-7201.

Fahey, J.J., Ross, M., and Axelrod, J.M. (1960) Loughlinite, a new hydrous sodium magnesium silicate. American Mineralogist, 45, 270-281.

Fairén, A.G., Chevrier, V., Abramov, O., Marzo, G.A., Gavin, P., Davilla, A.F., Tornabene, L.L., Bishop, J.L., Roush, T.L., Gross, C., Kneissi, T., Uceda, E.R., Dohm, J.M., Schulze-Makuch, D., Rodriguez, A.P., Amils, R., and McKay, C.P. (2010) Noachian and more recent phyllosilicates in impact craters on Mars. Proceedings of the National Academy of Science USA, 107, 12095-12200.

Ferris, J.P. and Ertem, G. (1992) Oligomerization of ribonucleotides on montmorillonite—reaction of the 5'-phosphorimidazolide of adenosine. Science, 257, 1387-1389.

Fisk, M.R., Popa, R., Mason, O.U., Storrie-Lombardi, M.C., and Vincenzi, E.P. (2006) Iron-magnesium silicate bioweahering on Earth (and Mars?). Astrobiology, 6, 48-68.

Fontanaud, A. and Meunier, A. (1983) Mineralogical facies of a weathered sepentinized lherzolite from the Pyrénées, France. Clay Minerals, 18, 77-88.

Fransolet, A.-M. and Bourguignon, P. (1975) Données nouvelles sur la fraipontite de Moresnet (Belgique). Bulletin de la Société Minéralogie de France, 98, 235-244.

Frondel, C. (1955) Two chlorites: gonyerite and melanolite. American Mineralogist, 40, 1090-1094.

Garvie, L.A.J. and Metcalfe, R. (1997) A vein occurrence of co-existing talc, saponite, and corrensite, Builth Wells, Wales. Clay Minerals, 32, 223-240.

Giese, R.F. (1988) Kaolin minerals: structures and stabilities. In S.W. Bailey, (Ed.), Hydrous phyllosilicates (exclusive of micas). Reviews in Mineralogy and Geochemistry, 19, 29-66. Mineralogical Society of America, Washington, DC.

Glickson, A. (1998) Eugene Shoemaker and the impact paradigm in Earth and planetary sciences. Celestial Mechanics and Dynamic Astronomy, 69, 1-7.

Golden, J., McMillan, M., Downs, R.T., Hystad, G., Goldstein, I., Stein, H.J., Zimmerman, A., Sverjensky, D.A., Armstrong, J., and Hazen, R.M. (2013) Rhenium variations in molybdenite (MoS_2): Evidence for progressive subsurface oxidation. Earth and Planetary Science Letters, 366, 1-5.

Gordon, A. S. and Millero, F. J. (1985) Adsorption mediated decrease in the biodegradation rate of organic compounds. Microbial Ecology, 11, 289-298.

Gradstein, F.M., Ogg, J.G., and Smith, A.G. (2004) A Geologic Timescale 2004. Cambridge University Press, UK.

Grew, E. and Hazen, R.M. (2009) Evolution of the minerals of beryllium, a quintessential crustal element [Abstract]. Geological Society of America Abstracts with Programs, 41(7), 99.

Grew, E. and Hazen, R.M. (2010a) Evolution of the minerals of beryllium, and comparison with boron mineral evolution [Abstract]. Geological Society of America Abstracts with Programs, 42(5), 199.

Grew, E. and Hazen, R.M. (2010b) Evolution of boron minerals: Has early species diversity been lost from the geological record? [Abstract]. Geological Society of America Abstracts with Programs, 42(5), 92.

Grew, E. and Hazen, R.M. (2013) Evolution of the minerals of beryllium. Stein, in press.

1387 Griffith, L.L. and Shock, E.L. (1997) Hydrothermal hydration of martian crust: illustration via
1388 geochemical model calculations. Journal of Geophysical Research, 102, 9135-9143.
1389 Grim, R.E., (Ed.) (1968) Clay Mineralogy. McGraw-Hill Book Company, New York, New
1390 York.
1391 Groves, D.I. and Bierlein, F.P. (2007) Geodynamic settings of mineral deposit systems. Journal
1392 of the Geological Society of London, 164, 19-30.
1393 Gruner, J.W. (1944) The composition and structure of minnestoaite, a common iron silicate in
1394 iron formations. American Mineralogist, 29, 363-372.
1395 Guggenheim, S. and Eggleton, R.A. (1988) Crystal chemistry, classification, and identification
1396 of modulate layer silicates. In S.W. Bailey, (Ed.), Hydrous phyllosilicates (exclusive of
1397 micas). Reviews in Mineralogy, 19, 675-725. Mineralogical Society of America,
1398 Washington, DC.
1399 Guggenheim, S. and Martin, R.T. (1995) Definition of clay and clay mineral: Joint report of the
1400 AIPEA nomenclature and CMS nomenclature committees. Clays and Clay Minerals, 43, 255-
1401 256.
1402 Guggenheim, S., Adams, J.M., Bain, D.C., Bergaya, F., Brigatti, M.F., Drits, V.A., Formoso,
1403 M.L.L., Galán, E., Kogure, T., and Stanjek, H. (2006) Summary of recommendations of
1404 nomenclature committees relevant to clay mineralogy: Report of the Association
1405 Internationale pour l'Etudes des Agrgiles (AIPEA) nomenclature committee for 2006. Clays
1406 and Clay Minerals, 54, 761-772.
1407 Guggenheim, S., Adams, J.M., Bain, D.C., Bergaya, F., Brigatti, M.F., Drits, V.A., Formoso,
1408 M.L.L., Galán, E., Kogure, T., and Stanjek, H. (2007) Corrigendum 1: Summary of
1409 recommendations of nomenclature committees relevant to clay mineralogy: Report of the

Association Internationale pour l'Etudes des Agrgiles (AIPEA) nomenclature committee for 2006. Clays and Clay Minerals, 55, 646-647.

Güven, N. (2009) Bentonites—clays for molecular engineering. Elements 5, 89-92.

Hajash, A. and Archer, P. (1980) Experimental seawater/basalt interactions: Effects of cooling. Contributions to Mineralogy and Petrology, 75, 1-13.

Hallam, A., Grose, J.A., and Ruffell, A.H., (1991) Palaeoclimatic significance of changes in clay mineralogy across the Jurassic-Cretaceous boundary in England and France. Palaeogeography, Palaeoclimatology, Palaeoecology, 81, 173-187.

Hanczyc, M.M., Fujikawa, S.M., and Szostak, J.W. (2003) Experimental models of primitive cellular compartments: Encapsulation, growth and division. Science, 302, 618-622.

Hand, E. (2009) When Earth greened over. Nature, 460, 161.

Harder, H. (1972) The role of magnesium in the formation of smectite minerals. Chemical Geology, 10, 31-39.

Harder, H. (1976) Nontronite synthesis at low temperatures. Chemical Geology, 18, 169-180.

Harrison, T.M., Blichert-Toft, J., Müller, W., Albarede, F., Holden, P., and Mojzsis, S.J. (2005) Heterogeneous hadean hafnium: evidence of continental crust at 4.4 to 4.5 Ga. Science, 310, 1947-1950.

Hazen, R. M. (2013) Paleomineralogy of the Hadean Eon: A preliminary list. American Journal of Science, in press.

Hazen, R.M. and Eldredge, N. (2010) themes and variations in complex systems. Elements, 6, 43-46.

Hazen, R.M., Papineau, D., Bleeker, W., Downs, R.T., Ferry, J.M., McCoy, T.J., Sverjensky, D.A., and Yang, H. (2008) Mineral evolution. American Mineralogist, 93, 1693-1720.

1433 Hazen, R.M., Ewing, R.C., and Sverjensky, D.A. (2009) Uranium and thorium mineral
1434 evolution. American Mineralogist, 94, 1293-1311.
1435 Hazen R.M., Bekker A., Bish D.L., Bleeker W., Downs R.T., Farquhar J., Ferry J.M., Grew E.S.,
1436 Knoll A.H., Papineau D., Ralph J.P., Sverjensky D.A., Valley J.W. (2011) Needs and
1437 opportunities in mineral evolution research. American Mineralogist, 96, 953-963.
1438 Hazen, R.M., J.Golden, R.T.Downs, G.Hysted, E.S.Grew, D.Azzolini, and D.A.Sverjensky
1439 (2012) Mercury (Hg) mineral evolution: A mineralogical record of supercontinent assembly,
1440 changing ocean geochemistry, and the emerging terrestrial biosphere. American Mineralogist,
1441 97, 1013-1042.
1442 Hazen, R.M., R.T.Downs, A.Jones, L.Kah, and A.Oganov (2013) The mineralogy of carbon. In
1443 Hazen, R.M., J.Baross, R.J.Hemley, A.Jones [Editors]. Carbon in Earth. Reviews in
1444 Mineralogy and Geochemistry, 75, 7-46. Mineralogical Society of America, Washington, DC.
1445 Hedges, J.I. and Keil, R.G. (1995) Sedimentary organic matter preservation: An assessment and
1446 speculative synthesis. Marine Chemistry, 49, 81–139.
1447 Hekinian, R., Hoffert, M., Larque, P., Cheminee, J., Stoffers, P., and Bideau, D. (1993)
1448 Hydrothermal Fe and Si oxyhydroxide deposits from South Pacific intraplate volcanoes and
1449 the East Pacific Rise axial and off-axial regions. Economic Geology, 88, 2099-2121.
1450 Helgeson, H.C. (1970) Description and interpretation of phase relations in geochemical
1451 processes involving aqueous solutions. American Journal of Science, 268, 415-438.
1452 Hesselbo, S.P., Deconinck, J.F., Huggett, J.M., and Morgans-Bell, H.S. (2009) Late Jurassic
1453 palaeoclimatic change from clay mineralogy and gamma-ray spectrometry of the Kimmeridge
1454 Clay, Dorset, UK. Journal of the Geological Society, 166, 1123-1133.

1455 Hower, J. and Mowatt, T.C. (1966) The mineralogy of illites and mixed-layer
1456 illite/montmorillonites. American Mineralogist, 51, 825-854.
1457 Hower, J., Eslinger, E.V., Hower, M., and Perry, E.A. (1976) Mechanism of burial
1458 metamorphism of argillaceous sediments: 1. Mineralogical and chemical evidence. Geological
1459 Society of America Bulletin, 87, 725-737.
1460 Huang, W.H. (1974) Stabilities of kaolinite and halloysite in relation to weathering of feldspars
1461 and nepheline in aqueous solution. American Mineralogist, 59, 365-371.
1462 Huang, W.H. and Keller, W.D. (1970) Dissolution of rock-forming silicate minerals in organic
1463 acids: simulated first-stage weathering of fresh mineral surfaces. American Mineralogist, 55,
1464 2076-2094.
1465 Huang, W.H. and Keller, W.D. (1972) Geochemical mechanics for the dissolution, transport, and
1466 deposition of aluminum in the zone of weathering. Clays and Clay Minerals, 20, 69-74.
1467 Hurowitz, J.A. and McLennan, S.L.A. (2007) ~3.5 Ga record of water-limited, acidic weathering
1468 conditions on Mars. Earth and Planetary Science Letters, 260, 432-443.
1469 Hurowitz, J.A., Fischer, W.W., Tosca, N.J., and Milliken, R.E. (2010) Origin of acidic surface
1470 waters and the evolution of atmospheric chemistry on early Mars. Nature Geoscience, 3, 323-
1471 326.
1472 Ildefonse, P. (1980) Mineral facies developed by weathering in a meta-gabbro, Loire-Atlantique,
1473 France. Geoderma, 24, 257-274.
1474 Jackson, M.L., Hsueng, Y., Corey, R.B., Evans, E.J., and Vanden Heuvel, R.C. (1952)
1475 Weathering sequence of clay-size minerals in soils and sediments. II. Chemical weathering of
1476 layer silicates. Soil Science Society of American Journal, 16, 3-6.

Jacobs, D.C. and Parry, W.T. (1976) A comparison of the geochemistry of biotite from some basin and range stocks. Economic Geology, 71, 1029-1035.

Janardhanan, S., Newton, R.C., and Smith, J.V. (1979) Ancient crustal metamorphism at low PH_2O: Charnockite formation from Kabbaldurga, south India. Nature, 278, 511-514.

Jayananda, M., Kano, T., Peucat, J.J., and Channabasappa, S. (2008) 3.35 Ga komatiite volcanism in the western Dharwar craton, southern India: constraints from Nd isotopes and whole-rock geochemistry. Precambrian Research, 162, 160-179.

Johnson, (1964) Occurrence of regularly interstratified chlorite-vermiculite as a weathering product of chlorite in a soil. American Mineralogist, 49, 556-572.

Johnson, N.M., Likens, G.E., Bormann, F.H., and Pierce, R.S. (1968) Rate of chemical weathering of silicate minerals in New Hampshire. Geochimica et Cosmochimica Acta, 32, 531-538.

Jolliffe, F. (1935) A study of greenalite. American Mineralogist, 20, 405-425.

Jonas, E.C. (1964) Petrology of the Dry Branch, Georgia, kaolin deposits. Proceedings of the 12th National Conference on Clays and Clay Minerals, 199-205.

Joussein, E., Petit, S., Churchman, J., Theng, B., Righi, D., and Delvaux, B. (2005) Halloysite clay minerals – a review. Clay Minerals, 40, 383-426.

Karup-Moller, S. and Petersen, O.V. (1984) Tuperssuatsaiite, a new mineral species from the Ilimaussaq intrusion in South Greenland. Neues Jahrbuch für Mineralogie, Monatschefte, 501-512.

Keller, W.D. (1970) Environmental aspects of clay minerals. Journal of Sedimentary Research, 40, 788-813.

1499 Kendall, B., Anbar, A.D., Kappler, A., and Konhauser, K.O. (2012) In A.H. Knoll, D.E.
1500 Canfield, and K.O. Konhauser [Editors]. Fundamentals of Geobiology, p.65-92. Wiley-
1501 Blackwell, Chichester, UK.

1502 Kennedy, M.J., Droser, M., Mayer, L.M., Pevear, D., and Mrofka, D. (2006) Late Precambrian
1503 oxygenation: Inception of the clay mineral factory. Science, 311, 1446–1449.

1504 Khoury, H.N., MacKenzie, R.C., Russell, J.D., and Tait, J.M. (1984) An iron-free volkonskoite.
1505 Clay Minerals, 19, 43-57.

1506 Kim, J.W., Dong, H., Seabaugh, J., Newell, S.W., and Eberl, D.D. (2004) Role of microbes in
1507 the smectite-to-illite reaction. Science, 303, 830-832.

1508 Klein, C. (2005) Some Precambrian banded iron-formations (BIFs) from around the world: Their
1509 age, geologic setting, mineralogy, metamorphism, geochemistry, and origin. American
1510 Mineralogist, 90, 1473-1499.

1511 Klein, C. and Hurlbut, C.S. (Eds.) (1999) Manual of Mineralogy (Revised). 21st Edition. John
1512 Wiley and Sons, New York, New York.

1513 Knauth, L.P. and Kennedy, M.J. (2009) The late Precambrian greening of Earth. Nature, 460,
1514 728-732.

1515 Knoll, M.A. and James, W.C. (1987) Effect of the advent and diversification of vascular land
1516 plants on mineral weathering through geologic time. Geology, 15, 1099-1102.

1517 Kodama, H., Schnitzer, M., and Jaakkimainen, M. (1983) Chlorite and biotite weathering by
1518 fulvic acid solutions in closed and open systems. Canadian Journal of Soil Science, 63, 619-
1519 629.

1520 Kohyama N. and T. Sudo (1975) Hisingerite occurring as a weathering product of iron-rich
1521 saponite. Clays and Clay Minerals, 23, 215-218.

Konhauser, K.O., Newman, D.K., and Kappler, A. (2005) The potential significance of microbial Fe(III)-reduction during Precambrian banded iron formations. Geobiology, 3, 167-177.

Koster van Groos, A.F. (1988) Weathering, the carbon cycle, and the differentiation of the continental crust and mantle. Journal of Geophysical Research, 93, 8952-8958.

Kramm, U. (1980) Sudoite in low-grade metamorphic manganese rich assemblages. Neues Jahrbuch für Mineralogie, Abhandlungen, 138, 1-13.

Krot, A.N., Hutcheon, I.D., Brearley, A.J., Pravdivtseva, O.V., Petaev, M.I., and Hohenberg, C.M. (2006) Timescales and settings for alteration of chondritic meteorites. In D.S. Lauretta and H.Y. McSween, Jr., (Eds.), Meteorites and the early solar system II, 525-553. University of Arizona Press, Tucson.

Lalonde, K., Mucci, A., Ouellet, A., and Gélinas, Y. (2012) Preservation of organic matter in sediments promoted by iron. Nature, 483, 198-200.

Lawrence, D.J., Feldman, W.C., Goldsten, J.O., Maurice, M., Peplowski, P.N., Anderson, B.J., Bazell, D., McNutt, R.L. Jr., Nittler, L.R., Prettyman, T.H., Rodgers, D.J., Solomon, S.C., and Weider, S.Z. (2013) Evidence for water ice near Mercury's north pole from MESSENGER neutron spectrometer measurements. Science, 339, 292-296.

Lazerenko, E.K. (1941) Donbassites, a new group of minerals from the Donets basin. American Mineralogist, 26, 349.

Linares, J. (1985) The process of bentonite formation in Cabo de Gata, Almeria, Spain. Mineralogica Petrographica Acta, 29A, 17-33.

Linares, J. (1987) Chemical evolutions related to the genesis of hydrothermal smectites, Almeria, SE Spain. In R. Rodriguez-Clemente and Y. Tardy, (Eds.), Geochemistry and mineral formation in the earth surface, 567-584. CSIC-CNRS. Madrid.

London, D. (2008) Pegmatites. Mineralogical Association of Canada, Ottawa.

Lowell, J.D. and Guilbert, J.M. (1970) Lateral and vertical alteration-mineralization zoning in porphyry ore deposits. Economic Geology, 65, 373-408.

Macias-Vazquez, F. (1981) Formation of gibbsite in soils and saprolites of temperate-humid zones. Clay Minerals, 16, 43-52.

MacPherson, G.J. (2004) Calcium–aluminum-rich inclusions in chondritic meteorites. In: Davis AM (ed) Meteorites, Comets, and Planets. Treatise on Geochemistry, 1, 201-246. Elsevier, Amsterdam.

Maksimović, Z. and Bish, D.L. (1978) Brindleyite, a nickel-rich aluminous serpentine mineral analogous to berthierine. American Mineralogist, 63, 484-489.

Maksimović, Z. and Brindley, G.W. (1980) Hydrothermal alteration of a serpentinite near Takovo, Yugoslavia, to chromium-bearing illite/smectite, kaolinite, tosudite, and halloysite. Clays and Clay Minerals, 28, 295-302.

Marzo, G.A., Davila, A.F., Tornabene, L.L., Dohm, J.M., Fairén, A.G., Gross, C., Kneissi, T., Bishop, J.L., Roush, T.L., and McKay, C.P. (2010) Evidence for Hesperian impact-induced hydrotheralism on Mars. Icarus, 208, 667-683.

Mayer, L.M., Schtik, L.L., Hardy, K.R., Wagai, R., and McCarthy, J. (2004) Organic matter in small mesopores in sediments and soils. Geochimica et Cosmochimica Acta, 68, 3863–3872.

McDowell, S.D. and Elders, W.A. (1980) Authigenic layer silicate minerals in borehole Elmore 1, Salton Sea Geothermal Field, California, U.S.A. Contributions to Mineralogy and Petrology, 74, 293-310.

Mering, J. (1975) Smectites. Soil components. Inorganic Components, 2, 97-119.

Meunier, A. (1980) Les mécanismes de l'altération des granites et le rôle des microsystèmes. étude des arènes du massif granitique de Parthenay (Deux-Sèvres)). Memoires de la Société Géologique de France, 140, 80.

Meunier, A. and El Albani, A. (2007) The glauconite—Fe-illite—Fe-smectite problem: A critical review. Terra Nova, 19, 95-104.

Meunier, A. and Velde, B. (1979) Weathering mineral facies in altered granites: The importance of local small-scale equilibria. Mineralogical Magazine, 43, 261-268.

Meunier, A., Petit, S., Cockell, C.S., El Albani, A., and Beaufort, D. (2010) The Fe-rich clay microsystems in basalt-komatiite lavas: importance of Fe-smectites for pre-biotic molecule catalysis during the Hadean Eon. Origins of Life and evolution of the Biosphere, 40, 253-272.

Meunier, A., Petit, S., Ehlmann, B.L., Dudoignon, P., Westall, F., Mas, A., El Albani, A., and Ferrage, E. (2012) Magmatic precipitation as a possible origin of Noachian clays on Mars. Nature Geoscience, 5, 739-743. DOI: 10.1038/NGEO1572.

Meyer, C. (1981) Ore-forming processes in geologic history. Economic Geology, 75th Anniversary Volume, 6-41.

Milliken, R.E. and Bish, D.L. (2010) Sources and sinks of clay minerals on Mars. Philosphical Magazine, 90, 2293-2308.

Milliken, R.E., Fischer, W.W., and Hurowitz, J.A. (2009) Missing salts on early Mars. Geophysical Research Letters, 36, L11202.

Milton, C., Dwornik, E.J., and Finkelman, R.B. (1983) Pecoraite, the nickel analogue of chrysotile, $Ni_3Si_2O_5(OH)_4$ from Missouri. Neues Jahrbuch für Mineralogie, Monatschefte, 513-523.

Moore, D. and Reynolds, R.C., Jr. (1997) X-ray Diffraction and the Identification and Analysis of Clay Minerals, 2nd edition. Oxford University Press, New York.

Moore, W.J. and Czamanske, G.K. (1973) Compositions of biotites from unaltered and altered monzonitic rocks in the Bingham Mining District, Utah. Economic Geology, 68, 269-274.

Murchie, S.L., Mustard, J.F., Ehlmann, B.L., Milliken, R.E., Bishop, J.L., McKeown, N.K., Noe Dobrea, E.Z., Seelos, F.P., Buczkowski, D.L., Wiseman, S.M., Arvidson, R.E., Wray, J.J., Swayze, G., Clark, R.N., Des Marais, D.J., McEwen, A.S., and Bibring, J.P. (2009) A synthesis of martian aqueous mineralogy after 1 Mars year of observations from the Mars Reconnaissance Orbiter. Journal of Geophysical Research, 114, E00D06.

Murnane, R. and Clague, D.A. (1983) Nontronite from a low-temperature hydrothermal system on the Juan de Fuca Ridge. Earth and Planetary Science Letters, 65, 343-352.

Mustard, J.F., Murchie, S.L., Pelkey, S.M., Ehimann, B.L., Milliken, R.L., Grant, J.A., Bibring, J.P., Poulet, F., Bishop, J., Dobrea, E.N., Roach, L., Seelos, F., Arvidson, R.E., Wiseman, S., Green, R., Hash, C., Humm, D., Malaret, E., McGovern, J.A., Seelos, K., Clancy, T., Clark, R., Marais, D.D., Izenberg, N., Knudson, A., Langevin, Y., Martin, T., McGuire, P., Morris, R., Robinson, M., Roush, T., Smith, M., Swayze, G., Taylor, H., Titus, T., and Wolff, M. (2008) Hydrated silicate minerals on Mars observed by the Mars reconnaissance orbiter CRISM instrument. Nature, 454, 305-309.

Odin, G.S. (1988) Green marine clays. Development in Sedimentology, volume 45. Elsevier, Amsterdam.

Nance, R.D., Murphy, J.B., and Santosh, M. (2013) The supercontinent cycle: A retrospective essay. Gondwana research, in press.

1611 Nesbitt, H.W. and Young, G.M. (1984) Prediction of some weathering trends of plutonic and
1612 volcanic rocks based on thermodynamic and kinetic considerations. Geochimica et
1613 Cosmochimica Acta, 48, 1523-1534.
1614 Nesbitt, H.W., Markovics, G. and Price, R.C. (1980) Chemical processes affecting alkalis and
1615 alkaline earths during continental weathering. Geochimica et Cosmochimica Acta, 44, 1659-
1616 1666.
1617 Newman, A.C.D., (Ed.) (1987) Chemistry of clays and clay minerals. Mineralogical Society of
1618 Great Britain, Monograph 6. Longman, London.
1619 Newsom, H.E. (1980) Hydrothermal alteration of impact melt sheets with implications for Mars.
1620 Icarus, 44, 207-216.
1621 Newton, R.C., Smith, J.V., and Windley, B.F. (1980) Carbonic metamorphism, granulites and
1622 crustal growth. Nature, 288, 45-50.
1623 Nittler, L.R. (2003) Presolar stardust in meteorites: Recent advances and scientific frontiers.
1624 Earth and Planetary Science Letters, 209, 259-273.
1625 Novák, F., Vtelenský, J., Losert, J., Kupka, F., and Valcha, Z. (1957) The orthochamosite from
1626 the ore veins of Kank near Kutna Hora—a new specific mineral. Essays in honour of
1627 academician Frantis Slavik on the occasion of his eightieth birthday, p.315-344. Academy of
1628 Sciences of the Czech Republic, Prague.
1629 Nozaka, T., Fryer, P., and Andreani, M. (2008) Formation of clay minerals and exhumation of
1630 lower-crustal rocks at Atlantis Massif, Mid-Atlantic Ridge. Geochemistry Geophysics
1631 Geosystems, 9, 19.
1632 Oze C. and Sharma M. (2006) Serpentinization and the inorganic synthesis of H_2 in planetary
1633 surfaces. Icarus, 186, 557-561.

1634 Papavassiliou, C.T. and Cosgrove, M.E. (1981) Chemical and mineralogical changes during
1635 basalt-seawater interaction: Site 223, Leg 23, D.S.D.P., north-west Indian Ocean.
1636 Mineralogical Magazine, 44, 141-146.
1637 Papineau, D. (2010) Mineral environments on the earliest Earth. Elements, 6, 25-30.
1638 Paris, F., Bonnaud, P., Ranger, J. and Lapeyrie (1995) In vitro weathering of phlogopite by
1639 ectomycorrhizal fungi. Plant and Soil, 177, 191-201.
1640 Peacor, D.R. and Essene, E.J. (1980) Caryopilite—a member of the friedelite rather than the
1641 serpentine group. American Mineralogist, 65, 335-339.
1642 Peacor, D.R., Essene, E.J., Simmons, W.B. Jr., and Bigelow, W.C. (1974) Kellyite, a new Mn-Al
1643 member of the serpentine group from Bald Knob, North carolina, and new data on grovesite.
1644 American Mineralogist, 59, 1153-1156.
1645 Perrault, G., Harvey, Y., and Pertsowsky, R. (1975) La yofortierite, un noveau silicate hydraté de
1646 manganèse de St-Hilaire, P.Q. Canadian Mineralogist, 13, 68-74.
1647 Peterson, J.W. and Newton, R.C. (1989) CO_2-enhanced melting of biotite-bearing rocks at deep
1648 crustal pressure-temperature conditions. Nature, 340, 378-380.
1649 Pirajno, F. (2005) Hydrothermal processes associated with meteorite impact structures: evidence
1650 from three Australian examples and implications for economic resources. Australian Journal
1651 of Earth Sciences, 52, 587-620.
1652 Pirajno, F. (2009) Hydrothermal Processes and Mineral Systems. Springer, Amsterdam. Doi:
1653 10.1007/978-1-4020-8613-7_11
1654 Postinkova, V.P., Tsipurskii, S.I., Sidorenko, G.A., and Mokhov, A.V. (1991) Yakhontovite—a
1655 new copper-bearing smectite. American Mineralogist, 76, 668-669.

1656 Poulet, F., Bibring, J.P., Mustard, J.F., Gendrin, A., Mangold, N., Langevin, Y., Arvidson, R.E.,
1657 Gondet, B., and Gomez, C. (2005) Phyllosilicates on Mars and implications for early Mars
1658 climate. Nature, 438, 623-627.
1659 Proust, D. (1982) Supergene alteration of metamorphic chlorite in an amphibolite from the
1660 Massif Central, France. Clay Minerals, 17, 159-173.
1661 Proust, D. and Velde, B. (1978) Beidellite crystallization from plagioclase and amphibole
1662 precursors: local and long-range equilibrium during weathering. Clay Minerals, 13, 199-209.
1663 Proust, D., Caillaud, J., and Fontaine, C. (2006) Clay minerals in early amphibole weathering:
1664 tri- to dioctahedral sequence as a function of crystallization sites in the amphibole. Clays and
1665 Clay Minerals, 54, 351-362.
1666 Ranorosoa, N., Fontan, F., Fransolet, A.-M. (1989) Rediscovery of manandonite in the Sahatany
1667 valley, Madagascar. European Journal of Mineralogy, 1, 633-638.
1668 Ransom, B., Bennett, R.H., Baerwald, R, and Shea, K. (1997) TEM study of in situ organic
1669 matter on continental margins: Occurrence and the “monolayer” hypothesis. Marine Geology,
1670 138, 1-9.
1671 Ransom, B., Kim, D., Kastner, M., and Wainwright, S. (1998) Organic matter preservation on
1672 continental slopes: Importance of mineralogy and surface area. Geochimica et Cosmochimica
1673 Acta, 62, 1329-1345.
1674 Ransom, B., Bennett, R.H., Baerwald, R., Hulbert, M.H., and Burkett, P.-J. (1999) In situ
1675 conditions and interactions between microbes and minerals in fine-grained marine sediments:
1676 A TEM microfabric perspective. American Mineralogist, 84, 183-192.
1677 Rathbun, J.A. and Squyres, S.W. (2002) Hydrothermal systems associated with martian impact
1678 craters. Icarus, 157, 362-372.

Reitmeijer, F.J.M. (1998) Interplanetary dust particles. In J.J. Papike, (Ed.), Planetary Materials. Reviews in Mineralogy and Geochemistry, 36, 2.1-2.95. Mineralogical Society of America, Chantilly, Virginia.

Reitmeijer, F.J.M., Nuth, J.A., Rochette, P., Marfaing, J., Pun, A., and Karner, J.M. (2006) Deep metastable eutectic condensation in Al-Fe-SiO_2-H_2-O_2 vapors: Implications for natural Fe-aluminosilicates. American Mineralogist, 91, 1688-1698.

Rich, C.I. and Cook, M.G. (1963) Formation of dioctahedral vermiculite in Virginia soils. Clays and Clay Minerals, 10, 96-106.

Rogers, J.J.W. and Santosh, M. (2004) Continents and Supercontinents. Oxford University Press, New York.

Rollinson, H. (2007) Early Earth Systems. Blackwell, Oxford, UK.

Romero, R., Robert, M., Elsass, F. and Garcia, C. (1992) Abundance of halloysite neoformation in soils developed from crystalline rocks. Contribution of transmission electron microscopy. Clay Minerals, 27, 35-46.

Ronov, A.B., Migdisov, A.A., and Hahne, K. (1990) On the problem of abundance and composition of clays of the sedimentary cover of the Russian Platform. Geokhimiya, 1990, 467-482.

Ross, C.S. (1946) Sauconite—a clay mineral of the montmorillonite group. American Mineralogist, 31, 411-424.

Roy, R. and Romo, L.A. (1957) Weathering studies. 1. New data on vermiculite. The Journal of Geology, 65, 603-610.

Rule, A.C. and Radke, F. (1988) Baileychlore, the Zn end member of the trioctahedral chlorite series. American Mineralogist, 73, 135-139.

Ruzicka, A., Snyder, G.A., and Taylor, L.A. (1999) Giant impact hypothesis for the origin of the Moon: A critical review of some geochemical evidence. In G.A. Snyder, C.R. Neal, and W.G. Ernst, (Eds.), Planetary Petrology and Geochemistry, p.121-134. Geological Society of America, Boulder, Colorado.

Santosh, M., Harris, N.B.W., Jackson, D.H., and Mattey, D.P. (1990) Dehydration and incipient charnockite formation: A phase equilibria and fluid inclusion study from south India. Journal of Geology, 98, 915-926.

Scarfe, C.M. and Smith, D.G.W. (1977) Secondary minerals in some basalt rocks from DSDP Loeg 37. Canadian Journal of Earth Sciences, 14, 903-910.

Schoonen, M.A.A., Smirnov, A., and Cohn, C. (2004) A perspective on the role of minerals in prebiotic synthesis. Ambio, 33, 539-551.

Schrenk, M.O., Brazelton, W.J., and Lang, S.Q. (2013) Serpentinization, carbon and deep life. Reviews in Mineralogy and Geochemistry, 75, 576-606.

Schumann, D., Hartman, H., Eberl, D.D., Sears, S.K., Hesse, R., and Vali, H. (2012) Formation of replicating saponite from a gel in the presence of oxalate: Implications for the formation of clay minerals in carbonaceous chondrites and the origin of life. Astrobiology, 12, 549-561.

Schwartzman, D.W. and Volk, T. (1989) Biotic enhancement of weathering and the habitability of Earth. Nature, 340, 457–460.

Schwenzer, S.P. and Kring, D.A. (2009) Impact-generated hydrothermal systems capable of forming phyllosilicates on Noachian Mars. Geology, 37, 1091-1094.

Severmann, S., Mills, R.A., Palmer, M.R., and Fallick, A.E. (2004) The origin of clay minerals in active and relict hydrothermal deposits. Geochimica et Cosmochimica Acta, 68, 73-88.

1724 Seyfried, W.E., Jr. and Mottl, M.J. (1982) Hydrotherml alteration of basalt by seawater under
1725 seawater-dominated conditions. Geochimica et Cosmochimica Acta, 46, 985-1002.
1726 Shelobolina, E.S., Van Praagh, C.G., and Lovley, D.R. (2003) Use of ferric and ferrous iron
1727 containing minerals for respiration by *Desulfitobacterium frappieri*. Geomicrobiology
1728 Journal, 20, 143-156.
1729 Siffert, B. (1978) Genesis and synthesis of clays and clay minerals: recent developments and
1730 future prospects. Proceedings of the VI International Clay Conference, Oxford, UK, p.337-
1731 347.
1732 Silverman, M.P. and Munoz, E.F. (1970) Fungal attack on rock: solubilization and altered
1733 infrared spectra. Science, 169, 985-987.
1734 Singer, A. and Stoffers, P. (1987) A hydrothermal clay mineral sequence in a core from the
1735 Atlantis II Deep, Red Sea. Clay Minerals, 22, 251-267.
1736 Smith, W.C., Bannister, F.A., and Hey, M.H. (1946) Pennantite, a new manganese-rich chlorite
1737 from Benallt mine, Rhiw, Carnarvonshire. Mienralogical Magazine, 27, 217-220.
1738 Smithies, R.H., Van Kranendonk, M.J., and Champion, D.C. (2005a) It started with a plume –
1739 early Archaean basaltic proto-continental crust. Earth and Planetary Science Letters, 238,
1740 284-297.
1741 Smithies, R.H., Champion, D.C., Van Kranendonk, M.J., Howard, H.M., and Hickman, A.H.
1742 (2005b) Modern-style subduction processes in the Mesoarchaean: Geochemical evidence
1743 from the 3.12 Ga Whundo intra-oceanic arc. Earth and Planetary Science Letters, 231, 221-
1744 237.
1745 Smol'yaninova, N.N., Moleva, V.A., and Organova, N.I. (1961) A new aluminum-free member
1746 of the montmorillonite-sauconite series. American Mineralogist, 46, 241-242.

1747 Springer, G. (1976) Falcondoite, nickel analogue of sepiolite. Canadian Mineralogist, 14, 407-
1748 409.
1749 Spyridakis, D.E., Chesters, G., and Wilde, S.A. (1967) Kaolinization of biotite as a result of
1750 coniferous and deciduous seedling growth. Soil Science Society of America Journal, 31, 203-
1751 210.
1752 Squyres, S.W. and Kasting, J.F. (1994) Early Mars: How warm and how wet? Science, 265, 744-
1753 749.
1754 Srodon, J. (1984) X-ray powder diffraction identification of illitic materials. Clays and Clay
1755 Minerals, 32, 337-349.
1756 Stakes, D.S. and O'Neil, J.R. (1982) Mineralogy and stable isotope geochemistry of
1757 hydrothermally altered oceanic rocks. Earth and Planetary Science Letters, 57, 285-304.
1758 Stern, R.J. (2005) Evidence from ophiolites, blueschists, and ultra-high pressure metamorphic
1759 terranes that the modern episode of subduction tectonics began in Neoproterozoic time.
1760 Geology, 33, 557-560.
1761 Stoch, L. and Sikora, W. (1976) Transformation of micas in the process of kaolinitization of
1762 granites and gneisses. Clays and Clay Minerals, 24, 156-162.
1763 Stucki, J.W. and Kostka, J.E. (2006) Microbial reduction of iron in smectite. Comptes Rendue
1764 Geoscience, 338, 468-475.
1765 Su, C.M. and Harsh, J.B. (1998) Dissolution of allophane as a thermodynamically unstable solid
1766 in the presence of boehmite at elevated temperatures and equilibrium vapor pressures. Soil
1767 Science, 163, 299-312.

1768 Sugimori, H., Iwatsuki, T., and Murakami, T. (2008) Chlorite and biotite weathering, Fe^{2+}-rich
1769 corrensite formation, and Fe behavior under low P-O_2 conditions and their implication for
1770 Precambrian weathering. American Mineralogist, 93, 1080-1089.
1771 Summons, R.E., Amend, J.P., Bish, D., Buick, R., Cody, G.D., Des Marais, D.J., Dromant, G.,
1772 Eigenbrode, J.L., Knoll, A.H., and Sumner, D.Y. (2011) Preservation of martian organic and
1773 environmental records: Report of the Mars biosignature working group. Astrobiology, 11,
1774 157-181.
1775 Sverjensky, D.A. and N. Lee (2010) The Great Oxidation Event and mineral diversification.
1776 Elements, 6, 31-36.
1777 Tardy, Y. and Gac, J.Y. (1968) Minéraux argileux dans quelques sols et arenes des Vosges
1778 cristallines. Presence de vermiculite Al. Hypothese de la formation des vermiculites et
1779 montmorillonites. Bulletin. Service de la Carte Geologique of d'Alsace et de Lorraine, 21,
1780 285-304.
1781 Taylor, L.L., Leake, J.R., Quirk, J., Hardy, K, Banwart, S.A., and Beerling, D.J. (2009)
1782 Biological weathering and the long-term carbon cycle: Integrating mycorrhizal evolution and
1783 function into the current paradigm. Geobiology, 7, 171-191.
1784 Tazaki, K. (2005) Microbial formation of a halloysite-like mineral. Clays and Clay Minerals, 53,
1785 224-233.
1786 Thompson, G. (1983) Basalt-seawater interaction. In: Rona, P.A., Bostrom, K., Laubier, L.,
1787 Smith, K.L. (Eds.) Hydrothermal Processes at Seafloor Spreading Centers, p.225-278.
1788 Plenum, New York.

1789 Thompson, G., Mottl, M.J., and Rona, P.A. (1985) Morphology, mineralogy and chemistry of
1790 hydrothermal deposits from the TAG area, 26ºN Mid-Atlantic Ridge. Chemical Geology, 49,
1791 243-257.
1792 Tien, P.-L., Leavens, P.B., and Nelen, J.A. (1975) Swinefordite, a dioctahedral-trioctahedral Li-
1793 rich member of the smectite group from Kings Mountain, North Carolina. American
1794 Mineralogist, 60, 540-547.
1795 Tkachev, A.V. (2011) Evolution of metallogeny of granitic pegmatites associated with orogens
1796 throughout geological time. Geological Society of London Special Publications, 350, 7-23,
1797 Tomeoka, K. and Buseck, P.R. (1990) Phyllosilicate in the Mokoia CV carbonaceous chondrite:
1798 Evidence for aqueous alteration in an oxidizing condition. Geochimica et Cosmochimica
1799 Acta, 52, 1627-1640.
1800 Tonks, W.B. and Melosh, H.J. (1993) Magma ocean formation due to giant impacts. Journal of
1801 Geophysical Research, 98, 5319-5333.
1802 Tosca, N.J. and Knoll, A.H. (2009) Juvenile chemical sediments and the long term persistence of
1803 water at the surface of mars. Earth and Planetary Science Letters, 286, 379-386.
1804 Tosca, N.J., Johnston, D.T., Mushegian, A., Rothman, D.H., Summons, R.E., and Knoll, A.H.
1805 (2010) Clay mineralogy, organic carbon burial, and redox evolution in Proterozoic oceans.
1806 Geochimica et Cosmochimica Acta, 74, 1579-1592.
1807 Touboul, M., Kleine, T., Bourdon, B., Plame, H., and Wieler, R. (2007) Late formation and
1808 prolonged differentiation of the Moon inferred from W isotopes in lunar metals. Nature, 450,
1809 1206-1209.
1810 Ueshima, M. and Tazaki, K. (1998) Bacterial bio-weathering of K-feldspar and biotite in granite.
1811 Clay Science Japan, 38, 68–92.

1812 Ueshima, M. and Tazaki, K. (2001) Possible role of microbial polysaccharides in nontronite
1813 formation. Clays and Clay Minerals, 49, 292-299.
1814 Ueshima, M., Mogi, K., and Tazaki, K. (2000) Microbes associated with bentonite. Journal of
1815 the Clay Science Society of Japan, 39, 171-183.
1816 Van Kranendonk, M.J. (2011) Onset of plate tectonics. Science, 333, 413-414.
1817 Velde, B. (Ed.) (1985) Clay Minerals: A Physico-Chemical Explanation of their Occurrence.
1818 Elsevier, Amsterdam.
1819 Velde, B. and Weir, A.H. (1979) Synthetic illite in the chemical system K_2O-Al_2O_3-SiO_2-H_2O at
1820 300°C and 2 kbar. In M.M. Mortland and V.C. Farmer, (Eds.), Developments in
1821 Sedimentology, 27, 395-404. Proceedings of the Sixth International Clay Conference.
1822 Elsevier, Amsterdam.
1823 Versh, E., Kirsimäe, K., and Jõeleht, A. (2006) Development of potential ecological niches in
1824 impact-induced hydrothermal systems: The small-to-medium size impacts. Planetary and
1825 Space Science, 54, 156-1574. doi: 10.1016/j.pss.2005.12.022
1826 Vidal, O. and Dubacq, B. (2009) Thermodynamic modelling of clay dehydration, stability and
1827 compositional evolution with temperature, pressure and H_2O activity. Geochimica et
1828 Cosmochimica Acta, 73, 6544-6564.
1829 Von Engelhardt, W., Muller, G., and Kromer, H. (1962) Dioktaedrischer Chlorit ("Sudoite") in
1830 Sedimenten des Mittleren Keupers von Plochingen (Wurtt.). Naturwissenschaften, 49, 205-
1831 206.
1832 Wada, K. (1989) Allophane and imogolite. In J.B. Dixon and S.B. Weed, (Eds.), Minerals in Soil
1833 Environments, 2nd edition, chapter 21, p.1051-1087. SSSA Book Series, Madison, Wisconsin.
1834 Weaver, C.E. (Ed.) (1989) Clays, Muds and Shales. Elsevier, Amsterdam.

Weed, S.B., Davey, C.B., and Cook, M.G. (1969) Weathering of mica by fungi. Soil Science Society of America Journal, 33, 702-706.

Weir, A.H. and Greene-Kelly, R. (1962) Beidelite. American Mineralogist, 47, 137-146.

Whitney, G. and Eberl, D.D. (1982) Mineral paragenesis in a talc-water experimental hydrothermal system. American Mineralogist, 67, 944-949.

Wilde S.A., Valley J.W., Peck W.H., and Graham C.M. (2001) Evidence from detrital zircons for the existence of continental crust and oceans on the Earth 4.4 Gyr ago. Nature, 409, 175-178.

Witze, A. (2006) The start of the world as we know it. Nature, 442, 128-131.

Wollast, R. (1967) Kinetics of the alteration of K-feldspar in buffered solutions at low temperature. Geochimica et Cosmochimica Acta, 31, 635-648.

Yin, A. (2012) Structural analysis of the Valles Marineris fault zone: Possible evidence for large-scale strike-slip faulting on Mars. Lithosphere, 4, 286-330.

Zagorsky, V.Y., Peretyazhko, I.S., Sapozhnikov, A.N., Zhukhlistov, A.P., and Zvyagin, B.B. (2003) Borocookeite, a new member of the chlorite group from the Malkhan gem tourmaline deposit, Central Transbaikalia, Russia. American Mineralogist, 88, 830-836.

Zega, T.J., Garvie, L.A.J., and Buseck, P.R. (2003) Nanometer-scale measurements of iron oxidation states of cronstedtite from primitive meteorites. American Mineralogist, 88, 1169-1172.

Ziegler, K., Hsieh, J.C.C., Chadwick, O.A., Kelly, E.F., Hendricks, D.M., and Savin, S.M. (2003) Halloysite as a kinetically controlled end product of arid-zone basalt weathering. Chemical Geology, 202, 461-478.

Figures

Figure 1. Relative abundances of smectite- versus illite-group clay minerals during the Phanerozoic Eon. Data for Russian platform sediments from Ronov et al. (1990). Labels represent abbreviations for geologic time intervals (Supplementary Table S1).

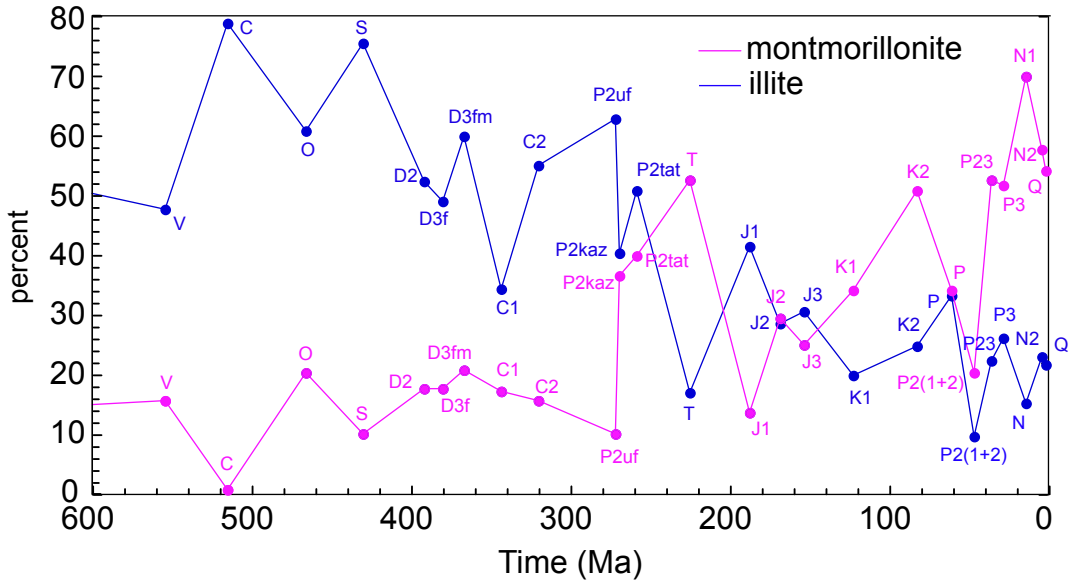

Figure 2. Relative abundances of chlorite- versus kaolinite-group clay minerals during the Phanerozoic Eon. Data for Russian platform sediments from Ronov et al. (1990). Labels represent abbreviations for geologic time intervals (Supplementary Table S1).

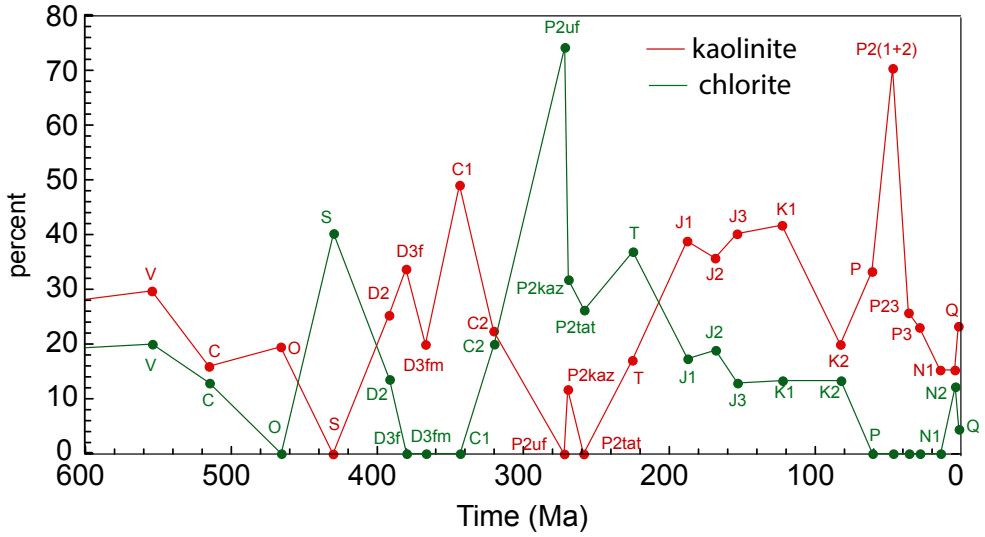

Figure 3. Relative abundance of kaolinite-group minerals in shales from the Russian platform (Ronov et al. 1990) versus values of the level of atmospheric O_2 from the GEOCARBSULF model (Berner 2006a) as functions of age. Labels represent abbreviations for geologic time intervals (Supplementary Table S1). Closed circles on O_2 curve are model calculations; open circles are interpolations to times of sampled clays. PMCC = Pearson moment correlation coefficient (see text).

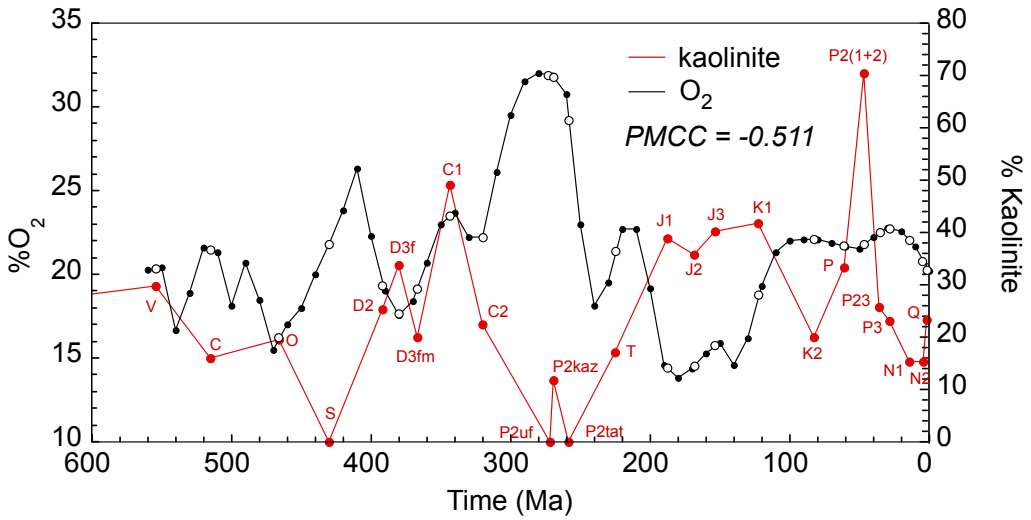

Figure 4. Relative abundance of chlorite-group minerals in shales from the Russian platform (Ronov et al. 1990) versus values of the level of atmospheric O_2 from the GEOCARBSULF model (Berner 2006a) as functions of age. Labels represent abbreviations for geologic time intervals (Supplementary Table S1). Closed circles on O_2 curve are model calculations; open circles are interpolations to times of sampled clays. PMCC = Pearson moment correlation coefficient (see text).

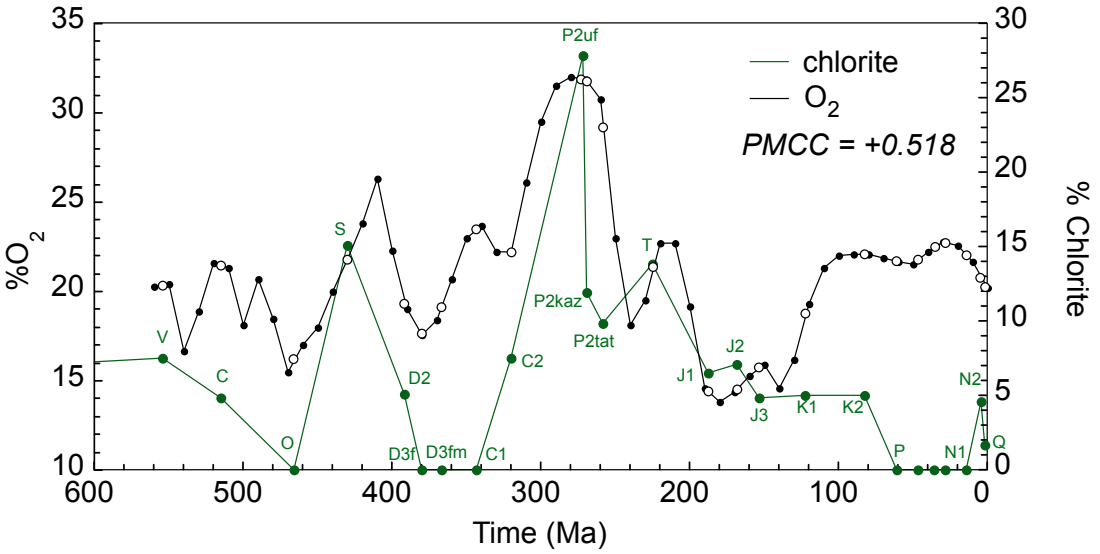

Figure 5. Relative abundances of smectite-group minerals (reported as "montmorillonite") in shales from the Russian platform (Ronov et al. 1990) versus values of the level of atmospheric CO_2 from the GEOCARBSULF model (Berner 2006a) as functions of age. RCO_2 denotes CO_2 concentration relative to present-day. Labels represent abbreviations for geologic time intervals (Supplementary Table S1). Closed circles on CO_2 curve are model calculations; open circles are interpolations to times of sampled clays. PMCC = Pearson moment correlation coefficient (see text).

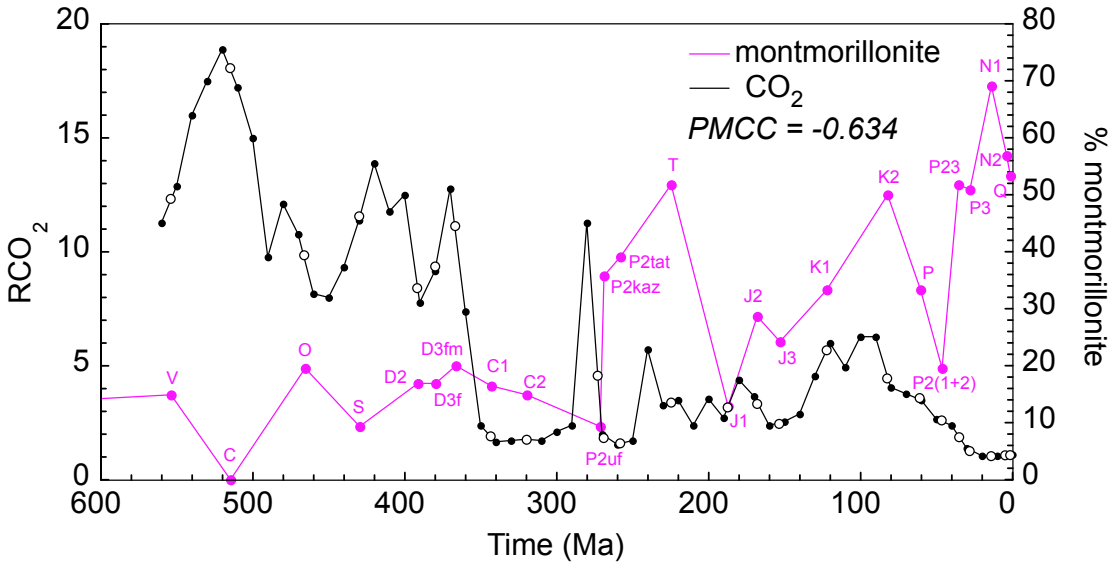

Figure 6. Relative abundances of illite-group minerals in shales from the Russian platform (Ronov et al. 1990) versus values of the level of atmospheric CO_2 from the GEOCARBSULF model (Berner 2006a) as functions of age. RCO_2 denotes CO_2 concentration relative to present-day. Labels represent abbreviations for geologic time intervals (Supplementary Table S1). Closed circles on CO_2 curve are model calculations; open circles are interpolations to times of sampled clays. PMCC = Pearson moment correlation coefficient (see text).

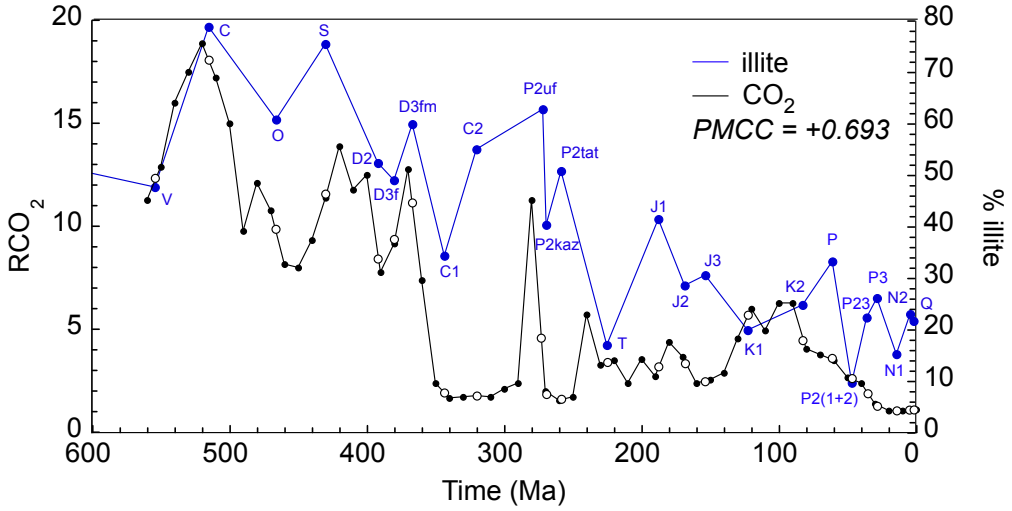

SUPPLEMENTARY INFORMATION

This document provides detailed information on the sources of the data for the atmospheric O_2 and CO_2 time series of Berner (2006, 2009), and the clay abundance time series of Ronov et al. (1990), and the statistical procedure that was used to examine their correlations.

A. Russian Platform clay abundance time series

The relative abundances of the kaolinite group, chlorite group, smectite group (reported as "montmorillonite"), and illite group minerals were taken from Table 1 in Ronov et al. (1990). The times assigned to the values were adjusted to GTS 2004 (Gradstein et al. 2004), using Russian zonation-to-standard chronostratigraphy information and geochronologic updates in *TS Creator* (2010). Specific ages were assigned by taking the average of the beginning and end of each series or stage. This procedure provides four clay abundance time series sampled at 25 time points throughout the Phanerozoic at a mean spacing of 23 Ma. Data are reported in Tables S1 and S3 below and plotted in Figs. 3-6 of the main manuscript.

B. Model O_2 and CO_2 time series

Values and times for the GEOCARBSULF-modeled atmospheric O_2 and CO_2 time series were obtained by digitizing the data points in Berner (2009) and (2006), respectively, as reported in Table S2 of this document. These values were smoothed and interpolated graphically to give values at the same ages represented by the mineral abundance data in order to carry out the statistical tests referred to below. The data are given in Table S3 below.

C. Statistical correlation

The sample Pearson product-moment correlation coefficient (PMCC) is a standard statistical measure of linear correlation between two variables X_1 and Y_1 (Snedecor and Cochran 1989):

$$r = \frac{\sum_{i=1}^{n}\left(X_i - \overline{X}\right)\left(Y_i - \overline{Y}\right)}{\sqrt{\sum_{i=1}^{n}\left(X_i - \overline{X}\right)^2}\sqrt{\sum_{i=1}^{n}\left(Y_i - \overline{Y}\right)^2}}$$

In this case, X corresponds to the set of *n* clay abundances and Y to the set of *n* modeled O_2 (or CO_2) values, that are paired with respect to time, with *n*=25, and $\overline{X}$ and $\overline{Y}$ correspond to sample means of X and Y.

The value of *r* falls in the range of ±1, where *r* = –1 signifies a perfect negative correlation, *r* = +1 a perfect positive correlation, and 0 no correlation between the variables. If X and Y are uncorrelated and normally distributed, the distribution of *r* follows Student's t distribution with *n* – 2 degrees of freedom, centered on *r* = 0. Hypothesis testing can be carried out with Student t critical values. An alternative approach, known as Fisher transformation, transforms *r* into a variable that is effectively normally distributed with a standard error $s_z=1/(n\text{-}3)^{-0.5}$:

$$z = 0.5\ [\ln(1+r)\text{-}\ln(1\text{-}r)]$$

for which the 95% confidence limits are the usual $z \pm 95\% = \pm 1.96 s_z$. Inverse transformation gives $r \pm 95\% = \pm\exp[2(1.96 s_z)\text{-}1] / \exp[2(1.96 s_z)+1]$.

As an example, PMCC computation for the kaolinite versus modeled O_2 time series gives the following: *r* = –0.5105, s_z = 0.2132, and $r \pm 95\% = \pm 0.3951$. The null hypothesis that the two time series are not correlated (actual *r* = 0) requires that calculated *r* occur within the $r \pm 95\%$ confidence limits. It does not; consequently, the two time series are significantly negatively correlated. The $r \pm 95\%$ confidence limits of ±0.3951 are assumed for all of the correlations discussed in this study.

Values of PMCC were determined for all possible pairs of clay minerals and the atmospheric variables O_2 and CO_2 and are listed in Table S4.

Supplemental References

Berner, R.A. (2006) GEOCARBSULF: a combined model for Phanerozoic O_2 and CO_2. Geochimica et Cosmochimica Acta, 70, 5653–5664.

Berner, R.A. (2009) Phanerozoic atmospheric oxygen: New results using the GEOCARBSULF model. American Journal of Science, 309, 603-606.

Gradstein, F., Ogg, J.G., and Smith, D.G. (2004) A Geologic Time Scale 2004. Cambridge, UK: Cambridge University Press.

Ronov, A.B., Migdisov, A.A., and Hahne, K. (1990) Abundance and composition of clays in the Russian-Platform sedimentary cover. Geokhimiya, No. 4, 467-482.

Snedecor, G.W. and Cochran, W.G. (1989) Statistical Methods, Eighth Edition. Ames, Iowa: Blackwell Publishing.

TSCreator visualization of enhanced Geologic Time Scale 2004 database (Version 4.2.1; 2010) James Ogg (database coordinator) and Adam Lugowski (software developer) http://www.tscreator.org

Table S1. Relative abundances of clay minerals from Ronov et al. (1990) as percentages of the total clays for individual time intervals through the Phanerozoic and late Precambrian.

Name[a.]	Age[b.]	Label	Kaolinite	Illite	Montmor.	Chlorite	Name[c.]
L. Riphean	1300	R1	17.5	68.4	8.8	5.3	Ectasian Period
M. Riphean	1100	R2	16.4	78.7	3.3	1.6	Stenian Period
U. Riphean	925	R3	16.4	70.5	8.2	4.9	Tonian Period
Vendian	554.5	V	29.9	47.8	14.9	7.5	Vendian
Cambrian	515.15	C	16.1	79.0	0.0	4.8	Cambrian
Ordovician	466	O	19.6	60.8	19.6	0.0	Ordovician
Silurian	429.85	S	0.0	75.5	9.4	15.1	Silurian
M. Devonian	391.4	D2	25.4	52.5	16.9	5.1	M. Devonian
Frasnian	379.9	D3f	33.9	49.2	16.9	0.0	Frasnian
Famennian	366.85	D3fm	20.0	60.0	20.0	0.0	Famennian
L. Carboniferous	343.75	C1	49.2	34.4	16.4	0.0	L.+M. Miss.
M. Carboniferous	320	C2	22.4	55.2	14.9	7.5	U. Miss. + L. Penn.
Ufa Stage	271.6	P2uf	0.0	63.0	9.3	27.8	Ufimian Stage
Kazanian Stage	269.3	P2kaz	11.9	40.5	35.7	11.9	Kazanian Stage
Tatar Stage	258.4	P2tat	0.0	51.0	39.2	9.8	Tatarian Stage
Triassic	225.3	T	17.2	17.2	51.7	13.8	Triassic
L. Jurassic	187.6	J1	39.0	41.6	13.0	6.5	L. Jurassic
M. Jurassic	168.4	J2	35.7	28.6	28.6	7.1	M. Jurassic
U. Jurassic	153.35	J3	40.3	30.6	24.2	4.8	U. Jurassic
L. Cretaceous	122.55	K1	41.7	20.0	33.3	5.0	L. Cretaceous
U. Cretaceous	82.55	K2	20.0	25.0	50.0	5.0	U. Cretaceous
Paleocene	60.65	P	33.3	33.3	33.3	0.0	Paleocene
L.+M. Eocene	46.5	P2(1+2)	70.6	9.8	19.6	0.0	L. + M. Eocene
U. Eocene	35.55	P23	25.9	22.4	51.7	0.0	U. Eocene
Oligocene	28.45	P3	23.1	26.2	50.8	0.0	Oligocene
Miocene	14.15	N1	15.4	15.4	69.2	0.0	Miocene
Pliocene	4.05	N2	15.4	23.1	56.9	4.6	Pliocene
Quaternary	1.4	Q	23.3	21.7	53.3	1.7	Quaternary

a. Geologic time intervals listed by Ronov et al. (1990).
b. Age in Ma.
c. Geologic time intervals from Gradstein et al. (2004)

Table S2. Values of the atmospheric O_2 and CO_2 levels from the GEOCARBSULF model of Berner (2006, 2009).

Age[a.]	% O_2[b.]	R(CO_2)[c.]	Age	% O_2	R(CO_2)
560	20.3	11.3			
550	20.4	12.9	270	31.9	2.01
540	16.7	16.0	260	30.8	1.56
530	18.9	17.5	250	23.0	1.70
520	21.6	18.9	240	18.1	5.71
510	21.3	17.2	230	19.5	3.27
500	18.1	15.0	220	22.7	3.49
490	20.7	9.81	210	22.7	2.39
480	18.5	12.1	200	19.2	3.55
470	15.5	10.8	190	14.6	2.72
460	17.0	8.18	180	13.8	4.40
450	18.0	8.01	170	14.4	3.67
440	20.0	9.32	160	15.3	2.39
430	21.8	11.4	150	15.9	2.58
420	23.8	13.9	140	14.6	2.90
410	26.3	11.8	130	16.2	4.56
400	22.3	12.5	120	19.3	6.03
390	19.0	7.79	110	21.3	4.93
380	17.6	9.19	100	22.0	6.30
370	18.4	12.8	90	22.1	6.27
360	20.7	7.42	80	22.1	4.08
350	23.0	2.39	70	21.9	3.77
340	23.7	1.68	60	21.7	3.48
330	22.2	1.73	50	21.5	2.68
320	22.2	1.80	40	22.2	2.41
310	26.1	1.70	30	22.8	1.42
300	29.5	2.14	20	22.6	1.06
290	31.5	2.40	10	21.7	1.04
280	32.0	11.3	0	20.2	1.11

a. Age in Ma.
b. Atmospheric O_2 level in percent from the GEOCARBSULF model (Berner, 2009).
c. Atmospheric CO_2 level from the GEOCARBSULF model (Berner, 2006), where R(CO_2) refers to the ratio of CO_2 in the past to that at present.

Table S3. Relative abundances of clay minerals from Ronov et al. (1990) and smoothed atmospheric O_2 and CO_2 levels from GEOCARBSULF at the same time intervals used for statistical analyses (see text).

Name[a.]	Age[b.]	Label	Kaolinite	Illite	Montmor.	Chlorite	Name[c.]
L. Riphean	1300	R1	17.5	68.4	8.8	5.3	Ectasian Period
M. Riphean	1100	R2	16.4	78.7	3.3	1.6	Stenian Period
U. Riphean	925	R3	16.4	70.5	8.2	4.9	Tonian Period
Vendian	554.5	V	29.9	47.8	14.9	7.5	Vendian
Cambrian	515.15	C	16.1	79.0	0.0	4.8	Cambrian
Ordovician	466	O	19.6	60.8	19.6	0.0	Ordovician
Silurian	429.85	S	0.0	75.5	9.4	15.1	Silurian
M. Devonian	391.4	D2	25.4	52.5	16.9	5.1	M. Devonian
Frasnian	379.9	D3f	33.9	49.2	16.9	0.0	Frasnian
Famennian	366.85	D3fm	20.0	60.0	20.0	0.0	Famennian
L. Carboniferous	343.75	C1	49.2	34.4	16.4	0.0	L.+M. Miss.
M. Carboniferous	320	C2	22.4	55.2	14.9	7.5	U. Miss. + L. Penn.
Ufa Stage	271.6	P2uf	0.0	63.0	9.3	27.8	Ufimian Stage
Kazanian Stage	269.3	P2kaz	11.9	40.5	35.7	11.9	Kazanian Stage
Tatar Stage	258.4	P2tat	0.0	51.0	39.2	9.8	Tatarian Stage
Triassic	225.3	T	17.2	17.2	51.7	13.8	Triassic
L. Jurassic	187.6	J1	39.0	41.6	13.0	6.5	L. Jurassic
M. Jurassic	168.4	J2	35.7	28.6	28.6	7.1	M. Jurassic
U. Jurassic	153.35	J3	40.3	30.6	24.2	4.8	U. Jurassic
L. Cretaceous	122.55	K1	41.7	20.0	33.3	5.0	L. Cretaceous
U. Cretaceous	82.55	K2	20.0	25.0	50.0	5.0	U. Cretaceous
Paleocene	60.65	P	33.3	33.3	33.3	0.0	Paleocene
L.+M. Eocene	46.5	P2(1+2)	70.6	9.8	19.6	0.0	L. + M. Eocene
U. Eocene	35.55	P23	25.9	22.4	51.7	0.0	U. Eocene
Oligocene	28.45	P3	23.1	26.2	50.8	0.0	Oligocene
Miocene	14.15	N1	15.4	15.4	69.2	0.0	Miocene
Pliocene	4.05	N2	15.4	23.1	56.9	4.6	Pliocene
Quaternary	1.4	Q	23.3	21.7	53.3	1.7	Quaternary

a. Geologic time intervals listed by Ronov et al. (1990).
b. Age in Ma.
c. Geologic time intervals from Gradstein et al. (2004)
d. Atmospheric O_2 level in percent at the same time interval as the clay abundances.
e. Atmospheric CO_2 level at the same time interval as the clay abundances. $R(CO_2)$ refers to the ratio of CO_2 in the past to that at present.

Table S4. Summary of the correlations between clay mineral relative abundances and atmospheric O_2 and CO_2 levels. Values cited are Pearson product-moment correlation coefficients (PMCC).

	Kaolinite	Illite	Smectite	Chlorite	% O_2
Kaolinite Group					
Illite Group	-0.497				
Smectite Group	-0.154	-0.742			
Chlorite Group	-0.551	0.362	-0.254		
% O_2	-0.498	0.131	0.115	0.510	
R(CO_2)	-0.137	0.716	-0.617	-0.035	-0.273

Table 1: Clay mineral evolution. Ten stages of Earth's mineral evolution saw changing rates and diversity of clay mineral formation. Note that the timings of some of these stages overlap, and several stages continue into the present (adapted from Hazen et al. 2008; Elmore 2009). Cumulative species refers to the total number of mineral species present, not just clay minerals.

Stage	New Clay Minerals*	Age (Ga)	~# species
1. Chondrites; Nebular processes	Primary high-T condensates; No clay minerals	>4.56 Ga	60
2. Aqueous alteration of C chondrites	Primarily Mg-Fe^{2+} species: 8-10, 12-14, 34, 39, 46	>4.56 to 4.55 Ga	250
3. Earliest Hadean Earth; alteration of ultramafic and basaltic crust	Serpentinization and seafloor alteration dominate: 1, 2, 4, 5, 7, 11, 16, 17, 22, 24, 25, 27, 33, 35, 40, 50	<4.55 Ga	420
4. Formation of granitoids and pegmatites	Saprolites from granites/rare pegmatite clays: 3, 21, 31, 43, 44, 51, 55, 56	uncertain, >3.5 Ga	~1000
5. Initiation of plate tectonics	Metamorphic clay minerals from tectonic facies: 47, 49, 52	uncertain, > 3.0 Ga	~1500
6. Origin of life; chemolithoautotrophs	Chemical weathering of terrestrial environments: 19, 23	>3.6 to 2.5 Ga	~1500
7. Great Oxidation Event	Clay minerals from oxidation reactions: 6, 18, 20, 26, 32, 36-38, 41, 42, 45, 53, 54	2.5 to 1.9 Ga	>4000
8. Intermediate Ocean	No new clay minerals; Global sedimentation/widespread clay deposition	1.9 to 1.0 Ga	>4000
9. Snowball Earth/Hothouse cycles	No new clay minerals; Episodic clay mineral production	1.0 to 0.542 Ga	>4000
10. Rise of the terrestrial biosphere	Increased biogenic clay mineral production: 15, 28-30, 48	0.542 Ga to present	>4700

*See Table 2, column 1 for clay mineral number key.

Table 2: Ten clay mineral groups and 56 phyllosilicate clay mineral species (as listed on http://rruff.info/ima/) cited in text, with their distributions through Earth history, paragenetic modes, and precursor minerals. Modified and expanded from Hower and Mowatt (1966), Brindley (1980), Bailey (1980, 1988a), Srodon (1984), Moore and Reynolds (1997), and web databases, including http://www.mindat.org and http://webmineral.com/data.

#. Group/Species Name	Ideal Formula	Stages[1]	Paragenetic Modes[2]; Precursor Minerals	References[3]
Kaolinite Group (7 Å dioctahedral 1:1 layer structure)				
1. Kaolinite	$Al_2Si_2O_5(OH)_4$	(3),4	HYDR—feldspars, feldspathoids, muscovite, biotite	1-3
		4	WEAT—granite, aluminosilicates	4, 5
		4	DEHY—halloysite-10Å	6
		4	AUTH—detrital sediments	4
		10	SOIL,BIOL—illite, vermiculite	7-9
2. Dickite	$Al_2Si_2O_5(OH)_4$	(3),4	HYDR—aluminosilicates; DIAG—kaolinite	10
		(3),4	AUTH—sediments	10
3. Nacrite	$Al_2Si_2O_5(OH)_4$	4	HYDR—aluminosilicates	10
4. Halloysite-7Å	$Al_2Si_2O_5(OH)_4$	3	HYDR—aluminosilicates in mafic and ultramafic rocks	1, 11,12
		4	WEAT—felsic igneous and metamorphic rocks	13-18
		4	DEHY—halloysite-10Å above 110°C	19
5. Halloysite-10Å	$Al_2Si_2O_5(OH)_4 \cdot 2H_2O$	3	HYDR—aluminosilicates in mafic and ultramafic rocks	1,11,12
		3,10	WEAT,SOIL—mafic and ultramafic rocks	13-18
6. Hisingerite	$(Fe^{3+})_2Si_2O_5(OH)_4.2H_2O$	7,10	OXID,WEAT—Fe silicates or sulfides	20
Serpentine Group (7 Å trioctahedral 1:1 layer structure)				
7. Amesite	$Mg_2Al(SiAl)O_5(OH)_4$	(3),(5)	RMET,HYDR—Al-Mg-rich rocks	10
8. Antigorite	$Mg_3Si_2O_5(OH)_4$	(2)	ACHN—C chondrites	21

		3	HYDR,SERP—ultramafics	22
		6	CMET—dolostone transformed to forsterite	10
9. Chrysotile	$Mg_3Si_2O_5(OH)_4$	(2)	ACHN—CM chondrites	21
		3	HYDR,SERP—mafic and ultramafic rocks	22
10. Lizardite	$Mg_3Si_2O_5(OH)_4$	(2)	ACHN—C chondrites	21
		3	HYDR,SERP—olivine, orthopyroxene	10,22
11. Caryopilite	$(Mn^{2+})_3Si_2O_5(OH)_4$	(3),(5)	CMET,HYDR—Mn minerals, such as rhodonite	23
		(6)	WEAT—Mn deposits	23
12. Berthierine	$(Fe^{2+},Fe^{3+},Al)_3(Si,Al)_2O_5(OH)_4$	(2)	ACHN—CM chondrites	21
		(3),4	AUTH—banded iron formations, marine sediments	24
		10	LATR,BIOL—soils	24
13. Cronstedtite	$(Fe^{2+}_2Fe^{3+})_3(Si,Fe^{3+})_2O_5(OH)_4$	(2)	ACHN—CM chondrites	21
		7	OXID,HYDR—ore veins	10
14. Greenalite	$(Fe^{2+},Fe^{3+})_{2-3}Si_2O_5(OH)_4$	(2)	ACHN—CM chondrites	21
		(6),7	AUTH—banded iron formations	25
15. Odinite	$(Fe^{3+},Mg,Al,Fe^{2+})_{2.5}(Si,Al)_2O_5(OH)_4$	(10)	BIOL,AUTH—tropical reefs	26
16. Népouite	$Ni_3Si_2O_5(OH)_4$	(3)	HYDR,SERP—Ni-rich ultramafic rocks	27
		(10)	LATR—Ni laterites	27
17. Pecoraite	$Ni_3Si_2O_5(OH)_4$	(3)	HYDR—Ni-rich ultramafic rocks	28
		(4)	WEAT—millerite (NiS)	28
18. Brindleyite	$(Ni,Al)_3(Si,Al)_2O_5(OH)_4$	(7)	OXID,WEAT—ultramafic rocks, bauxite deposits	29
19. Kellyite	$(Mn^{2+},Mg,Al)_3(Si,Al)_2O_5(OH)_4$	6	HYDR,WEAT—Mn-bearing carbonates and basic rocks	30
20. Fraipontite	$(Zn,Al)_3(Si,Al)_2O_5(OH)_4$	(7)	OXID,HYDR,WEAT—Zn-bearing rocks	31
21. Manandonite	$Li_2Al_4(Si_2AlB)O_{10}(OH)_8$	(4)	HYDR,WEAT—complex Li-B pegmatites	32
<u>Talc Group (10 Å trioctahedral, non-expandable 2:1 layer structure; no interlayer cations):</u>				
22. Talc	$Mg_3Si_4O_{10}(OH)_2$	3	HYDR—olivines and non-Al pyroxenes	7,10,33

		(3),4	WEAT—ultramafic	1,34
		5	RMET—Mg-rich rocks	1
23. Minnesotaite	$(Fe^{2+})_3Si_4O_{10}(OH)_2$	(6),7	RMET—banded iron formations	10,35
24. Willemseite	$Ni_3Si_4O_{10}(OH)_2$	(3)	HYDR—Ni-bearing igneous rocks	36
Pyrophyllite Group (10 Å dioctahedral, non-expandable 2:1 layer structure; no interlayer cations):				
25. Pyrophyllite	$Al_2Si_4O_{10}(OH)_2$	(3),4	HYDR—feldspar	10
		(5)	RMET—kyanite, Al-pyroxene	10
26. Ferripyrophyllite	$Fe^{3+}{}_2Si_2O_{10}(OH)_2$	(7)	OXID,HYDR—iron formations	37
Palygorskite-Sepiolite Group (10 Å di- and trioctahedral, expandable 2:1 layer structure; usually in fibrous habit):				
27. Sepiolite	$Mg_4Si_6O_{15}(OH)_2•6H_2O$	3	SERP—mafic rocks	10,38
		4	AUTH—alkaline saline waters in arid environments	10
28. Loughlinite	$Na_2Mg_3Si_6O_{16}·8H_2O$	(10)	RMET—dolomitic shale	39
29. Falcondoite	$Ni_4Si_6O_{15}(OH)_2·6H_2O$	(10)	LATR—serpentinized Ni-rich harzburgite	40
30. Palygorskite	$(Mg,Al)_2Si_4O_{10}(OH)•4H_2O$	10	SOIL—Mg silicates	10,38
31. Yofortierite	$Mn^{2+}{}_5Si_8O_{20}(OH)_2•8\text{-}9H_2O$	(4)	HYDR—pegmatite in nepheline syenite	41
32. Tuperssuatsiaite	$NaFe^{3+}{}_3Si_8O_{20}(OH)_2•4H_2O$	(7)	OXID,HYDR—sodalite-nepheline syenite pegmatite	42
Smectite and Vermiculite Groups (10 Å di- and trioctahedral, expandable 2:1 layer structure; no interlayer cations):				
33. Vermiculite	$Mg_{0.7}(Mg,Fe^{3+},Al)_6(Si,Al)_8O_{20}(OH)_4•8H_2O$	(3),4	HYDR,WEAT—Mg micas, muscovite	1,10,33,43-48
		4	SOIL—clay minerals	45,46
		(5)	RMET—limestone	10
34. Saponite	$(Ca,Na)_{0.3}(Mg,Fe^{2+})_3(Si,Al)_4O_{10}(OH)_2•4H_2O$	(2)	ACHN—CAIs, matrix, and chondrules in chondrites	21
		3	HYDR,SERP—basalt, skarns, amphibolites	33,48-50
35. Ferrosaponite	$Ca_{0.3}(Fe^{2+},Mg,Fe^{3+})_3(Si,Al)_4O_{10}(OH)_2·4H_2O$	(3)	HYDR—basalt	49,51

36. Sauconite	$Na_{0.3}Zn_3(Si,Al)_4O_{10}(OH)_2{\cdot}4H_2O$	(7)	OXID,HYDR—Zn ores	52
37. Zincsilite	$Zn_3(Si,Al)_4O_{10}(OH)_2{\cdot}4H_2O$	(7)	OXID, HYDR—Zn ores	53
38. Yakhontovite	$(Ca,Na,K)_{0.2}(Cu,Fe,Mg)_2Si_4O_{10}(OH)_2.3H_2O$	(7)	OXID,WEAT—Cu sulfide ore	54
39. Montmorillonite	$(Na,Ca)_{0.3}(Al,Mg)_2Si_4O_{10}(OH)_2{\bullet}nH_2O$	2	ACHN—CAIs and matrix in chondrites	21
		3	HYDR—volcanic and intrusive rocks	1,2,10,55,56
		3	WEAT--volcanic tuff and ash	1,2,10,57,58
40. Beidellite	$(Na,Ca)_{0.3}Al_2(Si,Al)_4O_{10}(OH)_2{\bullet}nH_2O$	3	HYDR—volcanics (bentonites)	10,43,56,59,60
		4	SOIL—mafic rocks	10,59
		(5)	HYDR—porphyry Cu	10,59
41. Nontronite	$Na_{0.3}Fe^{3+}{}_2(Si,Al)_4O_{10}(OH)_2{\bullet}nH_2O$	7	OXID,WEAT—basalt and ultramafic rocks	10,61,62
		7	OXID, HYDR—mafic rocks	10,55,56,63,64
		(7)	CMET—limestone	10
		7	OXID,AUTH—marine sediments	10,58,65
42. Volkonskoite	$Ca_{0.3}(Cr,Mg)_2(Si,Al)_4O_{10}(OH)_2{\bullet}4(H_2O)$	(7),(10)	OXID,WEAT—serpentinites	66
		(10)	AUTH,BIOL—sediments with organics	66
43. Swinefordite	$Ca_{0.2}(Li,Al,Mg,Fe)_3(Si,Al)_4O_{10}(OH,F)_2{\bullet}nH_2O$	(4)	AUTH—spodumene in pegmatites	67
Illite Group (10 Å dioctahedral, 2:1 layer structure; with interlayer cations):				
44. Illite[4]	$[K_{0.6}(H_3O)_{0.4}]Al_{1.3}Mg_{0.3}Fe^{2+}{}_{0.1}Si_{3.5}O_{10}(OH)_2{\bullet}(H_2O)$	4	AUTH,WEAT—feldspar	1,2,10,43,44,68
		4	HYDR—muscovite-phengite	1,2,10,12,33,68
		4	SOIL—smectite	1,10,69
45. Glauconite[4]	$(K,Na)(Fe^{3+},Al,Mg)_2(Si,Al)_4O_{10}(OH)_2$	7	DIAG,RDUC—biotite in shallow water	10,70
		7,10	BIOL—biotite alteration with organics	71
Chlorite Group (14 Å di- and trioctahedral, 2:1:1 layer structure):				
46. Clinochlore	$Mg_6Si_4O_{10}(OH)_8$	(2)	ACHN—chondrite	21
		3	HYDR—amphibole, pyroxene, biotite	10

		5	RMET—chlorite schist, marble, amphibolite, ultramafic	10,22,72
47. Chamosite	$(Fe^{2+},Mg,Al,Fe^{3+})_6(Si,Al)_4O_{10}(OH,O)_8$	5	RMET—Fe, Mg silicates	22,72
		7,10	AUTH,RDUC—sedimentary ironstones and organics	10
48. Orthochamosite	$Fe^{2+}{}_5Al(Si,Al)O_{10}(O,OH)_8$	(10)	LATR—olivine basalt	73
49. Pennantite	$(Mn^{2+},Al)_6(Si,Al)_4O_{10}(OH)_8$	(5)	RMET—Fe, Mg silicates	22,72
		(7)	HYDR—Mn deposits	74
50. Nimite	$(Ni,Mg,Al)_6(Si,Al)_4O_{10}(OH)_8$	(3)	HYDR,SERP—Ultramafic Ni deposits	75
		(5)	RMET—Fe, Mg silicates	22,72
51. Donbassite	$Al_2(Si_3Al)O_{10}(OH)_2{\cdot}Al_{2.33}(OH)_6$	(4)	AUTH—Al-rich sediments	76
		(5)	HYDR—andalusite	76
52. Sudoite	$Mg_2Al_3(Si_3Al)O_{10}(OH)_8$	(6),(7)	OXID,HYDR—hematite ore	77
		(5)	AUTH—aeolian sandstones	78
		(5)	RMET—low-grade assemblages	79
53. Gonyerite	$Mn^{2+}{}_5Fe^{3+}(Si_3Fe^{3+})O_{10}(OH)_8$	(7)	OXID,HYDR—Mn deposits, skarns	80
54. Baileychlore	$(Zn,Fe^{2+},Al,Mg)_6(Si,Al)_4O_{10}(OH)_8$	(7)	OXID;WEAT—Zn ores, skarns	81
55. Cookeite	$(Al,Li)_3Al_2(Si,Al)_4O_{10}(OH)_8$	(4)	HYDR—tourmaline and lepidolite in pegmatites	10
56. Borocookeite	$LiAl_4(Si_3B)O_{10}(OH)_8$	(4)	HYDR; tourmaline in pegmatites	82

[1]See Table 1 for the list of 10 stages of mineral evolution. Parentheses indicate relatively minor clay mineral production during that stage.

[2]Paragenetic modes include: ACHN = achondrite alteration; AUTH = authigenesis; BIOL = biological mediated; CMET = contact metamorphism; DEHY = dehydration; DIAG = diagenesis; HYDR = hydrothermal alteration; LATR = laterite formation; META = regional metamorphism; OXID = oxidative weathering; RDUC = reduction; RMET = regional metamorphism; SERP = serpentinization; SOIL = Phanerozoic soil formation; WEAT = subaerial weathering

[3]References: 1. Weaver (1989); 2. Berner (1971); 3. Stoch & Sikora (1976); 4. Keller (1970); 5. Meunier (1980); 6. Giese (1988); 7. Newman (1987); 8. Calvert et al. (1980); 9. Siffert (1978); 10. Deer et al. (1962); 11. Joussein et al. (2005; 12. Maksimović & Brindley (1980); 13. Huang (1974); 14. Dudas & Harward (1975); 15. Romero et al. (1992); 16. Ziegler et al. (2003); 17. Churchman (2000); 18. Brindley & Goodyear (1948); 19. Tazaki (2005); 20. Eggleston and Tilley (1998); 21. Brearley & Jones (1998); 22. Alt & Bach (2001); 23. Peacor & Essene (1980); 24. Brindley (1982); 25. Jolliffe (1935); 26. Bailey (1988b); 27. Brindley and Wan (1975); 28. Milton et al. (1983); 29. Maksimović & Bish (1978); 30. Peacor et al. (1974); 31. Fransolet & Bourguignon (1975); 32. Ranorosoa

et al. (1989); 33. Velde (1985); 34. Whitney & Eberl (1982); 35. Gruner (1944); 36. De Waal (1970a); 37.Badaut et al. (1992); 38. Bailey (1988a); 39. Fahey et al. (1960); 40. Springer (1976); 41. Perrault et al. (1975); 42. Karup-Moller & Petersen (1984); 43. Meunier & Velde (1979); 44. Velde & Weir (1979); 45. Roy & Romo (1957); 46. Jackson et al. (1952); 47. Johnson (1964); 48. Caillaud et al. (2006); 49. Nozaka et al. (2008); 50. Ames and Sands (1958); 51. Chukanov et al. (2003); 52. Ross (1946); 53. Smol'yaninova et al. (1961); 54. Postnikova et al. (1991); 55. Singer & Stoffers (1987); 56. Linares (1987); 57. Christidis & Huff (2009); 58. Harder (1972); 59. Weir & Greene-Kelly (1962); 60. Proust & Velde (1978); 61. Harder (1976); 62. Ducloux et al. (1976); 63. Murname & Clague (1983); 64. Alt (1988); 65. Bischoff (1972); 66. Khoury et al. (1984); 67. Tien et al. (1975); 68. Hower & Mowatt (1966); 69. Kim et al. (2004); 70. Meunier & El Albani (2007); 71. Odin (1988); 72. Alt et al. (1995); 73. Novák et al. (1957); 74. Smith et al. (1946); 75. De Waal (1970b); 76. Lazerenko (1941); 77. Eggleston & Bailey (1967); 78. von Engelhardt et al. (1962); 79. Kramm (1980); 80. Frondel (1955); 81. Rule and Radke (1988); 82. Zagorsky et al. (2003)

[4]IMA status uncertain

Table 3. IMA approved and provisional clay-like minerals cited in text, selected widely cited but not IMA approved clay minerals, and related clay-like materials.

IMA Approved Mixed-Layer Clay Minerals		
Corrensite	$(Ca,Na,K)_{1-x}(Mg,Fe,Al)_9(Si,Al)_8O_{20}(OH)_{10}\cdot nH_2O$	Interstratified trioctahedral chlorite with trioctahedral vermiculite ("corrensite-1") or with trioctahedral smectite ("corrensite-2")
Rectorite	$(Na,Ca)Al_4(Si,Al)_8O_{20}(OH)_4\cdot 2H_2O$	Interstratified dioctahedral mica and smectite; alteration of K-feldspar or muscovite
Dozyite	$Mg_7Al_2(Si_4Al_2)O_{15}(OH)_{12}$	Interstratified serpentine and chlorite; altered skarn
Tosudite	$Na_{0.5}(Al,Mg)_6(Si,Al)_8O_{18}(OH)_{12}\cdot 5H_2O$	Interstratified dioctahedral chlorite and smectite; hydrothermal alteration of tuffs, andesites
Kulkeite	$Na_{0.3}Mg_8Al(Si,Al)_8O_{20}(OH)_{10}$	Interstratified trioctahedral chlorite and talc; meta-evaporite sequence
Aliettite	$Ca_{0.2}Mg_6(Si,Al)_8O_{20}(OH)_4\cdot 4H_2O$	Interstratified talc and saponite; occurs in low-T ancient lake sediments; low-grade Mg-rich metamorphic rocks
Hydrobiotite	$K(Mg,Fe^{2+})_6(Si,Al)_8O_{20}(OH)_4\cdot nH_2O$	Interstratfied biotite and vermiculite; sedimentary environments
Lunijianlaite	$Li_{0.7}Al_{6.2}(Si_7Al)_{20}(OH,O)_{10}$	Interstratified cookeite and pyrophyllite; pegmatite alteration
Saliotite	$(Li,Na)Al_3(Si_3Al)O_{10}(OH)_5$	Interstratified cookeite and paragonite; pegmatite alteration
Selected Oxide-Hydroxides		
Boehmite	$AlO(OH)$	
Brucite	$Mg(OH)_2$	
Diaspore	$AlO(OH)$	
Gibbsite	$Al(OH)_3$	
Amorphous Clay-Related Phases		
Allophane	$Al_2O_3(SiO_2)_{1.3\text{-}2.0}\cdot 2.5\text{-}3.0H_2O$	Weathering of volcanic ash; hydrothermal alteration of feldspar

Imogolite	$Al_2SiO_3(OH)_4$	Soils derived from volcanic ash
Neotocite	$(Mn^{2+},Fe^{2+})SiO_3 \cdot H_2O$	Alteration of Mn-bearing sediments

Clay Minerals Widely Cited but not Approved by the International Mineralogical Association.

Hectorite	$Na_{0.3}(Mg,Li)_3Si_4O_{10}(OH)_2$	Discredited vermiculite group; Hot springs alteration of volcanic tuff
Stevensite	$(Ca_{0.5},Na)_xMg_3Si_4O_{10}(OH)_2$	Discredited vermiculite group; Hydrothermal replacement of pectolite
Phengite	$K(Mg,Al)_2(Si,Al)_4O_{10}(OH)_2$	Discredited illite group; Equivalent to fine-grained muscovite-celadonite
Kerolite	$(Mg,Ni)_3Si_4O_{10}(OH)_2 \bullet H_2O$	Discredited talc group; Lateritic soils

Unofficial clay-related terms, including clay rocks and commonly used designations for clay-like substances.

Attapulgite	A soil rich in smectite and palagorskite; mined in southern U.S. as binder for paints and numerous other applications.
Bauxite	An aluminum ore consisting primarily of the aluminum oxide-hydrides gibbsite, diaspore and boehmite.
Bentonite	A clay rock formed principally of smectite, especially members of the montmorillonite-beidellite series
Endellite	Synonym for halloysite-10Å
Hydrated halloysite	Synonym for halloysite-10Å
Kandites	The kaolinite group
Laterite	A soil rich in Al and Fe, formed by extensive weathering and rich in clay minerals
Pelite	Historic term for a fine-grained sedimentary rock rich in clay minerals
Ripidolite	Historical name used for undetermined members of the chamosite-clinochlore series of chlorites
Saprolite	A chemically weathered rock, typically rich in clay minerals
Saprock	Fractured bedrock with alteration restricted to fracture zones; saprock lies below saprolite in a soil column.
Smectite-1	General term for dioctahedral (notably Al, Fe^{3+}) smectites
Smectite-2	General term for trioctahedral (notably Mg, Fe^{2+}) smectites
Steatite	Soapstone: a metamorphic rock rich in talc

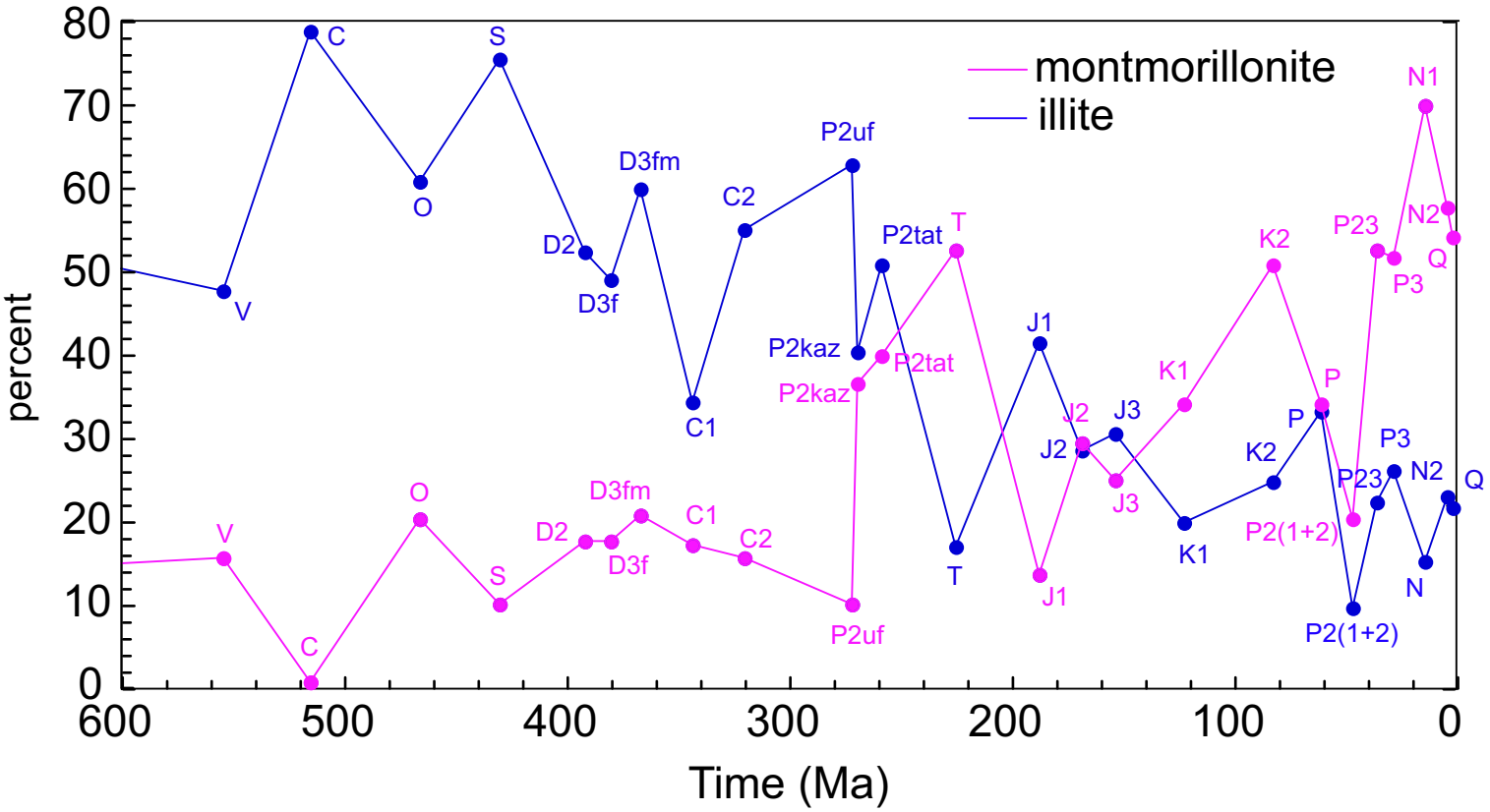
montmorillonite
illite
percent
Time (Ma)
0
10
20
30
40
50
60
70
80
600
500
400
300
200
100
0
C
S
V
O
D2
D3f
D3fm
C2
P2uf
C1
P2tat
T
J1
P2kaz
J2
J3
K1
K2
P
P23
P3
N1
N2
Q
N
P2(1+2)

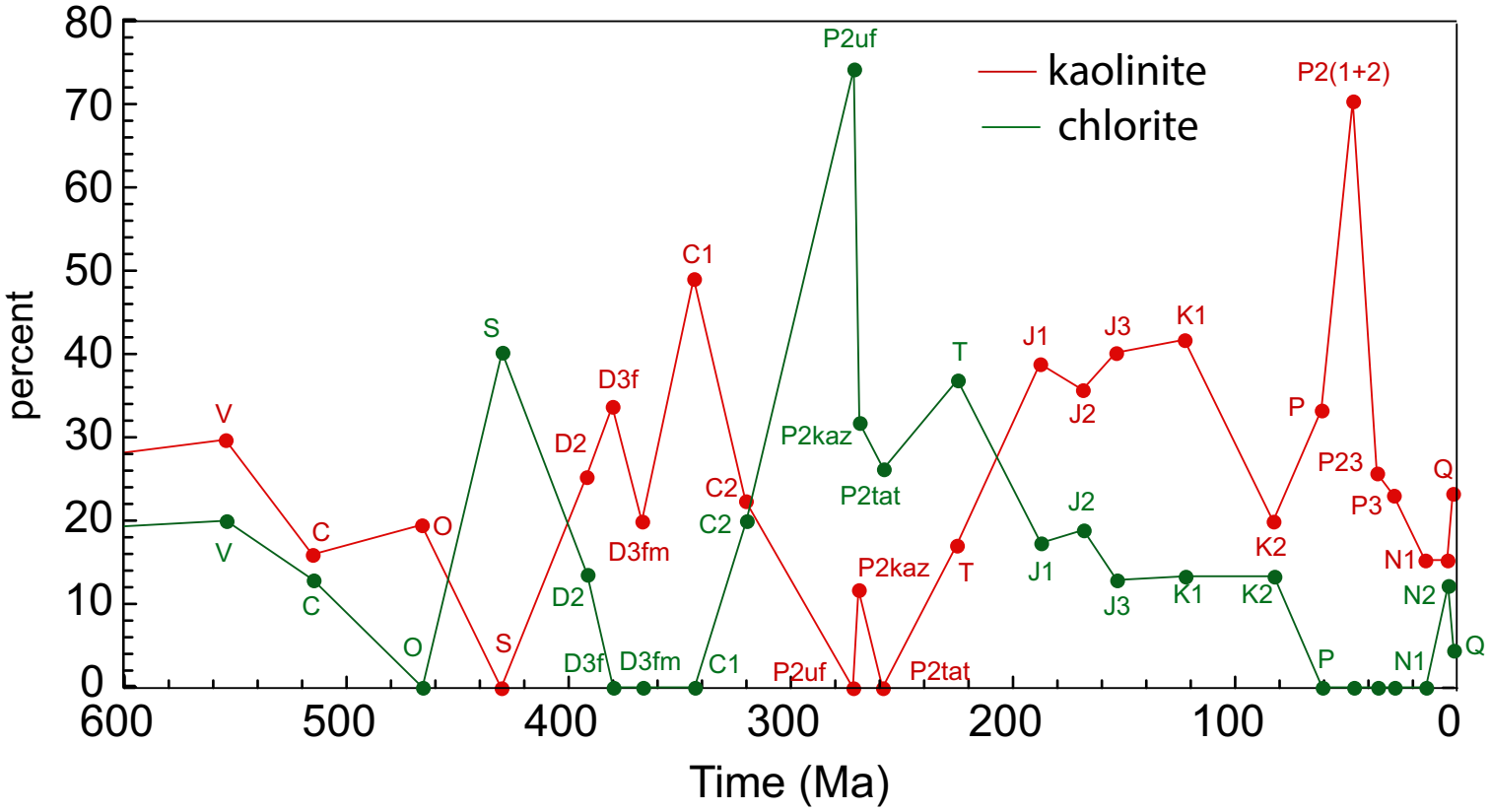
kaolinite
chlorite
percent
Time (Ma)
0
10
20
30
40
50
60
70
80
600
500
400
300
200
100
0
V
C
O
S
D2
D3f
D3fm
C1
C2
P2uf
P2kaz
P2tat
T
J1
J2
J3
K1
K2
P
P23
P3
N1
N2
Q
P2(1+2)

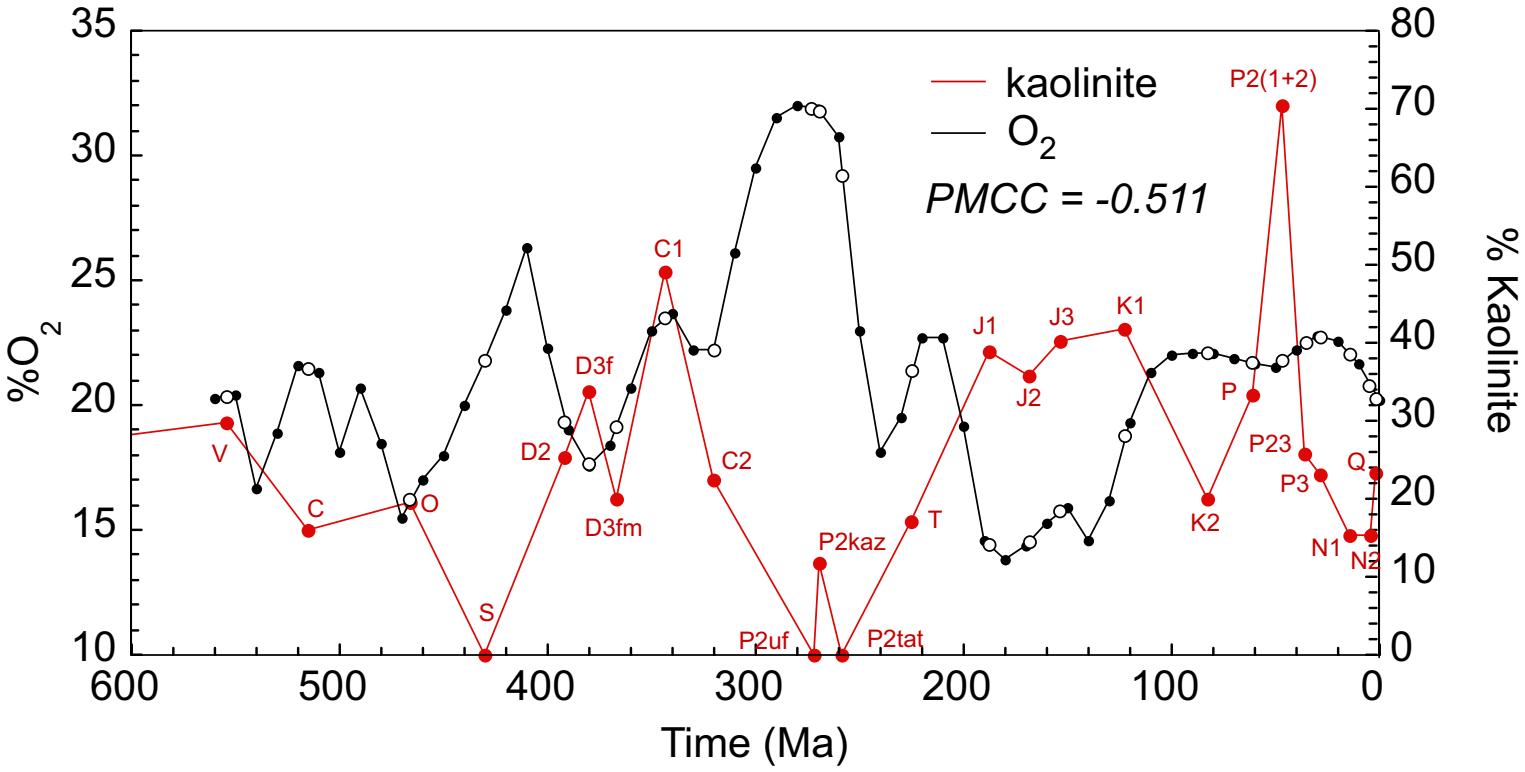
kaolinite
O_2
PMCC = -0.511
%O_2
% Kaolinite
Time (Ma)
35
30
25
20
15
10
80
70
60
50
40
30
20
10
0
600
500
400
300
200
100
0
V
C
O
S
D2
D3f
D3fm
C1
C2
P2uf
P2kaz
P2tat
T
J1
J2
J3
K1
K2
P
P2(1+2)
P23
P3
Q
N1
N2

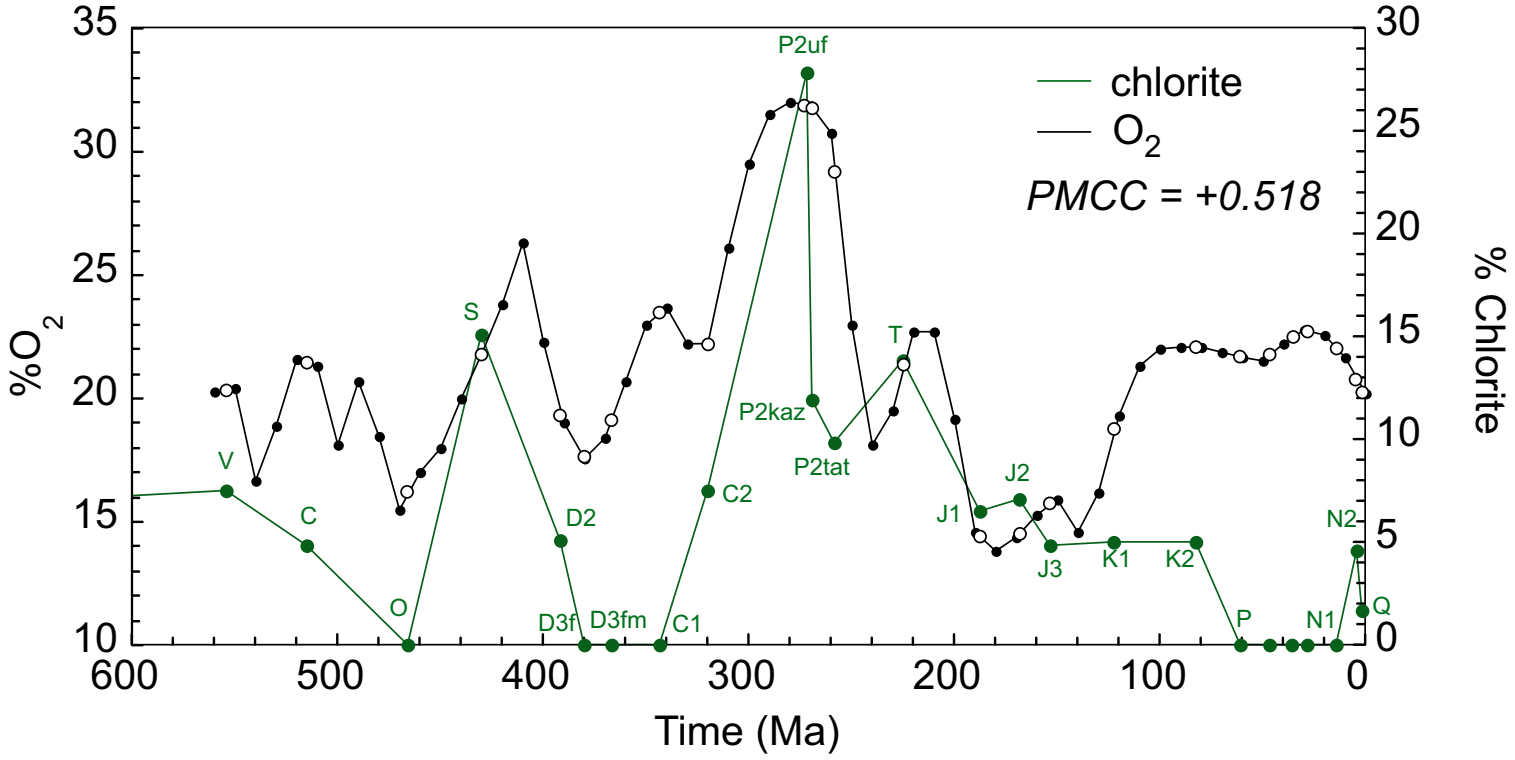
chlorite
O_2
PMCC = +0.518
%O_2
% Chlorite
Time (Ma)
V
C
O
S
D2
D3f
D3fm
C1
C2
P2uf
P2kaz
P2tat
T
J1
J2
J3
K1
K2
P
N1
N2
Q

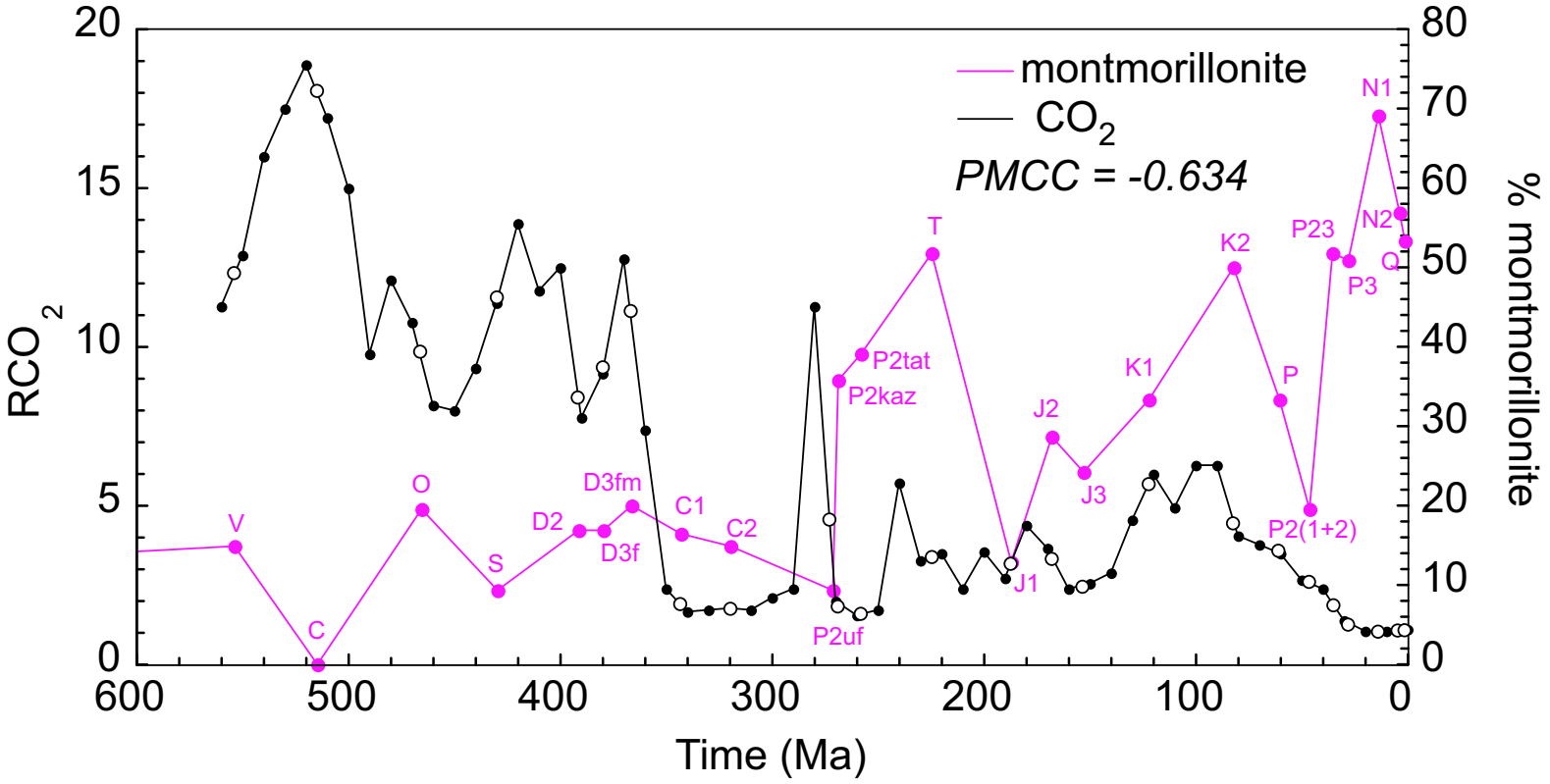
montmorillonite
CO2
PMCC = -0.634
RCO2
% montmorillonite
Time (Ma)
V
C
O
S
D2
D3fm
D3f
C1
C2
P2uf
P2tat
P2kaz
T
J1
J2
J3
K1
K2
P
P2(1+2)
P23
P3
N2
N1
Q

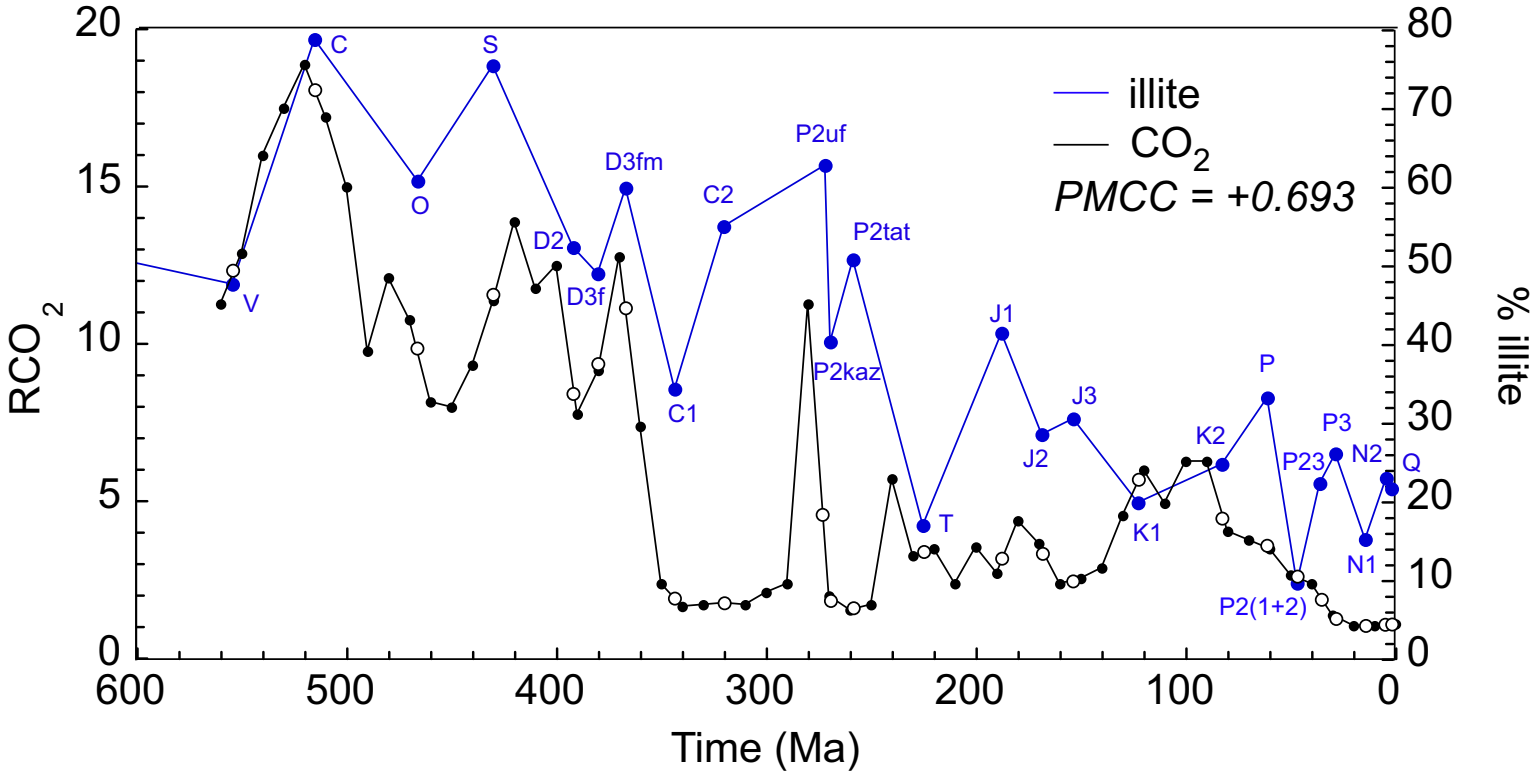
illite
CO2
PMCC = +0.693
RCO2
% illite
Time (Ma)
V
C
O
S
D2
D3f
D3fm
C1
C2
P2uf
P2kaz
P2tat
T
J1
J2
J3
K1
K2
P
P23
P3
N2
N1
Q
P2(1+2)